



TECHNISCHE UNIVERSITÄT MÜNCHEN

Lehrstuhl für Ernährung und Immunologie

**Murine susceptibility to intestinal inflammation by
in utero exposure to maternal inflammation and
maternal obesity**

Jana Hemmerling

Vollständiger Abdruck der von der Fakultät Wissenschaftszentrum Weihenstephan für Ernährung, Landnutzung und Umwelt der Technischen Universität München zur Erlangung des akademischen Grades eines

Doktors der Naturwissenschaften

genehmigten Dissertation.

Vorsitzende:

Univ.-Prof. Dr. H. Daniel

Prüfer der Dissertation:

1. Univ.-Prof. Dr. D. Haller

2. Univ.-Prof. Dr. M. Klingenspor

Die Dissertation wurde am 14.10.2015 bei der Technischen Universität München eingereicht und durch die Fakultät Wissenschaftszentrum Weihenstephan für Ernährung, Landnutzung und Umwelt am 23.02.2016 angenommen.

Zusammenfassung

Chronisch entzündliche Darmerkrankungen (CED) sind immun-vermittelte rezidivierende Entzündungen des Gastrointestinaltrakts einschließlich Morbus Crohn und Colitis Ulcerosa. Das Zusammenspiel von Risikofaktoren (z. B. genetische Prädisposition, Diät, Mikrobiota) führt durch die gestörte intestinale Homöostase zu einer übersteigerten mukosalen Immunantwort. Als Risikofaktor für die Entstehung chronischer Erkrankungen (z. B. Diabetes, Adipositas) wird die pränatale Exposition gegenüber bestimmten maternalen Reizen (z. B. Adipositas) diskutiert.

Ziel dieser Arbeit war es, den pränatalen Einfluss von maternaler Entzündung und maternaler Nahrungs-induzierter Adipositas (mDIO) auf die epitheliale transkriptionelle Programmierung des Darmepithels zu analysieren und die postnatale Entwicklung von intestinaler Entzündung an Mausmodellen mit genetisch-getriebener Ileitis [$Tnf^{ARE/+}$ (ARE)] und mit Natriumdextransulfat (DSS)-induzierter Colitis zu untersuchen.

Während frühere Arbeiten zeigten, dass maternale Entzündung das epitheliale Genexpressionsprofil des fötalen Ileums maßgeblich verändert, zeigt diese Arbeit, dass mDIO das Genexpressionsprofil kaum beeinflusst. Allerdings wurde die postnatale Entwicklung einer genetisch-getriebenen Entzündungspathologie im terminalen Ileum (Ileitis) durch keinen der beiden maternalen Stimuli verändert. Nur eine Kombination von mDIO mit einer postnatalen Hochfettdiät (HFD) beschleunigt die Entwicklung einer Ileitis, ohne dabei den Schweregrad zu verändern. Die pränatale Exposition gegenüber maternaler Entzündung wirkte sich protektiv auf den Schweregrad der DSS-Colitis aus, wohingegen mDIO keinen Einfluss zeigte. Das epitheliale Genexpressionsprofil des fötalen Colons wurde dabei durch maternale Entzündung nicht maßgeblich beeinflusst. Mit Hinblick auf die metabolische Programmierung, steigerte mDIO das Körpergewicht im fötalen Stadium (17.5 dpc) unabhängig vom fötalen Genotyp (WT und ARE). Dabei wirkte mDIO sich protektiv in WT Nachkommen aus (Körpergewicht, Fettmasse, Leptin), die mit postnataler HFD gefüttert wurden. ARE Nachkommen zeigten dagegen eine entzündungsabhängige Resistenz gegenüber HFD, welche durch mDIO nicht zusätzlich moduliert werden konnte.

Schlussfolgernd scheint die pränatale Programmierung des Darmepithels keinen entscheidenden Einfluss auf die intestinale Entzündung zu haben. Lediglich der Verlauf einer genetisch-getriebenen Ileitis (z. B. durch mDIO) wird durch pränatale Exposition gegenüber maternal-entzündlichen Reizen beeinflusst, nicht aber der Schweregrad. Im Gegensatz dazu wirkt sich maternale Entzündung protektiv auf den Schweregrad einer experimentellen Colitis aus.

Abstract

Inflammatory bowel diseases (IBD) are chronically relapsing immune-mediated disorders of the gastrointestinal tract such as Crohn's disease and ulcerative colitis. The interplay of risk factors (e.g. genetic predisposition, diet, microbiota) disturbs the intestinal homeostasis resulting in an overreacting mucosal immune response. Prenatal exposure to maternal stimuli (such as inflammation or obesity) is linked to chronic diseases.

The aim of this work was to investigate the effects of murine maternal inflammation or maternal diet-induced obesity (mDIO) on prenatal programming of the intestinal epithelium and on the postnatal development of intestinal inflammation using mouse models for genetically-driven ileitis [*Tnf^{ΔARE/+}* (ARE) mouse] and for dextrane sulfate sodium (DSS)-induced colitis.

As a result, and contradictory to previously published results that show that maternal inflammation highly impacts the epithelial transcriptome of the fetal ileum, no extensive influence on the fetal intestinal epithelial transcriptome was observed by mDIO. However, the postnatal development of a genetically-driven pathology in the terminal ileum (ileitis) was not affected by either maternal stimulus alone, indicating the strong influence of the postnatal environment on this disease. However, mDIO in combination with a postnatal high-fat diet (HFD) accelerated ileitis development, but not the ileitis severity at later stages. Consequently, risk factors from the postnatal environment were crucial in the development of TNF-driven ileitis, whereas mDIO reflects a risk factor for the onset of ileitis. In contrast, the responses to DSS colitis susceptibility were different. Maternal inflammation attenuated the severity of DSS colitis, whereas mDIO did not influence colitis development. However, the fetal epithelial transcriptome of the colon was not affected by maternal inflammation. In the context of metabolic programming, mDIO increased fetal body weights (17.5 dpc) independently of the fetal genotype (WT and ARE), but attenuated body weight gain, mesenteric fat gain and plasma leptin increase in HFD-fed WT offspring. Due to postnatal inflammation, HFD-fed ARE offspring showed resistance to diet-induced obesity, which was not modulated by mDIO.

In conclusion, fetal programming of the intestinal epithelium is hardly influenced by maternal stimuli and is not a determining factor for postnatal intestinal inflammation. Maternal inflammatory stimuli did not alter the severity of inflammation in a genetically-driven ileitis, but were able to modulate the disease onset (in case of mDIO). This is different in an experimental model, where maternal inflammation attenuated the severity of colitis.

Aims of the work

Maternal changes during gestation (i. e. inflammation, nutrition and infection) cause alterations in intrauterine availability to nutrients, oxygen and hormones, thus affecting the programming of tissues. It has been reviewed that intrauterine programming of fetal organ systems (e. g. cardiovascular, metabolic, reproductive and nervous system) can be related to diseases later in life (hypertension, obesity, type 2 diabetes, asthma). However, the role of maternal inflammatory conditions such as IBD or obesity as risk factors for long-term adverse consequences on the offspring's intestinal health remains poorly understood.

This work was conducted to investigate whether maternal inflammation or maternal diet-induced obesity (mDIO) program the fetal gut towards intestinal inflammation by using two mouse models of intestinal inflammation: genetically-driven CD-like ileitis (*Tnf^{ΔARE/+}* mice, ARE) and experimentally-induced colitis (*Tnf^{+/+}* mice, WT).

Laser microdissection (LMD) microscopy was used to characterize the transcriptional response of the fetal epithelium. Tissue pathology and hallmarks of tissue inflammation typical for the *Tnf^{ΔARE/+}* mouse model, such as infiltration of neutrophils (Ly6G-positive cells), were assessed in ileal tissue sections from adult WT and ARE offspring in order to investigate whether prenatal exposure to maternal inflammation or mDIO influences the postnatal development of ileitis. Characteristics of intestinal permeability and systemic inflammation were addressed by analysing portal vein endotoxin and plasma TNF. Furthermore, a putative coherent influence of prenatal and postnatal obesity on ileitis was proven by additional exposure of ARE offspring to postnatal HFD. To evaluate the severity of DSS colitis, body weight development and disease activity indices from DSS-treated WT offspring were monitored.

Metabolic programming in response to mDIO was evaluated in WT offspring that were exposed to a postnatal HFD feeding by monitoring offspring's body weight, mesenteric fat mass as well as plasma leptin at different time points.

Table of contents

Zusammenfassung	II
Abstract	III
Aims of the work	IV
Table of contents	V
1. Introduction	1
1.1. Inflammatory bowel diseases	1
1.2. Risk factors contributing to the development of IBD	2
1.2.1. Susceptibility loci for genetic changes and epigenetic modifications.....	2
1.2.2. Microbiota	3
1.2.3. Diet	5
1.2.4. Early life exposure to maternal environments	6
1.3. Prenatal gut development and lineage allocation of the epithelium.....	15
1.4. Perinatal development of immune homeostasis as a consequence of the microbial burden	16
1.5. The postnatal intestinal epithelium as first line of defence	19
1.6. Immunologic features of innate and adaptive immunity in the postnatal gut during IBD	22
1.7. Mouse models resembling human IBD	23
1.7.1. <i>Tnf^{flARE/+}</i> mouse model resembling CD-like ileitis	24
1.7.2. Dextrane sulfate sodium (DSS)-induced colitis model	24
2. Material and Methods	26
2.1. Ethics statement for animal studies	26
2.2. Breeding pairs for maternal inflammation studies	26
2.3. Breeding pairs for maternal obesity studies	27
2.4. Prenatal studies	27
2.4.1. Breeding for prenatal sampling.....	27
2.4.2. Fetal gut sampling at 17.5 dpc	27
2.5. Postnatal studies.....	28

2.5.1.	Development of genetically driven CD-like ileitis under maternal inflammation or obesity under conventional housing	28
2.5.2.	Development of genetically driven CD-like ileitis under maternal inflammation under specific-pathogen-free conditions	29
2.5.3.	DSS colitis susceptibility studies.....	29
2.6.	Histology	29
2.6.1.	Histopathological scoring of the distal ileum and proximal colon	29
2.6.2.	Mesenteric adipocyte sizes	30
2.6.3.	Immunofluorescence analysis on paraffin-embedded and frozen sections of the distal ileum	30
2.7.	Laser microdissection (LMD) of fetal intestinal epithelial cells	31
2.7.1.	Cryosectioning of distal ileum and colon.....	31
2.7.2.	Hematoxylin/Eosin (H&E) staining of cryosections prior to LMD	31
2.7.3.	Laser microdissection microscopy.....	32
2.7.4.	RNA isolation and quality control.....	32
2.7.5.	Microarray processing	33
2.7.6.	Microarray data analysis	33
2.7.7.	Preamplification of laser microdissected low input RNA	33
2.8.	Gene expression analysis of laser microdissected IEC or whole tissue sections	34
2.9.	Flow cytometry of T cells in spleens and mesenteric lymph nodes (MLNs)	35
2.10.	Microbial ecology	35
2.10.1.	Cecal content collection and bacterial DNA extraction	35
2.10.2.	Illumina Sequencing of 16S rRNA gene amplicons from caecal contents	36
2.11.	Plasma Measurements	36
2.11.1.	Measurements of proinflammatory cytokines TNF, IFN γ and IL-6.....	36
2.11.2.	Leptin measurements	36
2.11.3.	Endotoxin concentration of portal vein plasma.....	37
2.12.	Statistics	37
3.	Results	38

3.1. The severity of murine Crohn's disease-like ileitis is dependent on the microbial environment and on dietary factors.	38
3.2. The influence of maternal inflammation on genetically-driven postnatal development of CD-like ileitis in <i>Tnf^{ΔARE/+}</i> mice	39
3.2.1. <i>Tnf^{ΔARE/+}</i> dams are locally and systemically inflamed	39
3.2.2. Maternal inflammation does not change CD-like ileitis in <i>Tnf^{ΔARE/+}</i> mice.....	40
3.2.3. Maternal inflammation influences energy homeostasis in WT and <i>Tnf^{ΔARE/+}</i> offspring	43
3.2.4. Inflammation-driven shift of microbial ecology is not additionally influenced by early life exposure to maternal inflammation.	44
3.3. Fetal exposure to maternal diet-induced obesity and its potential to affect postnatal development of CD-like ileitis.....	46
3.3.1. The maternal diet-induced obesity environment during pregnancy and at weaning.....	46
3.4. Establishment of a workflow for large scale targeted gene expression analysis from laser microdissected murine fetal intestinal epithelium.....	48
3.4.1. Single primer isothermal amplification enables large-scale targeted gene expression analysis of fetal intestinal epithelial cells.....	49
3.4.2. Epithelial expression of <i>Muc2</i> and <i>Hoxb13</i> discriminates fetal ileum from colon	51
3.5. Maternal diet induced obesity (mDIO) hardly influenced the epithelial transcriptome of the fetal ileum in WT and <i>Tnf^{ΔARE/+}</i> mice	52
3.6. Maternal diet induced obesity accelerates intestinal inflammation in high-fat diet-fed <i>Tnf^{ΔARE/+}</i> mice.....	55
3.7. Maternal diet-induced obesity protects WT offspring from metabolic dysfunction induced by post weaning HFD.	59
3.8. Protection against DSS-induced colitis severity is attributed to maternal inflammation, but not to mDIO	60
3.9. The epithelial transcriptome in the fetal colon is hardly affected in response to maternal inflammation.	63
4. Discussion	64
4.1. Maternal inflammation has no impact on genetically-driven CD-like ileitis, but protects from DSS-induced colitis.....	64

4.2.	Maternal diet-induced obesity in the context of intestinal inflammation	67
4.2.1.	Fetal exposure to maternal-diet induced obesity has marginal effects on the epithelial transcriptome	67
4.2.2.	Changing control dams diet to HFD at birth equalized the offspring's metabolic conditions during breastfeeding	70
4.2.3.	Maternal diet-induced obesity combined with postnatal HFD accelerates TNF-driven intestinal inflammation in <i>Tnf^{ΔARE/+}</i> mice.	71
4.2.4.	Maternal-diet induced obesity protects from metabolic dysfunction	73
5.	References	76
6.	Appendix	91
7.	List of Figures	93
8.	List of Tables	95
9.	List of Supplementary Tables	96
10.	List of Abbreviations	96
11.	Acknowledgments	102
12.	Curriculum Vitae	103
13.	Eidesstattliche Erklärung	Fehler! Textmarke nicht definiert.

1. Introduction

1.1. Inflammatory bowel diseases

Chronic pathologies (i. e. obesity, diabetes, cancer) are long-lasting conditions that cause the major morbidity and mortality across the globe. They are characterized by a complex causality, multiple risk factors (often shared between pathologies), long latency periods, prolonged course of illness and functional impairment, which make it difficult to understand their pathogenesis.

Inflammatory bowel diseases (IBD) are such relapsing systemically immune-mediated chronic pathologies mainly affecting the gastrointestinal tract with its two main idiopathic forms, Crohn's disease (CD) and ulcerative colitis (UC).

CD and UC show distinct disease phenotypes. CD can affect the whole digestive tract represented by a patchy inflammation pattern of rocky appearance and UC develops in the large intestine continuously throughout areas. Patients mainly suffer from lower right (in CD) or left (UC) abdominal pain. Ulcers are deeply and transmurally located in CD, whereas in they reside in the mucus lining in UC. Both forms have in common that genetic abnormalities can cause overly aggressive T cell responses to a subset of commensal enteric bacteria. In addition, microbial adjuvants activate innate immune mechanisms through pattern recognition receptors (PRR) and subsequent NF κ B activation causing the expression of proinflammatory cytokines (such as TNF, IL1 β , IL-6 and IL-8) in active disease [1]. The overall immunologic phenotype of CD is driven by a Th1/Th17 response causing T cell expression and secretion of IFN- γ , IL-22 and IL-17 [2]. In contrast, the T cell profile in UC is more difficult to characterize. It is considered as an atypical Th2-like response in which natural killer T cells (NKT cells) produce IL-13 and IL-5 as the major response, but the concentrations of IL-4 and IL-5 which are elevated in a typical Th2 response may vary in UC.[1].

From a public health standpoint, IBD is a global health problem with increasing annual incidence rates especially in westernized countries during the 2nd and 3rd decade of life. In 2013, 10.58 million prevalent cases of IBD were reported worldwide, which was a 9.6% increase compared to 1990 [3]. UC has an annual incidence of 0-19.2 per 100,000 inhabitants in North America and 0.6-24.3 per 100,000 inhabitants in Europe with a corresponding prevalence of 37.5-248.6 per 100,000 and 4.9-505 per 100,000 inhabitants, respectively [4]. The incidence of CD is comparable to UC (0-20.2 per 100,000 in North America and 0.3-12.7 per 100,000 in Europe [4]. Distinct incidence rates around the globe point to potential environmental risk factors for IBD. The incidence is higher in urban than in rural populations and there is a north-south gradient of IBD incidence (multivariate-adjusted Hazard Ratio for

women residing in southern latitudes compared to northern latitudes was 0.48 (95% CI 0.30 to 0.77) for CD and 0.62 (95% CI 0.42 to 0.90) for UC [5]. However, the environment is not the only confounder for the outcome of IBD. Basic science, animal models, genetic analyses, and clinical trials provide some insights in the pathogenesis of IBD and already clarified that interactions of various risk factors contribute to IBD [1, 4, 6].

1.2. Risk factors contributing to the development of IBD

There are several risk factors described for the development of IBD [4]. It is a complex interplay between genetic predisposition (leading to immunological abnormalities), environmental influences and dysbiosis of the gut microbial ecology causing the onset of IBD, whereas one factor alone is not sufficient to trigger IBD [4].

1.2.1. Susceptibility loci for genetic changes and epigenetic modifications

The interplay between genetic predisposition and the environment became clear in genome wide association studies (GWAS) when susceptibility loci which are triggered by environmental signals (i. e. *NOD2*, *CARD*, *PTPN22*) were linked to disturbances in innate (i. e. intestinal barrier defects, Paneth cell dysfunction, impaired recognition of microbes) and adaptive (i. e. imbalanced effector and regulatory T cells and cytokines) immune responses [6]. In detail, 163 susceptibility loci (30 CD-specific and 23 UC-specific) were identified. 110 loci contribute to both phenotypes. A recently published study reported on 38 new risk loci for IBD [7]. Interestingly, some risk alleles have opposite effects in CD and UC. For instance, *PTPN22* and *NOD2* are risk alleles in CD, but show protective effects against UC. 70% of IBD loci are shared with other immune-mediated diseases (e. g. psoriasis) and link IBD to inflammatory extra-intestinal symptoms and autoimmune-diseases (e. g. asthma, diabetes type1) [8]. 25,075 single nucleotide polymorphisms (SNPs) are associated with at least one of CD or UC or both. Gene ontology analyses of 300 prioritized genes highlight 286 GO terms and 56 pathways involved in cytokine production, lymphocyte activation, IL-17 production and JAK-STAT signalling [8]. Concordance studies in mono- and dizygotic twins revealed that IBD is familial aggregated. In monozygotic twins 35% (CD) and in 16% (UC) of twin pairs were concordant for IBD, but a low concordance was observed in dizygotic twin pairs (3% (CD) and 2% (UC)) [9]. As well, genetic anticipation was confirmed by earlier disease onset in offspring from IBD parents. Nevertheless, a large fraction of risk is driven by non-coding variation and the fact that susceptibility loci and low concordance rates in monozygotic twins only explain a low percentage of the heritability of IBD [6]. This emphasizes towards the importance of further mechanisms such as epigenetics and environmental factors in IBD development.

Epigenetics may be defined as mitotically heritable changes in gene function that are not explained by changes in the DNA sequence. The main epigenetic mechanisms comprise DNA

methylation, histone modification, RNA interference, and the positioning of nucleosomes. Epigenetic modifications of genes can be understood as the link between genetic susceptibility loci and environmental influences. Thus, IBD-relevant genes are modulated by epigenetic modifications [10]. The most widely studied epigenetic mechanism is DNA methylation. Several methylation studies in monozygotic twins discordant for IBD or in patients with active and quiescent IBD showed that specific loci, such as *TNFRSF*, *IL12*, *CARD9*, *MAPK*, are differently methylated in IBD [11-15]. A prominent example of promoter hypermethylation is the cell-cell adhesion molecule E-cadherin (*CDH-1*) which is associated with a downregulation of *CDH-1* and a long-lasting inflammation in UC [16]. Newly identified IBD loci for DNA methylation are reviewed by Yi *et al.* 2015 [17]. DNA methylation appears to be a common phenomenon in UC, especially in mucosal biopsies from inflamed tissue. Unlike UC, limited data have been reported regarding the contribution of DNA methylation in CD pathogenesis.

Apart from genetics and epigenetics, IBD occurrence underlies a geographical pattern [5]. This is due to environmental shapes upon industrialization and urbanization of populations towards altered microbial exposures (e. g. infectious gastroenteritis, Mycobacterium infections), sanitation, occupations, diets (high-fat diet, breastfeeding), lifestyle behaviour (less exercise, smoking), medications (antibiotics) and pollution [8, 18-20]. In essence, the gut microbiome is important for maintaining host intestinal homeostasis. Vice versa, the host genotype clearly influences the microbiota composition as mentioned above.

1.2.2. Microbiota

The microbiota has a major impact on host energy metabolism and thus contributes to obesity, insulin resistance and even metabolic syndrome [21]. Regarding intestinal energy homeostasis microbes provide energy and nutrients by saccharolytic fermentation of non-digestible substrates (e. g. complex plant carbohydrates) such as short chain fatty acids (SCFA) for both, the host and symbiont communities. The intestinal epithelium covers 60-70% of its energy requirements by bacteria-derived SCFA such as acetate, propionate and butyrate indicating the importance of microbes in intestinal energy homeostasis. Furthermore, SCFA acidify the luminal environment and inhibit growth of pathogens emphasizing on the contribution of the microbiota on the intestinal mucosal immune homeostasis. This was also shown by local perfusion studies with SCFA showing improvement of 'diversion colitis' [22]. Despite its impact in energy homeostasis microbial components (such as lipopolysaccharides) are the main immunostimulants for the maturation and education of the mucosal immune system. For example, mice with a limited microbiota show reduced lymphoid subsets [23]. However, besides advantageous effects of the microbiota on intestinal health its promoting effects in IBD development are not fully clarified yet. A major hypothesis in the context of IBD development

is an abnormal communication between gut microbial communities and the host's mucosal immune system at different levels.

First of all, temporal, individual, dietary and drug-induced dynamics can affect the microbiota towards altered composition and less diversity (dysbiosis) and are tightly connected to IBD pathogenesis [24-26]. The general concept of dysbiosis (compositional changes of the microbiota) includes microbiota differences due to low biodiversity of dominant bacteria, high variability over time and changes in composition and spatial distribution (high concentrations of mucosal adherent bacteria). Dysbiosis might arise from either an enteric pathogen or a dysbalanced host-mediated innate and adaptive immunity or a combination of these two. Pathogens might benefit from a disturbed host immune response promoting bacterial translocation across the intestinal barrier and thus causing local and systemic inflammatory responses.

Secondly, alterations of the microbial composition are as well linked to IBD pathogenesis. Numerous studies demonstrate a decrease in strict anaerobes and a bloom of *Proteobacteria* in the microbiota of both CD and UC patients. In IBD, the predominant bacterial phyla *Bacteroidetes* and *Firmicutes* are less abundant (e. g. *Faecalibacterium prausnitzii*, [27]), whereas the phyla *Proteobacteria* and *Actinobacteria* [28] are increased in abundance. Murine studies revealed that reduced numbers of *Bacteroides fragilis* (a human symbiont) might contribute to intestinal inflammation, as it protects from *Helicobacter hepaticus*-induced colitis. In contrast to the loss of beneficial bacteria (such as *Faecalibacterium prausnitzii*), mucosa-associated *Enterobacteriaceae* (e. g. *E. coli*) were more abundant in CD patients. Intestinal colonization of the commensal *E. coli* correlates with CD-associated adherent invasive *E. coli* (AIEC). Tissue penetration of AIEC may be due to autophagy defects (ATG16L1 or IRGM) [29]. As well, it has to be taken into account that the microbiota of IBD patients has a closer contact to the mucosa. For example, mucolytic bacteria like *Ruminococcus gravus* and *Ruminococcus torques* are enriched in IBD [30]. This was shown by increased bacterial penetration through the mucus layer in IBD biopsies (30% of the patients) compared to healthy control specimen (3% of the controls).

Thirdly, the relationship of host-susceptibility loci and altered microbial composition is associated with IBD, but which factor is causative is not fully understood. For instance, host-susceptibility loci *NOD2*, *CARD9* and *IRGM1* for CD are required for *Mycobacteria* clearance in the intestine and might explain the character of *Mycobacteria*-related CD [31]. Many host factors that affect commensals in IBD are linked to barrier dysfunction (e. g. tight junctions, mucus layer and antimicrobial peptides). A pronounced barrier dysfunction was already observed in mild to moderately active CD [32], but the exact mechanism between discontinuous tight junctions and mucosal inflammation is not fully understood. Another

example is a follicle-associated epithelial barrier defect in the Payer's patches which is impaired in CD patients and might increase the load of commensals again activating the mucosal immune response [33]. Another host factor that affects bacterial composition is the mucus, which is significantly altered in UC patients (mucus composition and phospholipid content) [34]. Furthermore, antimicrobial peptides with bactericidal activities are also relevant in intestinal inflammation, because decreased levels of α -defensins and antimicrobial peptides deriving from Paneth cells are linked to ileal CD, whereas expression of β -defensins was reduced in colonic CD [35-37]. Unlike pathogens, commensals are crucial to promote barrier function. This is due to the fact that the expression of antimicrobial proteins such as regenerating islet-derived 3b and γ and angiogenin 4 were induced in response to commensal contact (e. g. *Bacteroidetes thetaiotaomicron*) [38, 39]. In summary, all described host factors can contribute to bacterial invasion across the gut barrier and lead to persisting immune cell exposure by mucosa-associated and macrophage-residing commensal enteric bacteria.

1.2.3. Diet

Besides microbial changes, many epidemiological studies associate dietary factors (e. g. fibre, dietary fat, vitamin D) with the onset of IBD. As an example it was shown that low intake of dietary fibre from fruit and vegetables and a low vitamin D status are associated with the risk of getting IBD [40-44]. Since an obesogenic diet is a risk factor for many diseases, such as cardiovascular diseases, diabetes, diet induced obesity (DIO) became a global health problem of industrialized countries. The worldwide incidence has increased dramatically during recent decades and the role of dietary fat in the development of IBD became an important issue. The World Health Organization (WHO) estimated more than 1 billion adults to be obese and 300 million of them are clinically obese with a body mass index (BMI) of 30kg/m² or higher [45]. It was already shown that dietary fat, particularly (trans)-saturated fat might play an important role in the pathogenesis of IBD [46, 47].

This is because a feature of DIO is a systemic low-grade inflammation characterized by abnormal cytokine production, increased acute phase reactants and other mediators that activate a network of inflammatory signalling pathways [48] and linking it to chronic inflammatory disorders such as diabetes, cancer, or atherosclerosis. Importantly, obesity and IBD share common characteristics, including chronic inflammation [49, 50]. Obese humans and DIO mouse models exhibited up-regulated TNF and IL-6 in serum, adipose tissue, liver or *Tnf* mRNA specifically in the ileum [50-53]. Interestingly, increased *Tnf* mRNA was strongly associated with the degree of weight gain, increased fat mass, plasma glucose or insulin [54]. The fact that adipose tissue performs a proinflammatory transformation during both, obesity and IBD, points to a possible link between these two conditions [55]. In CD patients the ratio of intra-abdominal fat to total abdominal fat is far greater than in healthy controls [56].

Mesenteric fat had been shown to be an important indicator of regional disease activity. “Creeping fat” has been recognized at least since the early 1930’s and was used to identify the most diseased regions of the gut. Creeping fat is defined as fat extending from the mesenteric attachment to partially cover the small or large intestine, resulting in a loss of the bowel-mesentery angle [57]. Diet-induced hypertrophic adipocytes are sources of proinflammatory cytokines including TNF, interleukin 6 (IL-6) and monocyte chemoattractant protein (MCP-1). They function like macrophages, surveying their environment for microbial products [56] and mediating innate immune responses [58]. HFD-driven activation of NFκB transcription in the ileum and to lesser extent in the colon was shown in an NFκBRE^{EGFP} reporter mouse model [54]. Interestingly, myeloperoxidase activity as a marker for intestinal inflammation was up-regulated in conditions of DIO, but not HFD alone [59]. However, this is in contrast to the observation of Gruber *et al.* 2013 showing in a murine model that high-fat diet-induced intestinal inflammation is independent of the presence of obesity [60].

Another aspect of how DIO can promote intestinal inflammation is the influence of HFD or obesity on the intestinal microbiota, which was intensely reviewed by Musso *et al.* [61]. Findings in germ-free (GF) mice being resistant to DIO and faecal transplant experiments of obese microbiota into GF mice [62] provide evidence that the gut microbiota integrates excess dietary components into adipose tissue. The fact that *Tnf* is not upregulated in HFD-fed GF mice points to interactions between HFD and the microbiota during the induction of intestinal inflammation. Additional evidence that HFD promotes inflammation is the fact that TLR4, a sensor of gram negative-derived lipopolysaccharide (LPS), is activated by HFD and links dietary components to innate immune mechanisms [59].

In addition, LPS is a key mediator of obesity and intestinal inflammation. HFD increases intestinal permeability by affecting tight junction proteins, favouring elevated translocation of LPS across the intestinal barrier. LPS obviously enters the lymph nodes and circulates systemically via chylomicrons [63].

In summary, animal models suggest that the interaction of HFD and microbes results in intestinal inflammation by increased intestinal permeability, translocation of bacterial products and upregulation of pro-inflammatory cytokines.

1.2.4. Early life exposure to maternal environments

Associations of environmental risk factors (e. g. smoking, hygiene, infections, medication) as well as life style factors with IBD are well described by Ananthakrishnan *et al.* 2015 [4] and Baumgart *et al.* 2012 [6]. However, the question at which time environmental exposures are most relevant for the pathogenesis of IBD remains unknown so far. The pre- and perinatal life is known to be a very sensitive period of life, where environmental factors may have a substantial programming effect towards disease onset later in life. This work puts special

emphasis on 'early life exposure to inflammation and to high-fat diet', in order to get insight in intrauterine risk factors that might contribute to the development of IBD.

In this work, it is hypothesized that environmental influences are most relevant during prenatal development, where the developing embryo or fetus is programmed by *in utero* conditions in order to be prepared for the predicted conditions in postnatal life. It is known that maternal changes (i. e. inflammation, nutrition and infection) cause alterations in intrauterine availability to nutrients, oxygen and hormones, thus programming tissue development. It has been reviewed that intrauterine programming of fetal organ systems (e. g. cardiovascular, metabolic, reproductive, nervous system) can be related to diseases later in life (hypertension, obesity, type 2 diabetes, asthma) [64]. However, the consequences on intestinal programming are not well understood.

A prominent example for prenatal programming is the Dutch famine in winter 1944, where maternal starvation caused limited intrauterine growth and was most importantly a contributor to coronary heart diseases as well as other chronic diseases later in life [65]. This was shown in a cohort study of 2414 people, born in the Dutch famine 1944. It was concluded that the exposure to the famine during any stage of gestation was associated with glucose intolerance. More coronary heart diseases, a more atherogenic lipid profile, disturbed blood coagulation, increased stress responsiveness and more obesity cases were observed among those exposed to famine in early gestation [65]. Women who were exposed to the famine in early gestation also had an increased risk of breast cancer indicating that especially the embryogenesis is highly susceptible to environmental changes. In contrast, they observed that people, who were exposed to the famine in mid gestation, had more microalbuminuria and obstructive airways disease. These findings agree well with Barker's hypothesis supporting the concept of a "thrifty phenotype", where maternal under-nutrition leads to a lower birth weight and to higher risks of chronic conditions in adult life [66].

According to this, it is hypothesized in this work that an inflammatory or obesity-related *in utero* environment may program the progeny towards increased susceptibility to IBD later in life. The two maternal risk factors (inflammation and diet induced obesity) will be highlighted in this context. These hypotheses are biologically plausible, since maternal IBD has a profound negative effect on gestational outcome and since there is mounting evidence linking HFD and diet induced obesity (DIO) to low-grade intestinal inflammation and IBD. Possible contributions of both maternal risk factors to the development of IBD are highlighted below.

Prenatal exposure to maternal intestinal inflammation

Epidemiological studies with IBD patients associate disease activity during pregnancy with adverse outcomes such as preterm birth, spontaneous abortion and labour complications [67,

68]. Getahun *et al.* showed in a retrospective cohort study (n= 395, 781) that IBD was associated with increased odds of small for gestational age, whereas only UC was associated with spontaneous preterm birth, preterm premature rupture of membranes and ischemic placental disease [69]. A Danish national birth cohort comprising 40, 640 mother-child pairs demonstrated that children of IBD mothers were significantly shorter at birth with a tendency towards decreased birth weight, however they recovered their body weight during first year of life [70]. This is in contrast to another IBD study, where significant lower birth weights and heights of IBD children lasted until 4 years of age [71]. Taken all studies together, there is no evidence that IBD or medication during pregnancy increases the risk of major congenital anomalies in children [72].

In the context of IBD development, there are no clear mechanism of intrauterine programming published. An insufficient maturation of the fetal intestinal barrier is the consequence of an altered maternal environment, thus affecting postnatal organ development and disease susceptibility [73]. Recently, maternal exposure to a high-fat diet-induced intestinal inflammation in fetal sheep supports the hypothesis that inflammatory stimuli affect the susceptibility to IBD in offspring [74].

During gestation, the intrauterine environment influences placental immune regulation, thus affecting fetal tolerance. The placenta enables the exchange of nutrients and metabolites between fetal and maternal compartments and initiates the temporal prevalence of cytokines. In physiological conditions, the placental immunology is very complex and underlies temporal $T_h1:T_h2$ shifts according to the gestational age [75]. Maternal T_{Reg} cells are important in pregnancy-induced immunological shifts to sustain maternal-fetal tolerance [76-78]. In the first trimester of pregnancy a pro-inflammatory T_h1 environment (IL1 β , IL-6 and TNF) facilitates embryonic invasion, proper implantation and placenta formation [79]. Placental expression of PRRs including TLR 2 and TLR 4 on normal human chorionic villi protects against bacterial or viral attack [80], clearly suggesting that innate immune mechanisms contribute to the placental environment and maintain its complex homeostasis [81, 82]. The second trimester characterizes the mid pregnancy phase with a T_h2 dominated anti-inflammatory environment (IL-4, IL-5 and IL-10) preventing fetal allograft rejection and supporting fetal development with materno-fetal synchrony. The third trimester is again characterized by a T_h1 dominated immune environment finally responsible for initiating birth. Thus, under normal physiological circumstances maternal T_{Reg} cells and placental chemokine and cytokine production prevent rejection of the fetal allograft in a physiological manner. For example, murine FOXP3+ T_{Reg} cell depletion triggers fetal resorption, decidual inflammation and abnormal spiral artery remodelling consistent with pathological features of preeclampsia in human pregnancy [83]. The fact that fetal tolerance is maintained by maternal T_{Reg} cells shows that infection and

inflammation-induced reductions in T_{Reg} cells have a critical potential to abrogate fetal tolerance with increased pregnancy complications. For instance, IBD-associated T_H1 inflammatory responses during pregnancy lead to peri- and postnatal complications including preterm labor and low birth weights [67, 84]. Figure 1 depicts putative immunomodulatory characteristics of materno-fetal crosstalk under physiological and pathological conditions.

However, whether maternal inflammatory stimuli during pathological conditions are transmitted into the fetus with consequences for later disease susceptibility is not well understood. A potential impact of inflammatory processes during pregnancy on fetal organ functions was recently shown in infection models, such as endotoxin-induced chorioamnionitis [85]. Elevated T_H1 cytokine levels by immune activation (endotoxin or bacterial infection) adversely affect both, the placenta and the fetus. For example, innate immune activation by low-dose endotoxin during early pregnancy initiates maternal TLR4 causing placental haemorrhages, hypoxia or fetal loss via production of TNF and TNFR [86]. Especially TNF exhibits detrimental effects on the placenta. Its cytotoxicity through TNFR1 activates caspase apoptosis pathways and TNF blocking during LPS response at late gestation prevents fetal loss [87]. Vice versa, recombinant TNF alone was sufficient to induce fetal and placental cell deaths [88, 89].

In essence, infection or inflammation-induced blunted maternal T_{Reg} suppression and consequently increased T_H1 cytokine flow into the placenta fracture fetal tolerance with ensuing immune mediated pregnancy complications [76] and it is plausible that this may cause a higher susceptibility to IBD in postnatal life.

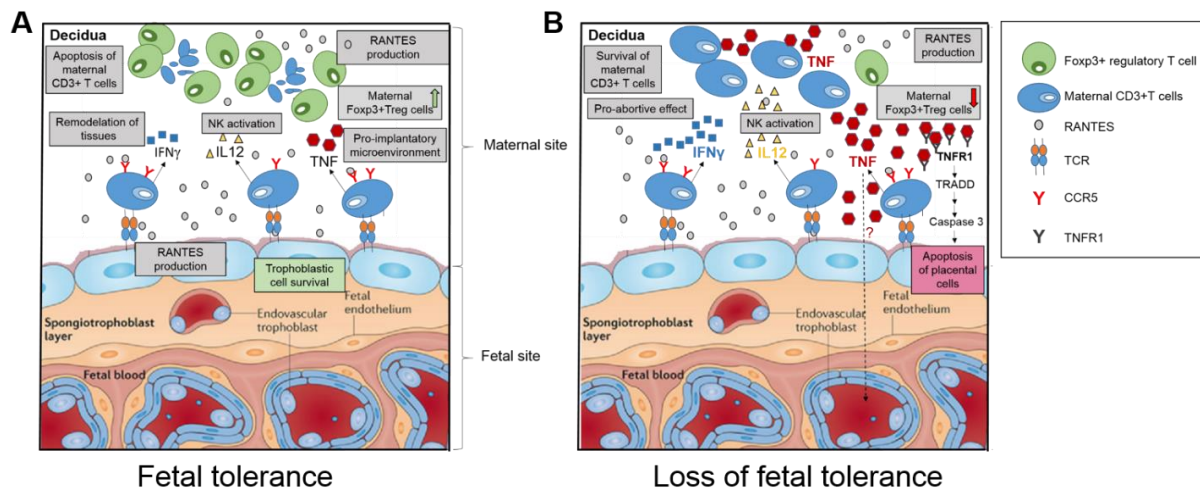


Figure 1 Immunoregulatory effects in the feto-maternal cross talk under physiological and inflammatory conditions adopted from [90]. (Left, physiological conditions) A mild proinflammatory environment causes fetal tolerance. Trophoblast cells constitutively secrete RANTES, and its production appeared to increase after the maternal-PBMCs trophoblast dialogue, accompanied by pro-inflammatory cytokines such as TNF-alpha, a low dose of IFN-gamma and IL-12 (necessary for uterine vascular modification), nitrite production (related to uterine quiescence and angiogenesis); characterizing a pro-implantatory microenvironment. This mild inflammatory context is a hallmark of normal implantation and could be later auto-controlled by RANTES through the modulation of the *Teffector/T_{Reg}* lymphocyte balance: First of all, an increase in RANTES results in the elevated apoptosis of potentially deleterious CD3+ lymphocytes. Second, RANTES has the ability to modulate the frequency of *T_{Reg}* cells during the maternal PBMCs-trophoblast cell dialogue, as evidenced by an increase in the frequency of CD4+CD25+Fcγ3+. Interestingly, the trophoblast-cell-line did not express CCR5, making these cells potentially resistant to apoptosis induced by RANTES and reflecting a potential mechanism whereby RANTES could selectively induce apoptosis of alloreactive maternal lymphocytes. **(Right, inflammatory conditions)** A proinflammatory environment e. g. during maternal inflammation or maternal obesity alters the dialogue between trophoblast cells and PBMCs altering RANTES immunomodulatory effects. Accumulating proinflammatory cytokines are associated with a decrease of fetal tolerance. A high frequency of TNF and subsequent binding to TNFR1 initiates apoptosis of placental cells via TRADD and Caspase 3, thus decreasing the number of CD4+CD25+Fcγ3+ cells. High levels of IL-12 and IFNγ promote NK cell activation and proabortive effects by survival of maternal CD3+T cells. Finally, fetal tolerance is lost.

Prenatal exposure to maternal diet-induced obesity and its inflammatory consequences on the offspring

Since the discovery of leptin in 1995 [91, 92] adipose tissue has been assigned to a secretory organ with endocrine and immunological features. Most of the studies associate maternal obesity during pregnancy with adverse offspring's metabolic phenotypes such as obesity and diabetes, but whether the susceptibility to intestinal inflammation is affected in offspring born by obese mothers is hardly reported. In sheep, maternal diet-induced obesity revealed increased gene expressions of pro-inflammatory cytokines *Tnf*, *Il-1α*, *Il-1β*, *Il-6*, *Il-8*, *Mcp-1* and macrophage marker *Cd11b*, *Cd14* and *Cd68* in the fetal and offspring's large intestine [74]. Increased *Tlr2* and *Tlr4* mRNA with corresponding NF-κB and JAK signalling point to an increased innate immune response upon maternal obesity. In essence, maternal obesity drives *T_h17* differentiation from naïve T cells via TGFβ and IL-6 [93], the same mechanism as in a CD-like inflammatory phenotype.

Another possible mechanism by which maternal obesity can program the offspring's intestine lies in the potential to shift the microbiota. Many studies reveal diet as a contributor to the gut microbiome, but studies about programming effects of the gut microbiota early in life are generally lacking. It is clinically evident that maternal body mass index and weight gain during pregnancy are associated with the faecal microbiota acquisition of the infant's favouring *Bacteroides*, *Clostridium* and *Staphylococcus* abundance on the expense of *Bifidobacterium* group in early life [94]. This is in accordance with Santacruz *et al.*, who claim that alterations of maternal microbiota during pregnancy are rather due to BMI and weight gain, than due to dietary changes [95]. By contrast, a recent study showed that HFD (maternal or postnatal), but not obesity per se, structures the offspring's intestinal microbiome in the primate *Macaca fuscata* (Japanese macaque) towards dysbiosis [96]. Post weaning low-fat control diet only partially corrects dysbiosis by early exposure to a HFD, clearly indicating that maternal diet programs the intestinal microbiome. Non-pathogenic *Campylobacter* is less abundant in the juvenile gut in response to maternal HFD. This demonstrates the potential of maternal diet in shaping commensal microbiome communities and maturation of the intestinal immune system. However, besides increasing risk for gestational complications by an increased inflammatory *in utero* environment, maternal obesity as well induces metabolic programming in offspring.

Prenatal exposure to maternal diet induced obesity and metabolic consequences on the offspring

The rising prevalence of obesity especially in women of child-bearing age is a global health concern for both, mothers and offspring. Alterations of dietary stimuli can trigger developmental programming during critical periods of organogenesis and tissue development, thus programming disease (metabolic and cardiovascular disorders) later in life [97]. The considerable effect of maternal overnutrition or obesity on developmental programming is not limited to the *in utero* environment because physiological systems develop after birth. Extensive epidemiological data connect maternal obesity and nutrition during pregnancy to offspring's risk for metabolic disease. But dynamics of the complex maternal-progeny relationship make it difficult to unravel whether diet, diet-induced obesity or weight gain are causal factors for disease programming. Another drawback is the attempt to identify the critical period of time that instigates a programmed phenotype. Many studies that have been reviewed by Alfaradhi and Ozanne *et al.* [98] restrict the onset of obesity to the early life period, either pre- or postnatal or both.

The "thrifty phenotype" hypothesis is one theory of how maternal nutrition can program the offspring's health and disease. It states that the fetal environment plays a crucial role in the risk for metabolic disorders. In essence, poor fetal nutrition drives metabolic adaptations to maximize the chance of survival in conditions of on-going nutritional deprivation. As a

consequence, metabolic adaptations are beneficial in continued poor postnatal conditions, but are detrimental in an environment characterized by high-energy food [99]. Therefore, low birth weight is associated with increased risk for heart disease, glucose intolerance, type 2 diabetes and metabolic syndrome [100-102]. Regarding maternal obesity, increased maternal BMI is associated to gestational diabetes and offspring's obesity. Sibpairs discordant for maternal type 2 diabetes show a greater prevalence for type2 diabetes and a higher BMI [103]. One possible mechanism is that obese mothers transmit more 'susceptibility genes' to their offspring than normal weight mothers. Other reasons might be *in utero* overnutrition through the placenta or neonatal overnutrition through the mother's milk. Interventional studies address *in utero* programming effects by using the same mother under different *in utero* conditions. For example, weight reduction due to maternal bariatric surgery, decreases the offspring's risk for obesity. Maternal obesity and maternal diet have differential effects on fetal development during gestation [104]. One study claimed that maternal programming effects are rather due to HFD than due to diet-induced obesity [105]. In order to dissect independent contributors of diet and obesity the induction of obesity without altering the diet is required. In contrast to Howie *et al.*, only obese rat dams fed a HFD transmitted obesity risk to their offspring, but not non-obese HFD rat dams [106].

The early postnatal period is highly vulnerable for developmental programming. Rapid postnatal growth in infancy following maternal undernutrition results in adult obesity. Overnutrition during early infancy in non-human primates elevated triglyceride levels and hypertrophy of adipocytes in adulthood [107]. Placental morphological changes in response to maternal diet-induced obesity result in increased nutrient delivery to the fetus in primates, sheep and humans [108]. As a result of maternal obesity, rhesus macaques showed signs of non-alcoholic fatty liver disease (NAFLD) in the fetal stage including triglyceride accumulation persisting throughout postnatal life. Interestingly, switching rhesus macaque mothers to a control diet between subsequent pregnancies prevented features of NAFLD [109]. Dietary manipulation studies in rodents confirmed the programming effects of maternal diet-induced obesity towards obesity, insulin resistance and hypertension [110, 111]. Crossfostering experiments in rats demonstrate that postnatal overnutrition contributes to the obese phenotype accompanied by hypertension and endothelial cell dysfunction later in life [111]. Interestingly, limiting maternal obesity to the gestational period caused no effects on offspring's body weight or obesity, but increased lipid synthesis, serum insulin and leptin. However, the combination of maternal obesity during gestation and lactation plus postnatal HFD clearly shows an accelerated weight gain and percent fat mass [112, 113]. Table 1 represents an overview about maternal obesity studies that were reported in the literature.

Table 1 Previously conducted rodent studies about maternal obesity with different setting of maternal dietary exposure. A.) Exposure during gestation and lactation. B.) Maternal HFD exposure is limited to the gestational period.

Rodent studies	Maternal diet during gestation	Maternal diet during lactation	Offspring 's diet after weaning
<i>A.) Maternal dietary exposure throughout gestation and lactation:</i>			
Buckley <i>et al.</i> 2005 ^[110]	Omega-6-fatty acids	Chow	Chow
Nivoit <i>et al.</i> 2009 ^[114]	HFD/ Chow	HFD/ Chow	Chow
Samuelsson <i>et al.</i> 2008 ^[115]	HFD/ CTRLD	HFD/CTRLD	Chow
Bayol <i>et al.</i> 2007 ^[116]	Junk food diet/CTRLD	Junk food diet/CTRLD	Junk food diet/CTRLD
Bayol <i>et al.</i> 2005 ^[117]	Cafeteria diet/CTRLD	Cafeteria diet/CTRLD	Cafeteria diet/CTRLD
King <i>et al.</i> 2014 ^[118]	Cafeteria diet/CTRLD	Cafeteria diet/CTRLD	Cafeteria diet/CTRLD
Page <i>et al.</i> 2009 ^[119]	HFD/ CTRLD	HFD/CTRLD	HFD/ CTRLD
Song <i>et al.</i> 2014 ^[120]	HFD/ CTRLD	HFD/CTRLD	HFD/ CTRLD
Hawkes <i>et al.</i> 2014 ^[121]	HFD/ CTRLD	HFD/CTRLD	HFD/ CTRLD
<i>B.) Maternal dietary exposure is limited to gestational phase: Crossfostering studies</i>			
Khan <i>et al.</i> 2005 ^[111]	HFD/Chow	HFD/Chow	Chow
Gorski <i>et al.</i> 2006 ^[122]	HFD/Chow	HFD/Chow	Chow
Mitra <i>et al.</i> 2009 ^[123]	HFD/ CTRLD	HFD/ CTRLD	HFD/ CTRLD
Shankar <i>et al.</i> 2008/2010 ^[112, 113]	Obesogenic Liquid diet/ Liquid CTRLD	Chow	HFD/ Chow
Umekawa <i>et al.</i> 2014 ^[124]	HFD/ CTRLD	HFD/ CTRLD	CTRLD

In essence, the sum of programming influences from the onset of pregnancy throughout weaning determines the risk for obesity or IBD later in life. However, whether exposure at conception, *in utero* or in the postnatal period primarily contributes to developmental programming and which factors program the developing fetus is still not clarified.

Maternal microbiota transition and postnatal IBD development

In the context of early life exposure to maternal inflammation or mDIO it has to be taken into account that a shifted maternal microbiota (due to inflammation or obesity) during perinatal development can contribute to an IBD-like microbiota. It is plausible that the maternal microbiota will be transmitted to the offspring during perinatal development, thus again increasing the risk for both, IBD and obesity.

The intestinal microbiota derives from the mother and depends on the mode of delivery. After natural birth, the progeny's microbiota reflects the maternal vaginal or gut microbiota, whereas the offspring's microbiota consists of a large number of environmental bacteria after

Caesarean sections [125]. However, the microbial colonization of the neonatal intestine is not fully understood. A paradigm of prenatal development is the existence of a microbiota-free intrauterine environment. It was thought that rupture of amniotic membranes establishes the naïve neonatal microbiota, with further modulation by vaginal microbial system at birth [125-127]. Therefore, the mode of delivery (vaginal versus caesarean section) determines the presence of essential microbial communities, such as *Escherichia-Shigella* and *Bacteroidetes* and the decrease of *Clostridium difficile* abundance. Vaginally delivered infants adapt a collection of bacterial communities similar to their mother's vagina and skin microbiota. By contrast Caesarean section-delivered infants acquire different and less diverse bacterial communities with increased risk of chronic inflammatory conditions such as coeliac disease, type 1 diabetes, asthma and obesity [128-131].

Recent studies demonstrate that even uninfected placentas harbour a unique low-abundance microbiome existing in the basal plate (directly at the maternal-fetal interphase), mainly composing commensal microbiota from *Firmicutes*, *Tenericutes*, *Proteobacteria*, *Bacteroidetes* and *Fusobacteria* with a high similarity to the human oral microbiome. Variations of the placental microbiome are associated with remote prenatal infections (*Streptococcus* and *Acinetobacter* enrichment), such as urinary tract infection in the first trimester, or preterm birth (enriched taxon *Burkholderia*) and highlight on the importance to modulate the offspring's microbiome later in life.

Within the first week of life neonates represent already complex microbial communities of the phyla *Actinobacteria*, *Proteobacteria*, *Bacteroides* and much less *Firmicutes* with high fluctuation in bacterial composition until 3 years of age [125, 127, 132, 133]. Interestingly, *Firmicutes* and *Tenericutes* dominated in neonates with small birth weights (<1200g) [134]. Especially, the early neonatal microbiome is highly vulnerable to alterations through nutritional changes of the mother's milk during breastfeeding. In conclusion, maternally transmitted inflammation-driven compositional changes of the microbiota might be an important factor contributing to offspring's disease susceptibility. One example was shown in crossfostering studies of TRUC-mice. Garrett *et al.* concluded that TRUC-derived strains can elicit colitis in WT and Rag2 deficient mice, but that a maternally transmitted endogenous microbial community is required for maximal colitic inflammation [135]. Whether this is also true for other animal models of IBD has to be analysed further and is part of this work.

1.3. Prenatal gut development and lineage allocation of the epithelium

One part of this work investigated the influence of maternal inflammation and maternal obesity on the murine fetal epithelium in order to evaluate a programming effect to IBD later in life. Organogenesis of the murine intestine and subsequent establishment of the intestinal immune system may be critical phases for the postnatal IBD development.

The development of the gut occurs after gastrulation (5-7.5 dpc) [136], the phase where the germ layers (ectoderm, mesoderm and endoderm) are formed. After gastrulation, the endoderm is a simple epithelial layer underlying the mesoderm. The gut tube (endodermal tubulogenesis) derives from the endoderm and mesoderm at 8-9.5 dpc (Figure 2), building the foregut, midgut and hindgut. In this context, the duodenum derives from the foregut and midgut, whereas the jejunum and ileum derive from the midgut only. In contrast, colonic compartments are midgut and hindgut derivatives. The intestinal epithelium develops out of the endoderm, whose fate determinant is TGF β -related growth factor Nodal. Duration and concentration of exposing growth factors are determining for the specification of anterior-posterior patterning of the endoderm. SOX2 and HHEX are regional determination factors for anterior endoderm, whereas CDX2 programs for posterior endoderm. The small and large intestine derives from the posterior endoderm. The endodermal gut tube is surrounded by the visceral peritoneum (mesoderm) and connected to the body wall by the mesentery. At 9.5-13.5 dpc the gut tube lengthens and increases its circumference. At 14.5 dpc the thickened epithelium is drastically remodelled, the previously flat luminal surface converts into finger-like epithelial projections with mesenchymal cores. The endoderm undergoes an extensive folding, through formation of clusters of mesenchymal cells (from the mesoderm) below the epithelium, which extend towards the center of the lumen, this creating villi. Cell dynamic studies of the early murine intestine reported a pseudostratified epithelium between 12.5 and 14.5 dpc that is driven by microtubule-actinomyosin-dependent apicobasal elongation [137], whereas previous studies described it as stratified [138, 139]. At 15 dpc epithelial-mesenchymal crosstalk regulates the differentiation of myofibroblasts and smooth muscle cells [140-142] and proliferation becomes less abundant at 17 dpc. Wnt/ β -catenin pathways are also implicated in proliferation and stem cell maintenance and crypt development throughout the developing intestine [143] until weaning.

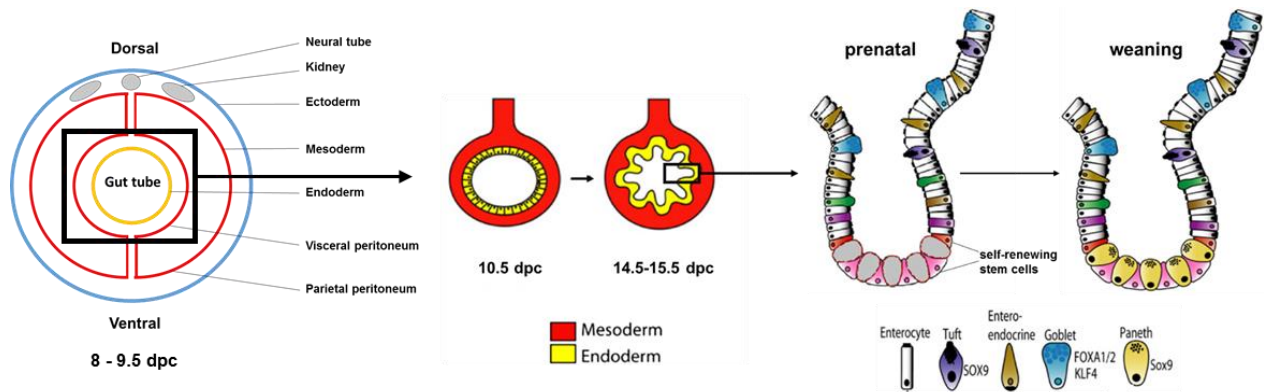


Figure 2 Early development of the intestinal epithelium adopted from [136]. (Left panel) After gastrulation endodermal tubulogenesis (8-9.5 dpc) occurs building the gut tube and the peritoneum (deriving from the mesoderm). The visceral peritoneum (mesoderm) surrounds the endoderm to enclose the gut tube and connects it to the dorsal body wall. Medial to lateral cross sections of the gut tube are shown. At 10.5 dpc the intestinal endoderm is a compact pseudostratified single layer epithelium; Villus formation initiates in a rostral to caudal wave at approximately 14.5 dpc, as clusters of mesenchymal cells form below the epithelium and extend toward the center of the lumen, creating villi. **(Right panel)** The cartoon depicts the crypt structure with individual cell types. Cells migrate out of the crypt and onto the villus as they terminally differentiate, except Paneth cells which develop during early postnatal development residing intercalated among the stem cells at the crypt base.

The initial sign of IEC differentiation (enterocytes, goblet cells and enteroendocrine cells) can be observed at the same time as villi emerge, whereas Paneth cells arise with crypt formation around weaning (Figure 1). Notch pathways are crucial to commit IEC lineages and regulates the choice of absorptive versus secretory lineages. This works by reciprocal regulation between *Hes1* and *Atoh1* which is dependent on Notch activity. Notch induces stem cell-derived *Hes1* and thereby programs cells to become enterocytes via inhibition of *Atoh1* [144]. *Hes1* deficient mice display fewer enterocytes and *Atoh1* overexpression, directing progenitors towards the secretory cell lineage [145]. Interestingly, Notch activity is not required for absorptive cell differentiation as its absence programs “default” progenitors towards enterocytes [146, 147].

1.4. Perinatal development of immune homeostasis as a consequence of the microbial burden

Birth is the event that converts a sterile fetal environment into an environment that is highly enriched in microbes, dietary components and other exogenous stimuli. Especially the microbiota initiates the maturation and education of the mucosal immune system [23]. An insufficiently matured immune system due to perinatal defects cannot cope with potential pathogens, thus increasing disease susceptibility later in life (e. g. rheumatoid arthritis, type I diabetes, chronic inflammation of the gut) [148, 149]. Mucosal surfaces have important barrier functions and play a crucial role in immunologic tolerance. Both, developmental and environmental signals (such as commensals) are of eminent importance in the perinatal establishment of the immune system, which in turn maintains mucosal tissue homeostasis and

induces immune tolerance later in life. In this context, Figure 2 represents an overview of how commensals can activate the maturation of the neonatal immune system.

The murine prenatal intestine is sterile and characterized by absent epithelial cell proliferation and high expression of cathelicidin-related antimicrobial peptides (CRAMP or LL37 in humans) [73]. Low levels of IgA-producing plasma cells and decreasing expression of Toll-Like receptor 4 (TLR4) induce adaptive and innate immune tolerance prior to birth. Secondary lymphoid structures (Peyer's patches and mesenteric lymph nodes) and specialized epithelial cells (M cells) are generated before birth, but their maturation occurs after birth. The production of T_{Reg} cells is already initiated in the prenatal period. CD4⁺CD25⁺ T_{Reg} cells are highly abundant in human fetal tissue (e. g. MLN) and control T cell responses *in utero* and in the neonatal period [150].

At birth, microbial colonization by commensals stimulates the maturation of innate and adaptive immune mechanisms (Figure 3). Unlike human new-borns, who already possess a mature villus-crypt structure in the small intestine, murine neonates reach this stage not until postnatal day 10-12 [151]. In the neonatal intestinal mucosa lymphocytes differentiate (e. g. T_{Reg} cells, intraepithelial lymphocytes), cryptopatches and isolated lymphoid follicles are formed. Cryptopatches are clusters of KIT⁺IL-7R⁺THY1⁺ T cell progenitors in the murine intestinal lamina propria. Isolated lymphoid follicles are small aggregates in the lamina propria of small and large intestines that contain B cells, T cells, dendritic cells and stroma cells. Both, cryptopatches and isolated lymphoid follicles are absent in germ-free mice indicating the role of bacterial colonization in their development [152, 153].

Around weaning, intestinal crypt formation starts and initiates increased proliferation, epithelial cell renewal and Paneth cells generation. Bacteria are the strongest immunostimulants in the postnatal environment and can activate an immune response via pattern recognition receptors (PRR), such as TLRs. In essence, alterations of the antimicrobial peptide repertoire during the perinatal period are associated with compositional changes of the microbiota [154, 155]. Rodent studies show that innate recognition of bacteria or bacterial components triggers epithelial expression of secreted C-type lectins *Reg3g* and *Reg3b* [38, 156]. To prevent an overshooting immune response of an immature immune system, minimized TLR4 expression and steadily increased NF- κ B inhibitor induce tolerance to bacterial lipopolysaccharides and other pro-inflammatory stimuli [73].

After weaning and in concert with bacterial colonization, immune cells home the intestinal mucosa and induce spatially reorganized adaptive and innate immune mechanisms in order to adapt adequately to the postnatal environmental triggers. M cells reside above innate lymphoid follicles and Peyer's patches in order to facilitate antigen transport to lymphoid cells.

Innate cells (e. g. innate lymphoid cells (ILC), innate lymphoid tissue inducer (LTi) cells, natural killer cells (NK), T cells, intraepithelial lymphocytes), CD103+ dendritic cells (DC) CX3CR1+ macrophages, and forkhead box protein 3 (FOXP3)⁺ regulatory T (T_{Reg}) cells home the mucosa. For example, innate lymphoid cells (e. g. RORγt⁺ILC=ILC3) translate microbial signals into immunomodulatory signals of the intestine. Upon macrophage stimulation IL-1β is released and engages IL-1 receptor on ILC3, thus producing colony-stimulating factor2 (CSF2). CSF2 then primes DC- and macrophage-production of T_{Reg} cell-stimulants, such as retinoic acid and IL-10, which in turn induce and expand T_{Reg} cells from naïve T cells [157]. Murine neonatal CD4⁺ T cells preferentially differentiate into FOXP3⁺ T_{Reg} cells, thus attenuating an overshooting immune response upon stimulation [158]. Therefore, T_{Reg} cells play an important role in the immunosuppression and control of T_{helper} (T_h) cells. Their expressions and migrations out of secondary lymphoid structures are sensed by signals (e. g. commensal antigens) that derived from dendritic cells and macrophages. For example, *Bifidobacterium infantis* markedly induces FOXP3⁺ T_{Reg} cells in mice [159] and protects against NF-κB activation. *Clostridium* clusters *IV* and *XIVa* are suspected to take over the promoting role of *B. infantis* on colonic induction of FOXP3⁺T_{Reg} cells [160]. *Clostridium* enhances TGFβ and other T_{Reg} cell -inducing molecules independent of TLR2 or NOD receptor signalling. Another example of inducing T_{Reg} responses is shown with the microbial immunomodulatory molecule polysaccharide A (PSA) that derives from the commensal *Bacteroides fragilis*. PSA stimulation of FOXP3⁺ T_{Reg} cells via TLR2 initiates the secretion of anti-inflammatory cytokines (e. g. IL-10) and reduces IL-17 production. In contrast, it was shown that pro-inflammatory T_h17 cells are induced by mucosa-attached segmented filamentous bacteria (SFB) and whether equivalents are existent in the human gut is not known [161, 162].

Intestinal immune modulation can also occur via humoral immunity. Similarly to T_{Reg} cell induction, the establishment of humoral immunity is dependent on environmental factors. For example, retinoic acid causes adequate differentiation of IgA⁺ plasma cells and secretory IgA (SIgA) inhibits overshooting immune activation by microbes and luminal antigens [163]. In essence, SIgA reinforces the intestinal epithelium, as SIgA-coated commensals are restricted in colonizing epithelial surfaces, which decreases the chance of antigen penetration through the epithelial barrier. This in turn decreases the risk of hypersensitivity reactions and infections. In the prenatal gut the epithelial barrier is reinforced by maternal SIgA. This function becomes more relevant during breast-feeding [164]. Murine studies of colonizing germ-free mice with commensals revealed a transient IgA production that seems to be necessary to allow penetration of microbial components into the gut-associated-lymphoid tissue (GALT) [165, 166]. Therefore, it is very likely that the intestinal SIgA response continuously adapts to microbial alterations.

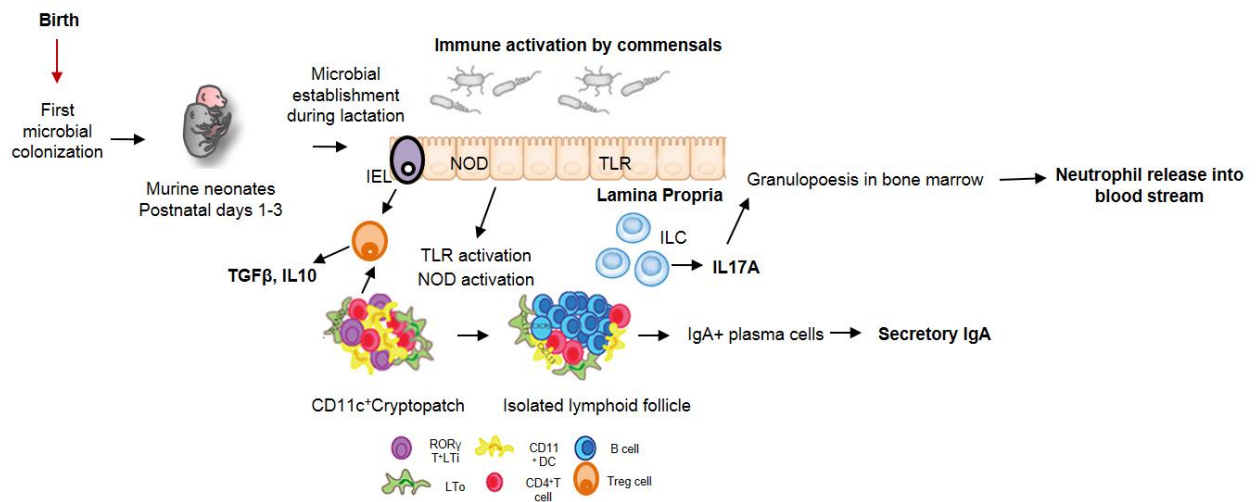


Figure 3 Neonatal development of the intestinal immune system. After birth, commensals of the environment e.g. through mother's milk reside the neonatal gut preparing an immunological barrier against future pathogens. Besides innate immune mechanisms via NOD and TLR activation (such as REG3β and γ production) adaptive immune responses are initiated by commensal structures, i.e. secretory IgA produced by plasma cells, which derive from B-cells of isolated lymphoid follicles located in the subepithelial compartments. Further, innate lymphoid cells (ILC) secrete IL-17, which drives granulopoiesis in the bone marrow, finally releasing neutrophils into the blood stream. On the other hand, an anti-inflammatory tone is generated by TGFβ and IL-10 secretion upon stimulation of intraepithelial lymphocytes (IEL) by commensals, preventing an overshooting inflammatory response to commensals.

Clinical features of IBD are tightly linked to dysfunctions in the intestinal barrier and therefore present its emerging importance in intestinal homeostasis. The first homeostatic mechanisms (innate immunity) will be generated during in utero development that is highly dependent on maternal stimuli. Therefore, this period is critical in the establishment of a well working intestinal homeostasis later in life.

1.5. The postnatal intestinal epithelium as first line of defence

The intestinal barrier selectively separates the luminal environment (containing pathogens, toxins, diet and digestive enzymes) from the host and is therefore the first line of defence. It comprises three different compartments, the mucus layer, which is an extrinsic layer that also contains secretory IgA, the intestinal epithelium and the underlying gut-associated-lymphoid tissue (GALT).

Particularly, the intestinal epithelium plays a crucial role in frontline defence, by harbouring specialized mechanisms to fulfil multiple functions, such as innate immune modulation, antimicrobial defence and mucus production. The intestinal epithelium is the largest mucosal surface of the body (~400 m² surface area) consisting of absorptive (enterocytes) and secretory (goblet cells, Paneth cells, enteroendocrine cells). Intestinal epithelial cells (IEC) undergo a continuous cell renewal by pluripotent stem cells at the crypt bottom. Enterocytes maintain the host's energy homeostasis, although they are in part capable to secrete small amounts of antimicrobial peptides (AMPs such as regenerating-islet derived 3b and g) and

support the defensive functions of highly specialized secretory IEC. Microfold cells (M cells) actively transport luminal antigens and intact microorganisms and mediate their presentation to the underlying immune system, such as dendritic cells or intestinal lymphoid structures (Peyer's patches and isolated lymphoid follicles) [167]. Enteroendocrine cells secrete hormone regulators of digestive functions and link the enteric neuroendrine system to the central one.

Paneth cells are uniquely specialized to produce and lumenally secrete many AMPs (defensins, cathelicidins, C-type lectins and lysozyme). For example, pore-forming defensins and cathelicidins disrupt surface membranes of bacteria and C-type lectins target peptidoglycans in Gram⁺ (REG3g) and Gram⁻ bacteria (REG3b) [168-170] enabling a broad regulation of commensals and pathogens. REG3 production is regulated by IEC-intrinsic recognition of commensal microbial signals. Regionally varying AMP production along the intestine may mirror anatomically restricted host-commensal interactions and their influence on IEC responses. For instance, Reg3g was recently described as a small intestinal factor that segregates microbes from the epithelial surface [171].

A similar function has been described for goblet cell-derived MUC2 in the colon. Goblet cells build a mechanical and biochemical barrier to avoid microbial contact with the epithelium and underlying immune cells. They are secretory IEC and produce different kinds of mucins (MUC2 most abundant mucin [172]) forming the mucus layer a defence line against bacteria. The fact that MUC2-deficient mice exhibit spontaneous colitis and have a predisposition to inflammation-induced colorectal cancer underlines the importance of the mucus layer in intestinal homeostasis [173, 174]. Furthermore, goblet cell-derived products, such as trefoil factor 3 (TFF3) and resistin-like molecule- β (RELM β) are also involved in mucus barrier functions. TFF3 crosslinks mucins and signals epithelial repair, epithelial migration and resistance to apoptosis [175, 176]. RELM β supports mucin secretion and regulates adaptive immune mechanisms during inflammation [169, 170].

However, combined functions of secretory IEC (e. g. Paneth cells and goblet cells; REG3 and MUC2 interactions) lead to even higher antimicrobial activity [177], thus limiting the quantity and diversity of bacteria at the epithelial surface. These diverging functions of the epithelium protect the host from infections and inflammatory stimuli. Therefore, genetic defects in autophagy and unfolded protein responses (UPR) impair Paneth cell and goblet cell functions, thus increasing the disease susceptibility (possible mechanisms in IBD). Side effects of autophagy are the support of packaging and exocytosis of Paneth cell granules [178]. Paneth cells engage autophagy and UPR, thereby massively contributing to intestinal homeostasis in mice and their combined absence results in spontaneous disease resembling human Crohn's disease [179]. This together with genetic evidence for autophagy and UPR involvement in IBD

provides an important link to impaired Paneth cell functions and the establishment of intestinal inflammation [180-182].

Important sentinels of IEC are pattern recognition receptors (PRR). They function as frontline sensors for microbial encounters and integrate bacteria-derived signals into antimicrobial and immunomodulatory responses. Toll-like receptor (TLR), NOD (nucleotide-binding oligomerization domain) -like receptor (NLR) and RIG-I-like receptor (RLR) families provide distinct pathways for bacterial recognition [183-186].

TLRs are located at the cell surface or at intracellular membranes and sense highly conserved structures from bacteria, viruses and fungi. IEC intrinsic-TLR signalling is dichotomic. TLRs support intestinal homeostasis via signalling through MyD88/ NF- κ B signalling that includes the expression of cytoprotective heat-shock proteins, epidermal growth factor receptor ligands and TFF3 and the mitogen-activated protein kinase (MAPK) pathway [187, 188]. IEC-specific deletion of elements downstream of TLR, including inhibitor of NF- κ B (I κ B) kinase (IKK) complex or NF- κ B essential modulator (NEMO) lead to enhanced DSS-induced or spontaneous colitis, indicating an important role for TLRs [189, 190].

NOD-like receptors are of cytosolic location and reorganize foreign structures (such as muramyl dipeptide) associated with pathogenesis. NOD2 was the first identified susceptibility gene locus for CD. NOD1 and NOD2 signal via receptor-interacting protein 2 (RIP2) and activates NF- κ B and MAPKs, whereas other NLRs (NOD-, LRR and pyrin-domain-containing 3 (NLRP3, NLRP6 and NOD-LRR- and CARD-containing 4 (NLRC4) form inflammasome complexes with pro-caspase 1 in order to cleave and activate IL-1 β , and IL-18. Polarized expression of PRRs in IEC (apical versus basolateral) may enable the discrimination between commensal and pathogenic signals. For example, TLR9 promotes the inhibition of NF- κ B signalling, whereas basolateral TLR expression activates NF- κ B signalling [191]. The complexity of microbial recognition receptors by IEC is of eminent importance to balance intestinal homeostasis and to switch, whenever needed, to inflammatory responses.

The adherens junctions (AJ) and tight junctions (TJ) are important key players in adhesive contacts between adjacent IEC to create a tight physical barrier between the harmful luminal structures and the host. AJ comprise the core transmembrane protein E-cadherin (CDH-1) and intracellular components like p120-catenin, α -catenin and β -catenin. They fulfil multiple functions such as initiation and stabilisation of cell-cell adhesion, regulation of the actin cytoskeleton, intracellular signalling and transcriptional regulation [192, 193]. Numerous human and mouse studies confirmed that dysfunctions in AJ or TJ are associated with IBD [194, 195]. TJ protein occludin is decreased in IBD patients, whereas claudin-2 expression is enhanced [196, 197]. Furthermore, in chronic active UC a downregulation of occludin was

associated to enhanced transepithelial migration of neutrophils into epithelium and intestinal lumen leading to crypt abscesses [198]. *CDH1* gene polymorphisms that results in a decreased E-Cadherin protein expression and mislocates TJ proteins is associated with CD [199]. Vice versa, an inflammatory milieu of the intestine causes also dysfunctions of AJ and TJ proteins [200]. For instance, TNF antagonizes epithelial barrier repair in active CD patients [201] and reduces E-cadherin expression *in vitro* [202]. The transcriptional inhibition of TJ by proinflammatory cytokines (e. g. TNF and IFN γ) and their influence on cellular redistribution works probably via myosin light chain kinase (MLCK)-dependent contraction of actin filaments [203, 204].

1.6. Immunologic features of innate and adaptive immunity in the postnatal gut during IBD

Microbial changes (e. g. microbial infection) and gene-polymorphisms (e. g. *NOD2*, *ATG16L1*) affecting the epithelial barrier (e. g. Mucin degradation) abrogate the tolerogenic milieu of the intestinal mucosa involving innate and adaptive immune responses. Disturbances of innate immune mechanisms comprise increased expression of the pattern recognition receptors TLR2 and TLR4 causing exaggerated LPS responses and abrogated abilities of dendritic cells to sense the production of tolerogenic T_{Reg} cell [205]. Cytosolic Nod-like receptors (NOD1 and NOD2) possess caspase recruitment domains and are therefore able to induce autophagy [206-209]. CD-associated NOD2-polymorphisms show reduced inflammatory cytokine responses towards NOD-ligand muramyl dipeptide, insufficient autophagy which then fails to appropriately induce adaptive T cell responses and reduced transcriptional expression of anti-inflammatory cytokine IL-10.

A hallmark for disturbed adaptive immunity in IBD is the loss of immune tolerance due to the imbalance of effector T cells versus T_{Reg} cells and inducible T_{Reg} (iT_{Reg}) cells. Interestingly, two main opposing phenotypes, T_h17 and T_{Reg}, are inversely controlled by transcription factors ROR γ T/FOXP3 [210]. In detail, the imbalance of T_h cells versus T_{Reg} cells is due to a general switch from anti-inflammatory properties to pro-inflammatory ones. Different immune cells such as, CD103⁺ DCs, IL-22-producing CD4⁺ T cells and ROR γ t⁺NKp46⁺ lymphocytes act in concert to produce pro-inflammatory cytokines (IL-6, IL-12, IL-23). Together with CX3CR1⁺ macrophage-derived IL-6 and IL-1 they induce the cytokine production of T_h1 (IFN γ , TNF, IL-2) and T_h17 cells (IL-17), which are important mediators of inflammation in IBD [211-214]. Consequently, neutrophils and IgG-producing plasma cells cause tissue destruction and organ dysfunction. Additional routes of clinical development in IBD are high levels of T_h1-associated transcription factors STAT4 and T-bet that were observed in CD lesions and experimental colitis [215, 216]. T_h17-involvement in IBD pathogenesis was also concluded by GWAS of *IL23*-

R gene (a surface marker for T_h17 cells) and genes involved in T_h17-differentiation (*IL-12B*, *JAK2*, *STAT3*, *CCR6* and *TNFSF15*). They were associated with the susceptibility to CD and partly UC [217, 218]. However, TNF- and IL-23-producing CD14⁺ macrophages contribute also to CD development, but more via IFN γ than IL-17 production [219].

In essence, in IBD, the interplay between disturbed innate and adaptive immunity towards pro-inflammatory pathways causes a rapid recruitment of leukocytes and diminishes their retention from effector sites of the intestinal mucosa.

1.7. Mouse models resembling human IBD

As the clinical appearance of IBD is extremely complex and heterogeneous it is challenging to assess the full scope of use of IBD animal models which address scientific questions. Dozens of animal models have been established. Since the maintenance of mucosal immune homeostasis prevents uncontrolled inflammation in the gut, the epithelial interface is the primary target to study IBD pathogenesis. This is supported by emerging evidence showing that defects of epithelial integrity comprise defects in innate immune responses, epithelial paracellular permeability, epithelial cell integrity, as well as in the production of mucus [220]. Well-established mouse models that are commonly utilized are chemically-induced or genetic models of intestinal inflammation (Table 2). While acute chemical-induced colitis models incorporate features of innate biology (epithelial barrier function and immune function), the chronic and progressive models typically illustrate a complex interplay between innate and adaptive immunities [221].

Table 2 Commonly used mouse models of IBD (adapted from [220, 221]).

Model	Background strain	Location	Nature of insult	Nature of response	Kinetics	Immune cells involved
DSS	Multiple C57BL/6 BALB/c	Colon	Chemical	Epithelial damage	Acute	Neutrophils, myeloid
TNBS	Multiple SJL BALB/c	Colon	Chemical	Epithelial damage	Acute	
CD45RBhi	BALB/c C57BL/6	Colon	Immune deficiency	Inflammatory	Chronic	
Piroxicam/ IL-10 KO	129sv C57BL/6	Colon	NSAID+ immune deficiency	Inflammatory	Chronic	Macrophages, CD8 T cells
<i>Tnf</i> ^{ΔARE/+}	C57BL/6	Ileum	TNF overexpression	Inflammatory	Chronic	Macrophages, neutrophils, CD8 T cells,
SAMP1/Yit Fc	SAMP1	Ileum	Immune activation	Inflammatory	Chronic	Macrophages, neutrophils, lymphocytes

In this work the effect of maternal inflammation and maternal obesity on the postnatal development of intestinal inflammation was investigated by using two different mouse models, the *Tnf^{fARE/+}* mouse (CD-like ileitis) and the DSS colitis model.

1.7.1. *Tnf^{fARE/+}* mouse model resembling CD-like ileitis

Although anti-TNF treatment is a successful therapeutic target in CD pathology, TNF-specific molecular and cellular mode of pathogenic action is not fully understood. The deletion mutation in the octanucleotide adenosine uracil-rich element (ARE) of the *Tnf* gene stabilizes *Tnf* mRNA and subsequent elevation of TNF protein. The clinical manifestation in this mouse model is very similar to CD that is characterized by transmural lesions and granulomatosis. *Tnf^{fARE/+}* mice exhibit an age-dependent chronic ileitis and polyarthritis [222]. Onset of chronic ileitis is at 4 weeks of age and of colitis between 12 and 16 weeks of age [60]. Disease progression is characterized by splenomegaly and significant increases of secondary lymphoid structures such as mesenteric lymph nodes (MLN). Histopathology is highly dependent on dietary factors and hygiene stages and requires bacterial stimulation [60, 223, 224]. Backcrossing of *Tnf^{fARE/+}* mice with recombina-ase activating gene (RAG)-1 deficient mice abrogated ileitis, but not polyarthritis. This points to two different disease mechanisms, strong involvement of adaptive immune mechanisms (T and B cells) is relevant in ileitis, but not in polyarthritis. In detail, loss of CD8aa⁺ and enhanced CD8ab⁺ in intraepithelial lymphocytes (IEL) are responsible for chronic ileitis [222, 225, 226]. This is also demonstrated by the fact that an abrogation of CD4⁺ T cell responses led to accelerated disease, whereas MHC-I/CD8⁺ exclusion delayed the disease onset. Overall chronic ileitis in the *Tnf^{fARE/+}* mouse model is a T_h1/ T_h17-mediated inflammation.

1.7.2. Dextrane sulfate sodium (DSS)-induced colitis model

DSS administration in drinking water induces a reproducible acute epithelial damage resembling UC-like colitis in mice with clinical signs of bloody diarrhea, weight loss, ulcerations and infiltrating granulocytes [227-229]. It is believed that DSS is toxic to IEC, increases intestinal permeability and activates macrophages, thus leading to neutrophil infiltration. DSS treatment over several days (e. g. 7 days) triggers an acute inflammation, whereas several cycles of DSS exposure (e. g. 7 days followed by 14 days water) result in a more chronic phenotype with weight loss and increasing numbers of infiltrated neutrophils. DSS treatment of T cell- and B cell-deficient *Rag1^{-/-}* mice showed no abrogation of colitis, demonstrating that the adaptive immune response is not a major target of DSS. In contrast, innate immune mechanisms are involved in the mode of DSS action as *Tlr4^{-/-}* and *Myd88^{-/-}* mice showed reduced susceptibility to DSS [230]. Fukata *et al.* showed that TLR4 and MyD88 are required for neutrophil recruitment into inflamed tissue regions. In addition, DSS treatment is used as supportive tool to study the potential role of genes which may be involved in IBD pathogenesis,

but do not spontaneously trigger intestinal inflammation. For example, transgenic mice overexpressing growth hormone exhibit enhanced survival and mucosal repair upon DSS-induced colitis [231]. Further, inflammation-driven colorectal cancer, which was observed in UC patients [232, 233], could be mimicked by a chronic DSS model with one initial dose of the genotoxic carcinogen azoxymethan (AOM) [234] and therefore plays an essential role to study IBD-related colorectal cancer besides the pathogenesis of IBD.

To bring all the aspects of this introduction together the primary objective of this work was to investigate whether *in utero* exposure to maternal inflammation and maternal diet-induced obesity influence the fetal epithelial transcriptome of the gut. As a secondary objective it was investigated whether *in utero* exposure to maternal inflammation or maternal obesity has a consequence on the outcome of postnatal intestinal inflammation. In this context it a further objective was to analyse whether a maternal inflammatory microbiome can shift the offspring's microbiota towards a more disease-supporting microbiota with the consequence of intestinal inflammation.

2. Material and Methods

2.1. Ethics statement for animal studies

Mouse experiments were performed in accordance to the German guidelines for animal care permitted by the Regierung von Oberbayern (Bavaria, Germany, proposal numbers 55. 2-1-54-253-163-10 and 55. 2. 1. 54-2532-43-12). Mice (C57BL/6N genetic background) were housed either under conventional or under specific pathogen-free conditions in groups of 3-5 mice per cage at a 12h light/dark cycle at 24-26°C. They received fresh tap water (autoclaved water for SPF-mice) and diet (Ssniff Chow and customized Ssniff experimental diet and Ssniff HFD (see table S1 Appendix) *ad libitum* and were sacrificed with CO₂.

2.2. Breeding pairs for maternal inflammation studies

For maternal inflammation studies conventionally raised $Tnf^{\Delta ARE/+}$ (ARE) dams were bred at the age of 8 weeks with age-matched $Tnf^{+/+}$ wildtype (WT) sires and vice versa (n=10-20 breeding pairs), generating offspring from healthy WT dams (WT and ARE) and inflamed ARE dams (iWT and iARE) (n=6-16 each). Average age of dams at weaning stage (3 weeks after delivery) was 16 ± 2 weeks for WT dams and 14 ± 1 weeks for ARE dams. Figure 4 represents an overview of the different offspring groups.

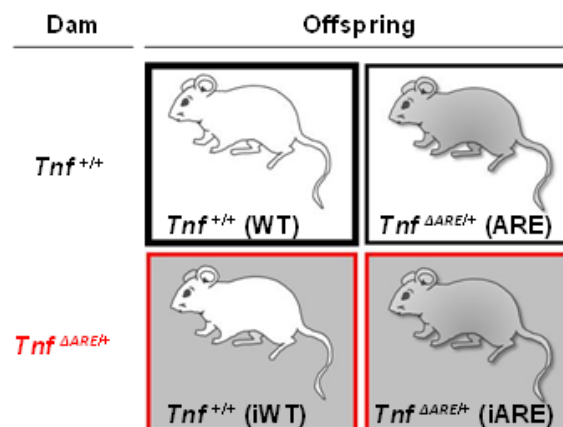


Figure 4 Offspring groups in maternal inflammation studies.

2.3. Breeding pairs for maternal obesity studies

For maternal obesity studies WT dams were fed an experimental control or high-fat diet (HFD) from the age of 4 weeks on (see Table S1, Appendix). At 12 weeks of age dams were bred with ARE sires (n=12-17 breeding pairs), generating WT and ARE offspring from lean (WT and ARE) and obese (oWT and oARE) dams (Figure 5). At the date of delivery, control diet fed dams received HFD (indicated as control diet→HFD dams) during breast-feeding period in order to synchronize fatty acid profiles during breast feeding. All dams were sacrificed either at 17.5 days post conception (dpc) or at weaning time point (3 weeks after giving birth).

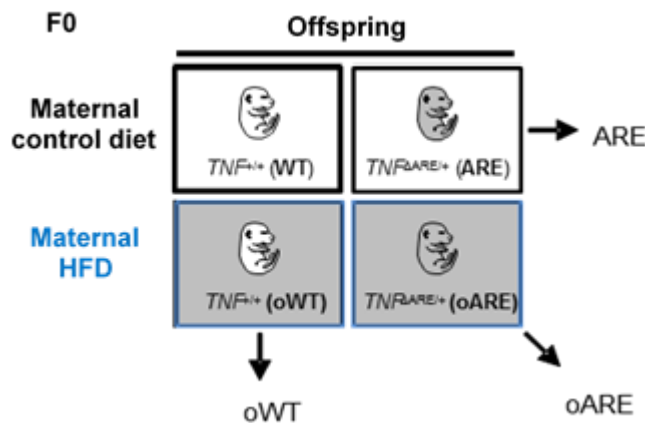


Figure 5 Offspring groups in maternal obesity studies

2.4. Prenatal studies

2.4.1. Breeding for prenatal sampling

For maternal obesity studies breeding was performed once a week (overnight) in order to determine dam's gestational age and fetal developmental stage. Breeding pairs were separated again for one week. Dams that were not pregnant after 2 nights of breeding were excluded from the study. Fetuses derived from lean WT dams (WT and ARE) or obese WT dams (oWT and oARE) (n= 5 each).

2.4.2. Fetal gut sampling at 17.5 dpc

17.5 dpc fetuses were dissected by Caesarean sectioning. Morphological criteria of fetuses were evaluated according to Theiler stage 25 (TS25) based on the onset of skin wrinkling, whiskers and eyelid closure. Fetus weight and size were measured prior to decapitation. The fetal gut was isolated by opening the abdomen and subsequent fixation of the stomach with forceps. The gut was dissected very carefully by cutting the mesentery in order to disconnect the intestine from the dorsal abdominal wall. The dissected gut was transferred into a petri dish with 1x PBS and the whole mesentery was removed in order to straighten the gut. Caecum

and colon were separated from the small intestine. The distal third of the small intestine was defined as ileum. Fetal ileum and colon were embedded longitudinally with a proximal versus distal orientation in Optimal Cutting Temperature (O.C.T.; Sakura Finetek, Torrance, USA) and stored at -80°C until use, respectively.

2.5. Postnatal studies

All offspring were generated from both, maternal inflammation and maternal obesity breeding pairs.

2.5.1. Development of genetically driven CD-like ileitis under maternal inflammation or obesity under conventional housing

WT and ARE offspring were weaned 21 days after birth and received Ssniff Chow diet until 4 weeks of age. Henceforward, diets were changed to experimental diet and/or HFD until sacrifice (8 or 12 weeks of age) (Figure 6). Body weight development was monitored on a weekly basis. Fasting blood glucose was measured in all offspring deriving from maternal obesity breeding pairs [60]. All Offspring were sacrificed by CO₂ inhalation. Portal vein and abdominal aorta blood were withdrawn posthumously and centrifuged (3000g, 10min, 4°C) to obtain plasma. Gut sections (distal ileum and proximal colon) were fixed in 10% formaldehyde for 24h. Mesenteric and perigonadal fat pads were fixed in 4% formaldehyde for 24h. Mesenteric lymph nodes and spleen halves were stowed in ice cold RPMI (10% FCS, 1 % AA) until subsequent flow cytometry.

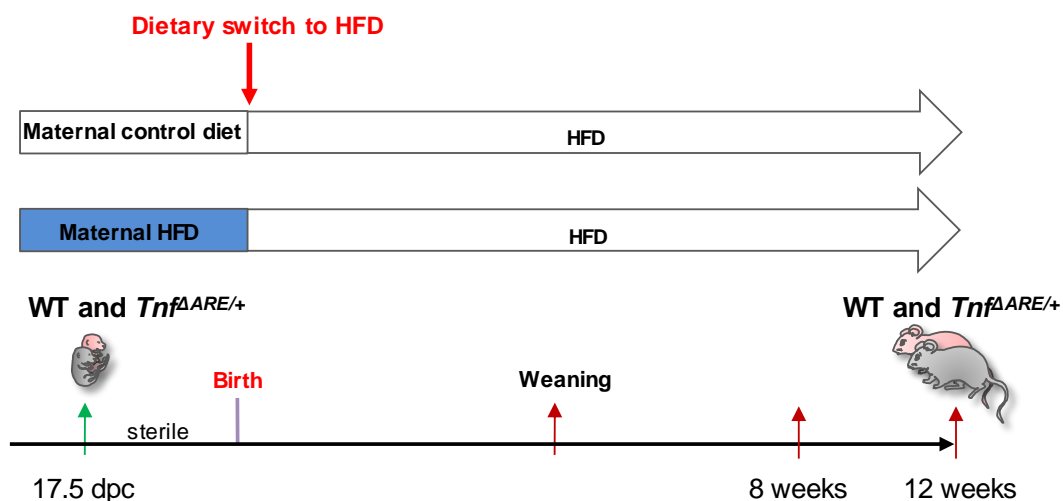


Figure 6 Regimen of maternal and offspring's dietary exposure.

2.5.1.1. Development of genetically driven CD-like ileitis under maternal inflammation under specific-pathogen-free conditions

WT and ARE offspring were weaned 21 days after birth and received Chow diet (Ssniff) until 4 weeks of age. ARE mice were randomly fed either a Chow diet or experimental control diet until date of culling (12 weeks). WT mice were fed a Chow diet throughout postweaning life. All offspring were sacrificed by CO₂ inhalation. Portal vein and abdominal aorta blood were withdrawn posthumously and centrifuged (3,000g, 10min, 4°C) to obtain plasma. Gut sections (distal ileum and proximal colon) were fixed in 10% formaldehyde for 24h. Mesenteric lymph nodes and spleen halves were stored in ice cold RPMI (10% FCS, 1 % Antibiotics/Antimycotics) until subsequent flow cytometry.

2.5.2. DSS colitis susceptibility studies

WT offspring (n=6, no littermates within one group) were generated and fed a Ssniff Chow diet throughout post weaning life. At 12 weeks of age offspring were exposed to 1% DSS (w/v) (MW 36,000-50,000, MP Biomedicals, LLC France) for 7 days in their drinking water, followed by 8 days drinking water without DSS as recovery phase. Control animals received only drinking water throughout the whole experiment. During that time mice were housed in single cages in order to monitor stool consistency, occurrence of rectal bleeding and body weight daily. Disease activity index was assessed as mean score of body weight loss, stool consistency and rectal bleeding. After recovery, mice were sacrificed by anaesthesia and final exsanguination.

In order to classify the severity of DSS colitis we evaluated the mean of 3 clinical signs: stool consistency (scores: 0=normal, 2=loose and 4=diarrhea), rectal bleeding (scores: 0=negative, 2=gross bleeding, 3=bleeding>1d, 4=bleeding>2d) and weight loss, indicated as weight change in % on basis of initial body weight at day 0 (scores: 0=none, 1=1-5%, 2=6-10%, 3=11-15%, 4>15%). The daily calculated mean of these scores expresses the disease activity index (DAI adapted by Cooper *et. al.* [235]).

2.6. Histology

2.6.1. Histopathological scoring of the distal ileum and proximal colon

Transversal sections (5µm thickness) were cut (Microtom, Leica) from 10% formaldehyde-fixed paraffin-embedded distal ileum and proximal colon. The histological score was ascertained in a blinded fashion on H&E-stained sections of the distal ileum (WT, iWT, ARE, iARE or WT, oWT, ARE, oARE), resulting in a score from 0 (non-inflamed) to 12 (highly inflamed) as previously described [236].

2.6.2. Mesenteric adipocyte sizes

Five μm sections were cut from paraffin-embedded mesenteric fat tissue of WT and ARE offspring. H&E-stained sections were analysed using a light microscope (Leica) at 200x magnification. Adipocyte size measurements were performed using Axion Software (Leica). Individual adipocyte sizes were calculated as means out of 25 measured cells per ROI (region of interest). In total 3 ROIs per mouse were evaluated.

2.6.3. Immunofluorescence analysis on paraffin-embedded and frozen sections of the distal ileum

After deparaffinization of tissue sections (Leica ST5020 Multistainer system), antigen demasking was performed by boiling in 1x sodium citrate buffer (pH 6, 900W, 23min) or by Proteinase K digestion (10 $\mu\text{g}/\text{ml}$ at 37°C for 14min and cool down for 10min followed by 2 times 2min washing with 1x PBST). After cool down to RT, slides were washed 3 times in dH_2O for 5min, followed by 5min in PBS. Frozen sections were equilibrated to room temperature (30min), fixed in ice cold acetone (-20°C) for 10min, followed by 30min air drying at RT and 3 times 5min washing in PBS.

Paraffin-embedded and frozen sections were blocked with 50 μl blocking buffer raised against the host species of the secondary antibody for 60min at RT in a humidified chamber. For co-incubations of two primary antibodies (Table 3) the respective blocking buffers were equally combined. For paraffin-embedded sections, diluted primary antibodies (in antibody diluent) raised against the antigen of interest were incubated overnight at 4°C in a humidified chamber. For frozen sections, primary antibodies were incubated at RT for 1-3 hours. For both, paraffin-embedded and frozen sections fluorochrome-conjugated secondary antibodies (Table 4), were diluted 1:200 and incubated for 1h at RT. Nuclei were counterstained using DAPI (1:2000) in secondary antibody solution. Sections were visualized using a confocal microscope (Olympus Fluoview 1000 using the FV10-ASW software). The amount of Ly6G positive (Ly6G+) cells per area was counted using the Volocity® 5.51 software (Perkin Elmer) defining the lamina propria as region of interest. For each individual mouse, 3 microscopic fields at a 600-fold magnification were quantified for mean Ly6G-positive (Ly6G+) cells per mm^2 .

Table 3 Primary antibodies

Antigen	Host	Dilution	Company	Antigen retrieval
Ly6G	Rat	1:500	BD Pharmingen	Sodium citrate buffer
MPO	Rabbit	1:200	Thermo Fisher	Proteinase K
Lysozyme	Rabbit	1:2000	DAKO	Sodium citrate buffer

Table 4 Secondary antibodies

Antigen	Host	Dilution	Conjugated with	Company
Rat	Goat	1:200	Alexa Fluor 546	Invitrogen
Rabbit	Goat	1:200	Alexa Fluor 594	Invitrogen
Rabbit	Donkey	1:500	Biotin	Dianova

In case of Lysozyme, an immunohistochemistry approach was performed after incubation with primary antibody. Donkey- anti-biotin antibody was incubated at RT for 30min followed by signal amplification with Avidin/Biotin Complex (ABC) according to the manufacturer's instructions (PK-4000, Vector laboratories, USA) and 10min incubation of the tyramide substrate (excitation wave length at 488 nm). The amount of lysozyme-positive (Lyz+) crypts was calculated in relation to present crypts per power field. For each individual mouse 3 different areas were quantified as mean number of Lysozyme-positive (Lyz+) crypts per total number of crypts.

2.7. Laser microdissection (LMD) of fetal intestinal epithelial cells

2.7.1. Cryosectioning of distal ileum and colon

Frozen sections were generated at -20°C from fetal ileum and colon (Microm, Walldorf, Germany). Briefly, 1cm of the distal parts from ileum or colon were cut out of the cryoblock and embedded transversally in O.C.T. Eight PET-frame slides per intestinal sample (MicroDissect, Herborn, Germany) were treated with RNase (Sigma-Aldrich, Steinheim, Germany) before use and dried at RT. Twenty transversal sections (10µm) were mounted on one slide, air-dried and stored at -80°C for short periods of time (<7d) until laser microdissection.

2.7.2. Hematoxylin/Eosin (H&E) staining of cryosections prior to LMD

Each slide was stained directly before LMD microscopy, in order to visualize the epithelial layer of the fetal intestine (Table 5). Respective staining solutions were always prepared with respect to an RNase free environment. Solutions were renewed after staining of 8 slides. All staining solutions were stored at RT and prepared using 0.1% DEPC (Diethylpyrocarbonate) water or nuclease-free water (Mol. biol. grade) as dilution reagent.

Table 5 H&E staining protocol for laser microdissection

Step	Treatment	Time
1.	Equilibration of cryosections to RT	2min
2.	Fixation with 70%(v/v) EtOH	1min
3.	Rinse with DEPC water	30sec
4.	Harris hematoxylin	1min
5.	Rinse with DEPC water	1min
6.	Bluing agent 0.1% (v/v) NH ₄ OH	30sec
7.	Counterstaining with 2.5% Eosin (alc.)	2min
8.	Dehydration with 96% EtOH	30sec
9.	Dehydration with EtOH abs.	30sec
10.	Air drying at RT	2-5min

2.7.3. Laser microdissection microscopy

Fetal intestinal epithelial cells (IEC) from ileum and colon were cut at a magnification of 630x using the UV laser-cutting system LMD 6000 and the Leica Application Suite software (Leica, Wetzlar, Germany) [237]. To avoid degradation of RNA, LMD procedure did not exceed 2h per slide. 100µl of lysis buffer supplied by the AllPrep® DNA/RNA Micro Kit (Qiagen, Hilden, Germany) were added into the lid of the tube in order to prevent loss of epithelial pieces after dissection. Samples were kept frozen at -80°C until DNA/RNA isolation. In total, mean areas of $1.6\pm 0.15\times 10^6\mu\text{m}^2$ (ileum) and $1.5\pm 0.19\times 10^6\mu\text{m}^2$ (colon) from ileal and colonic IEC were collected for total RNA isolation and subsequent analysis.

2.7.4. RNA isolation and quality control

All lysates were vortexed at least 30 seconds and incubated at 37°C for 10min (Peqstar, Peqlab, Germany). All lysates per biological sample were pooled into a 1.5ml tube. Total RNA was isolated using the column-based AllPrep® DNA/RNA Micro Kit (Qiagen, Hilden, Germany), following the manufacturer's instructions. RNA was eluted with 14µl nuclease-free water into a nuclease-free tube (1st elution). As back-up elution was repeated into a new tube with another 14µl nuclease-free water (2nd elution). 3µl from the 1st elution were used for subsequent measurements of RNA quantity and quality. Remaining RNA was immediately frozen at -80°C until further analysis. RNA quantity was measured using the Quant-iT RiboGreen® RNA Assay Kit (Invitrogen, Eugene, USA). Diluted RNA (1:100 in 1xTE-buffer) was analysed in triplicates followed by the manufacturer's instructions. Quantification was performed using the equation of the standard dilution curve. After obtaining a total RNA yield $\geq 60\text{ng}$ RNA integrity measurements were performed. Quality determination of 1µl diluted RNA (1:10 in nuclease-free water) was performed with the Bioanalyzer 2100 (Agilent, Waldbronn,

Germany). Using the RNA 6000 Pico Kit (Agilent, Waldbronn, Germany) according to the manufacturer's instructions. Quality threshold for microarray and preamplification procedure was a RNA integrity number (RIN) of 6. Total RNA (50ng) from laser microdissected fetal IEC were sent to the University of Wageningen in order to perform microarrays and subsequent data analysis.

2.7.5. Microarray processing

Microarrays were performed at the University of Wageningen (Mark Boekschoten, Michael Müller, The Netherlands). Briefly, total RNA (25ng) was labelled using the NuGEN Ovation PicoSL WTA V2 with the Encore Biotin Module (NuGEN Technologies, Leek, The Netherlands) and hybridized to Affymetrix GeneChip Mouse Gene 1.1 ST targeting 21,187 genes, (Affymetrix, Santa Clara, CA). Sample labelling, hybridization to chips and image scanning was performed according manufacturer's instructions.

2.7.6. Microarray data analysis

Microarray analysis was performed using MADMAX pipeline for statistical analysis of microarray data [238]. Quality control was performed and all arrays met our criteria. Expression values were calculated using robust multichip average (RMA) method, which includes quantile normalization. Significant differences in expression were assessed using paired Intensity-Based Moderated T-statistic (IBMT). Genes were defined as significantly changed when the p value was <0.05 and the log₂-based fold change (FC) was ± 1.3 . All microarray data are MIAME (Minimum Information About a Microarray Experiment) compliant. Significantly regulated gene lists were filtered, according to the control group with expression values higher than 50 in order to create a list of biologically relevant genes that are potent for microarray validation. Heatmaps and gene distance matrices (GDM) were generated using the MultiExperiment Viewer (TigrMEV) software. Gene Ontology (GO) terms were computed using the GeneRanker program (Genomatix, München, Germany) and the David tool [239]. Overrepresentation of biological terms were calculated and listed in the output together with respective p -values.

2.7.7. Preamplification of laser microdissected low input RNA

Depending on the RNA amount, either the 1st elution alone or pooled 1st and 2nd elutions of total RNA were additionally DNase digested and concentrated using the Clean and Concentrator Kit (Zymo Research) according to the manufacturer's instructions. Elution volume was 8 μ l nuclease-free water. Completely clean RNA was again quantified using the Quant-iT RiboGreen® RNA Assay (Invitrogen, Eugene, USA). Input material of 2-6ng total RNA was applied to whole transcriptome preamplification using the Ovation PicoSL WTA System V2 kit (NuGEN, Netherlands) and following the manufacturer's instructions. Quality of

preamplified cDNA was evaluated at the Bioanalyzer using RNA 6000 Nano Kit (Agilent, Waldbronn, Germany).

2.8. Gene expression analysis of laser microdissected IEC or whole tissue sections

Quantitative real-time PCR was performed on 10ng cDNA using the LightCycler® 480 System (Roche Diagnostics, Mannheim, Germany). Gene-specific nucleotide sequences and accession numbers were obtained from the National Center for Biotechnology Information (NCBI) website (<http://www.ncbi.nlm.nih.gov/gene>). Primer pairs (Table 6) were designed with the Universal ProbeLibrary (UPL) design center (Roche Diagnostics, Mannheim, Germany). Crossing points (Ct) were determined using the second derivative maximum method by the LightCycler® 480 software release 1.5.0. Data were normalized to the Ct mean of reference genes (*18s*, *Rpl13a* and *Gapdh*) and expressed as $2^{-\Delta Ct}$ values in order to compare expression levels among all groups.

Table 6 Primer sequences. Underlined genes are housekeeping genes

Gene	Forward primer	Reverse primer	Probe	Amplicon
<u><i>Gapdh</i></u>	5'-tcc act cat ggc aaa ttc aa	5'-ttt gat gtt agt ggg gtc tcg	#9	108 nt
<u><i>Rpl13a</i></u>	5'-atc cct cca ccc tat gac aa	5'-gcc cca ggt aag caa act t	#108	97 nt
<u><i>18s</i></u>	5'-aaa tca gtt atg gtt cct ttg gtc	5'-gct cta gaa tta cca cag tta tcc aa	#55	67 nt
<i>Afp10</i>	5'-gca tgc tgc aaa gct gac	5'-cct ttg caa tgg atg ctc tc	#63	64 nt
<i>Il12p40</i>	5'-atc gtt ttg ctg gtg tct cc	5'-gga gtc cag tcc acc tct aca	#78	80 nt
<i>Tnf</i>	5'-tgc cta tgt ctc agc ctc ttc	5'-gag gcc att tgg gaa ctt ct	#49	117 nt

2.9. Flow cytometry of T cells in spleens and mesenteric lymph nodes (MLNs)

Spleen halves and MLNs were stowed in RPMI 1640 (10% FCS+ 1AA) on ice until tissue lysis. Tissues were sieved through a nylon cell strainer (REF352360, 100µm pore size) and washed with 1ml FACS buffer (PBS, 5% FCS, 2mM EDTA). Cell suspension was centrifuged (300g, 10 min, 4°C) and resuspended in 1ml FACS buffer. A volume of 100µl was transferred into a well of a 96 well V-bottom microplate. Fluorochrom-conjugated antibodies (Table 7) and 20µl Fc(R)-Block were incubated for 15-20min in the dark (4°C). Unbound antibodies were washed away with 100µl FACS buffer 2 times (400g, 5min, 4°C). A volume of 100µl cell suspension was filled up with 900µl FACS buffer and fluorescence intensities were measured (BD LSR II, CA USA). Relative fluorescence intensities were analyzed with BD FACS diva software (BD Pharmingen, CA, USA).

Table 7 Fluorochrome-conjugated antibodies

Antigen	Conjugated with:	Volume/well [µl]	Company
CD3	APC-Cy7	0.4	BD Pharmingen
CD4	PE-Cy7	0.5	BD Pharmingen
CD8α	PE	8.0	Bio-RAD
CD8β	FITC	0.4	BD Pharmingen
CD44	APC	0.5	BD Pharmingen

2.10. Microbial ecology

2.10.1. Cecal content collection and bacterial DNA extraction

Caecal content was collected from 3 and 8 week-old offspring and snap frozen on dried ice. Prior to bacterial DNA extraction 100mg cecal content was diluted 1:10 with sterile PBS, centrifuged at 8,000g for 5min, followed by washing pellets 3 times. Pellet was resuspended in 750µl sterile filtered lysis buffer (200mM NaCl, 100mM Tris (pH8), 20mM EDTA, 20mg/ml Lysozyme) and shaken (800rpm) at 37°C for 30min. Sterile filtered 10% SDS (85µl) and 10mg/ml Proteinase K were added and incubated in a thermoshaker (60°C, 30min, 800rpm). Phenol-Chloroform-Isoamyl alcohol (Roth) (500µl) was added and cells were disrupted using a bead beater 4 x 30sec. After 5min centrifugation (10,000g) top layer was transferred to 500µl Phenol-Chloroform-Isoamyl alcohol briefly shaken, centrifuged again (4 new cycles of top layer transfer). DNA was precipitated by adding 2 volumes of EtOH (96-100%) at -20°C over night and subsequent centrifugation at full speed for 20min, washed with 70% EtOH and centrifuged again. DNA pellet was air-dried and resuspended with 100µl Tris buffer (10mM pH8). 100ng of bacterial DNA was used for PCR.

2.10.2. Illumina Sequencing of 16S rRNA gene amplicons from caecal contents

Amplicons of the V4 region of 16S rRNA genes were obtained after 25 PCR cycles as described previously [240]. They were sequenced in paired-end modus (PE200) using the MiSeq system (Illumina Inc., San Diego, USA). Sequences were analyzed using in-house developed pipelines partly based on UPARSE [241], the open source software package QIIME [242] and the Ribosomal Database Project [243]. Sequences were filtered at a base call accuracy of 99 %. Sequences containing any ambiguous nucleotide (N character) were discarded. The presence of chimeras was checked after dereplication using UCHIME [244]. Operational taxonomic units (OTUs) were picked at a threshold of 97 %. Only those OTUs occurring in at least one sample at abundances >0.5 % total sequences were included in the analysis. Sequence proportions of bacterial taxa were analyzed for significant differences using F-Test followed by Benjamini-Hochberg correction for multiple testing in the R programming environment (2008, ISBN 3-900051-07-0).

2.11. Plasma Measurements

2.11.1. Measurements of proinflammatory cytokines TNF, IFN γ and IL-6

TNF, IFN γ or IL-6 were measured in abdominal aorta plasma using respective Mouse ELISA Ready –SET-Go![®] according to the manufacturer's instructions (eBioscience, San Diego, USA). A volume of 100 μ l total plasma was incubated for 2h at RT on microplate wells pre-coated with anti-mouse TNF or anti-mouse IL-6 antibody, respectively. After washing and blocking captured antigens were incubated with Avidin/Biotin labelled anti-mouse TNF; IFN γ or IL-6 detection antibody, respectively. HRP-conjugated antibodies were incubated for 30min and substrate conversion was stopped after 15min with 2N H₂SO₄. The product absorbance of standard dilutions and plasma sample were measured at 405nm to the reference wavelength of 570nm. Quantification was performed using the linear equation of the standard dilutions.

2.11.2. Leptin measurements

Leptin concentrations were measured in abdominal aorta plasma using Mouse and Rat leptin ELISA (Biovendor, Karasek, Czech Republic). Briefly, 100 μ l of diluted plasma (20x in dilution buffer) from mothers (n=5 per group) and offspring (n=8-10 per group) were incubated in microplate wells pre-coated with anti-mouse leptin antibody for 1h at RT. After washing, biotin labelled polyclonal anti-mouse leptin antibody was added and incubated with the captured leptin for 1h at RT. After another washing, streptavidin-HRP conjugate was incubated for 30min, followed by a last washing and subsequent incubation with substrate solution for 10min. The absorbance of the resulting yellow product was measured at 450nm wavelength to the

reference wavelength 630nm. Quantification was performed using the linear equation of the standard dilutions.

2.11.3. Endotoxin concentration of portal vein plasma

Endotoxin concentrations in portal vein plasma were analyzed using LAL assay (Hycult Biotech, The Netherlands). Plasma samples were diluted 1:50 in endotoxin-free water (EFW, Hycult Biotech, The Netherlands). After vortexing, and 10min incubation at 70°C, 3.03µl Pyrospere was added. For standards a volume of 50µl diluted Pyrospere (1:100 in EFW) was pipetted per well. Standard concentrations were prepared by serial dilutions of the highest concentrated standard (25µl, 10EU/ml as final conc.). Samples were spiked with 5µl 10 EU/ml in order to determine recovery rate of samples. LAL reagent (50µl/well) was added and colour formation was monitored by absorbance measurements over time (50min) at 405nm wavelength.

2.12. Statistics

Statistical analyses were performed with Graph Pad Prism version 6 (GraphPad software, San Diego, USA) and SigmaPlot 11. 0 (Systat Software Inc. San Jose, USA) using unpaired T-test, Kruskal-Wallis test followed by Dunn's multiple comparison or ANOVA followed by pairwise comparisons testing (Holm-Sidak test). Data were expressed as mean \pm SD. Differences between groups were considered significantly if p -values were <0.05 (*), <0.01 (**), <0.001 (***). Graphs were created using GraphPad Prism version 6.00.

3. Results

3.1. The severity of murine Crohn's disease-like ileitis is dependent on the microbial environment and on dietary factors.

$Tnf^{\Delta ARE/+}$ mice were used to study the role of maternal inflammation and maternal obesity on the offspring's ileal inflammation. It was recently published that maternal inflammation does not affect the severity of genetically-driven ileitis and colitis [245] under Chow dietary conditions in a conventional housing environment. Thereafter, we additionally considered the fact that certain dietary and hygienic conditions influence the genetically-driven ileitis in the $Tnf^{\Delta ARE/+}$ mouse model.

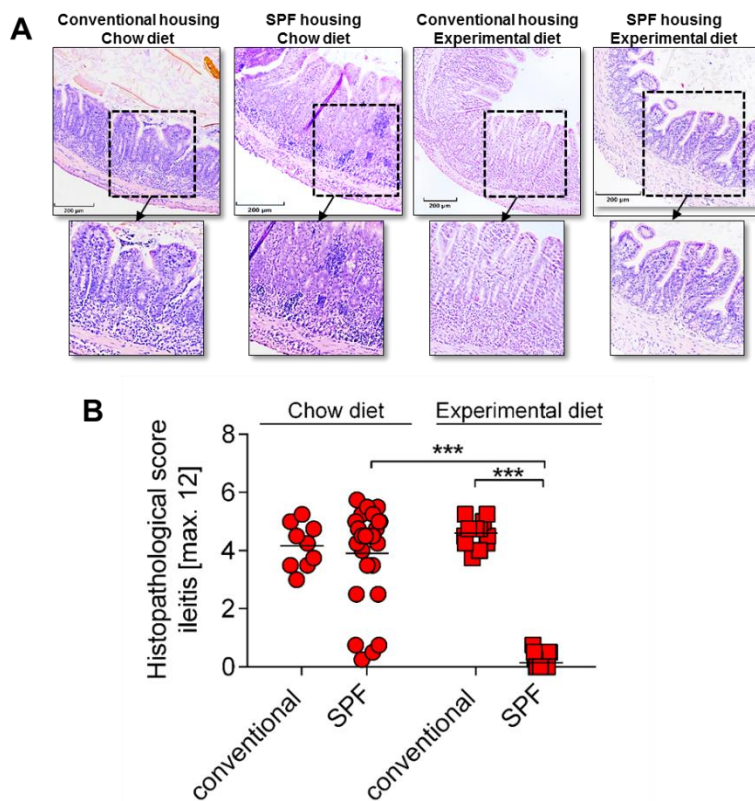


Figure 7 Severity of CD-like ileitis in response to diet and hygiene stage. $Tnf^{\Delta ARE/+}$ mice were housed until 12 weeks of age in different hygiene stages (conventional versus SPF conditions) on Chow or experimental diet, respectively. **(A)** Representative H&E-stained sections of the distal ileum from 12-week old $Tnf^{\Delta ARE/+}$ mice. **(B)** Histopathological ileitis scores were blindly assessed by blindly assessing the degree of lamina propria mononuclear cell infiltration, crypt hyperplasia, goblet cell depletion and architectural distortion on H&E-stained sections of the distal ileum in $Tnf^{\Delta ARE/+}$ mice ($n=9-26$ each). Two-Way ANOVA, *** $p<0.001$

To test this we assessed the chronic ileitis severity in 12 week-old $Tnf^{\Delta ARE/+}$ mice that derived from conventional or SPF-housing and received either Chow or experimental diet from 4 weeks of age on. We observed the highest inflammation scores of $Tnf^{\Delta ARE/+}$ mice on Chow diet independently of the hygiene stages (Figure 7). Interestingly, experimental diet feeding revealed no ileitis in SPF-raised $Tnf^{\Delta ARE/+}$ mice, whereas the same diet induced severe inflammation when mice were conventionally housed. Interestingly, Chow diet feeding under SPF conditions revealed 4 non-responder mice (ileitis score <1), 4 intermediate-responder mice (ileitis score 2-4) and 18 high-responders (ileitis score >4). Because of heterogeneous ileitis severity in Chow diet-fed $Tnf^{\Delta ARE/+}$ mice and because of absent pathology in SPF-housed

$Tnf^{\Delta ARE/+}$ mice on experimental diet further experiments were conducted in conventionally-raised $Tnf^{\Delta ARE/+}$ mice fed an experimental diet.

3.2. The influence of maternal inflammation on genetically-driven postnatal development of CD-like ileitis in $Tnf^{\Delta ARE/+}$ mice

3.2.1. $Tnf^{\Delta ARE/+}$ dams are locally and systemically inflamed

Consequences of maternal inflammation on WT and $Tnf^{\Delta ARE/+}$ offspring that received a postweaning experimental diet (from 4 weeks of age on) were investigated. The genetically-driven local and systemic inflammation in ARE dams was confirmed at weaning (3 weeks postnatal) by significantly increased ileal histological scores (WT vs. ARE dams: 0.5 ± 0 and 5.2 ± 0.5), elevated plasma TNF (WT vs. ARE dams: 2.93 ± 1.9 pg/ml and 100.3 ± 31.58 pg/ml) and increased relative spleen weights (WT vs. ARE dams: 3.12 ± 0.18 mg/g BW and 5.68 ± 0.74 mg/g BW) (Figure 8).

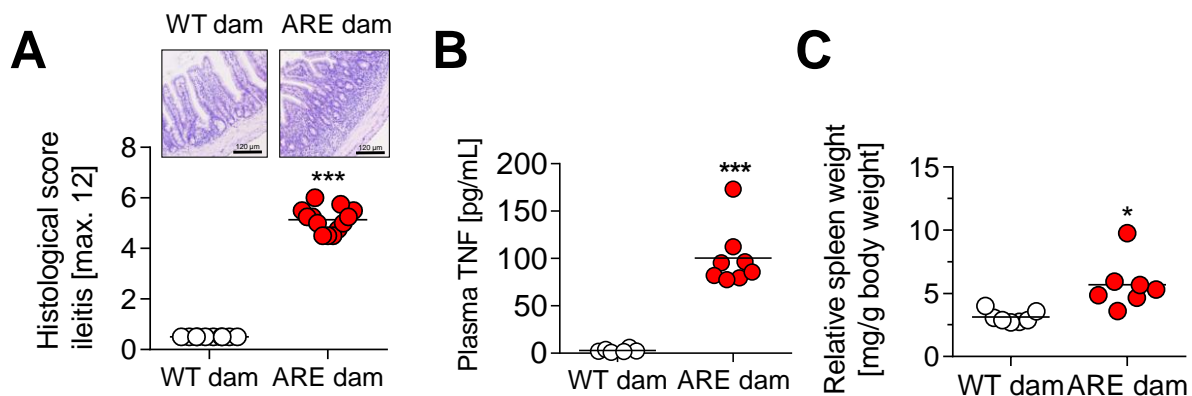


Figure 8. TNF-driven maternal inflammatory environment at weaning (3 weeks after giving birth). Local and systemic signs of intestinal inflammation in $Tnf^{\Delta ARE/+}$ (ARE) dams confirm the maternal inflammatory environment. (A) Histological ileitis scores were blindly assessed on H&E-stained sections of the distal ileum in WT and ARE dams ($n=6-9$ each). Local inflammation significantly increased (B) plasma TNF ($n=6-8$ each) and (C) relative spleen weights in ARE dams, thus, highlighting on increased systemic inflammatory stages. Unpaired, two tailed T-test with Welch's correction, * $p < 0.05$, *** $p < 0.001$.

3.2.2. Maternal inflammation does not change CD-like ileitis in *Tnf^{ARE/+}* mice

Although a maternal inflammatory environment during pregnancy was confirmed, 8 week-old ARE and iARE offspring showed the same grade of inflammation in the distal ileum (Figure 9). Although systemic and local signs of postnatal inflammation were observed in spleens and mesenteric lymph nodes (MLNs) of ARE and iARE compared to WT and iWT offspring. However, offspring's inflammation was independent of maternal inflammation (Figure 9B). Increased relative MLN weight served as a marker for tissue inflammation in the distal ileum, because it significantly correlated with the histological score ($r_{\text{Spearman}}=0.48$; $p=0.01$).

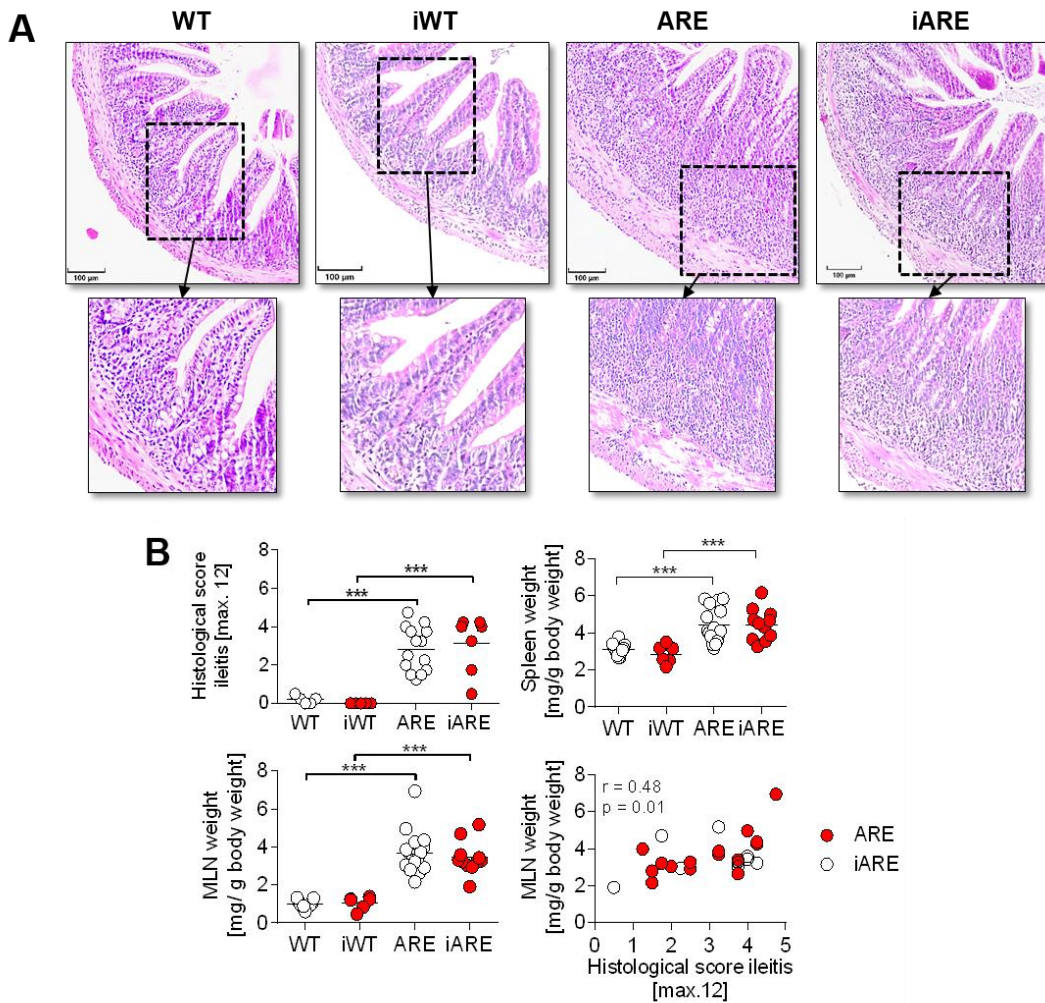


Figure 9. Severity of CD-like ileitis is not influenced by maternal inflammation. Offspring's intestinal and systemic inflammation is unaffected by in utero exposure to maternal inflammation. (A) Representative H&E-stained sections of the distal ileum from 8-week old WT, iWT, ARE and iARE offspring ($n=6-15$ each). **(B)** Histological ileitis scores, relative weights of spleen and mesenteric lymph nodes (MLN) were significantly increased in ARE groups compared to WT offspring independently of the exposure to maternal inflammation. There is significant correlation between relative MLN weight and the histological ileitis score ($r_{\text{Spearman}}=0.48$; $p=0.01$). Two-Way ANOVA, *** $p < 0.001$.

Immune cell infiltration into the lamina propria and submucosa of distal ileum sections in response to maternal inflammation was exemplarily assessed by the number of Ly6G+ neutrophils (Figure 10). The strong positive correlation of infiltrated Ly6G+ neutrophils with the histological ileitis score ($r_{\text{Spearman}}=0.82$, $p=0.0019$) indicated Ly6G as a reliable marker for tissue pathology.

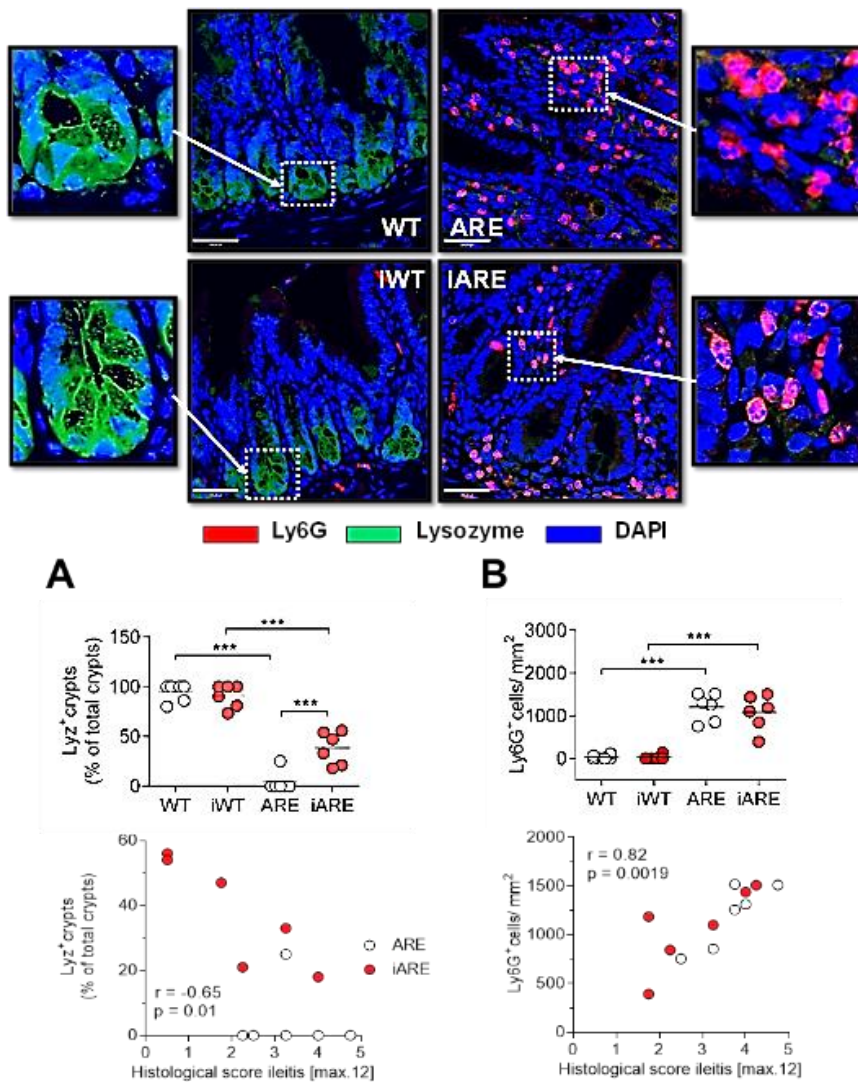


Figure 10 Loss of lysozyme and infiltration of neutrophils in distal ileum of $Tnf^{\Delta ARE/+}$ mice is not affected by maternal inflammation. (Upper panel) Representative microscopic immunofluorescence pictures (600x magnification) of confocal laser microscopy for Lysozyme (Lyz, green) as hallmark for Paneth cells and Ly6G+ neutrophils (red) from distal ileum in 8-week old WT, iWT, ARE and iARE offspring on experimental diet. Nuclei were counterstained with DAPI (blue). Three pictures per mouse were analyzed. (A) The percentage of Lyz+ crypts compared to total number of crypts was ascertained per mouse ($n=5-6$ each). Individual data and means are shown (Two-Way ANOVA and Holm-Sidak multiple comparisons, $*p<0.05$, $**p<0.01$, $***p<0.001$). Correlation analysis in $Tnf^{\Delta ARE/+}$ offspring indicated negative associations between histopathological scores and the percentage of Lyz+ crypts ($r_{\text{Spearman}}=-0.65$, $p=0.01$). (B) Lamina propria and submucosa were defined as regions of interest. The numbers of Ly6G+ cells per mm² from all 3 pictures per mouse were counted. Individual data and means are shown (Two-Way ANOVA and Holm-Sidak multiple comparisons, $*p<0.05$, $**p<0.01$, $***p<0.001$). Correlation analysis in $Tnf^{\Delta ARE/+}$ offspring indicated strong associations between histopathological scores and infiltration of Ly6G+ neutrophils ($r_{\text{Spearman}}=0.82$, $p=0.0019$).

Despite increased Ly6G+ cell number in inflamed ARE and iARE mice, maternal inflammation did not additionally alter immune cell infiltration in both, WT and ARE offspring. Furthermore, ARE and iARE showed a significant loss of Lysozyme-positive (Lyz⁺) crypts compared to WT and iWT offspring. Interestingly, maternal inflammation attenuated loss of Lyz⁺ crypts in iARE offspring (ARE vs. iARE: $4\pm 9\%$ of crypts vs. $38\pm 15\%$ of crypts were Lyz⁺), whereas no changes were observed in WT offspring. In essence, the proportion of Lyz⁺ crypts negatively correlated ($r_{\text{Spearman}}=-0.65$, $p=0.01$) with the histological ileitis scores, but unexpectedly it was

not consistently in both, ARE ($r_{\text{Spearman}}=0.00$; $p=0.33$) and iARE ($r_{\text{Spearman}}=-0.92$, $p=0.0056$) groups.

A closer look into immune modulatory effects by immunophenotyping of lymphocytes from MLN and spleens revealed alterations of CD4+ T helper cells and CD8+ cytotoxic T cell subsets in response to maternal and postnatal inflammation (Figure 11). This indicates a potential systemic and local (intestinal) shift of T cell subsets due to maternal or postnatal inflammation.

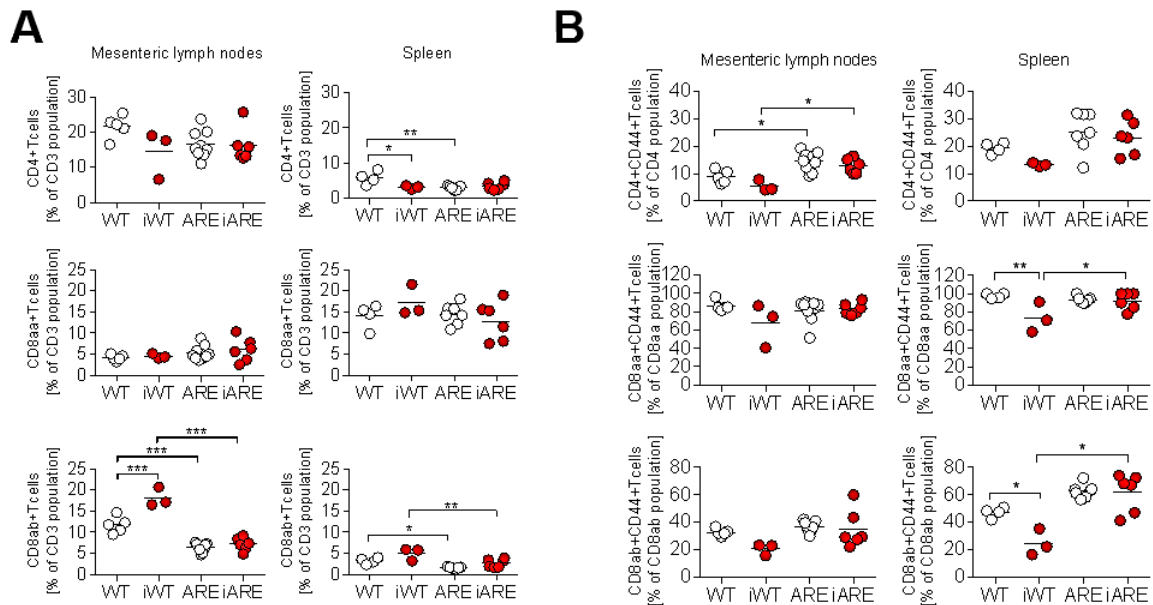


Figure 11. Immunophenotyping of offspring's mesenteric and splenic lymphocytes in response to maternal inflammation. (A+B) Spleen halves and MLNs were stowed in RPMI 1640 (10% FCS+ 1AA) on ice until tissue lysis. Fluorochrom-conjugated antibodies (Table 7) and 20 μ l Fc(R)-Block were incubated for 15-20min in the dark (4°C). Unbound antibodies were washed away with 100 μ l FACS buffer 2 times (400g, 5min, 4°C). A volume of 100 μ l cell suspension was filled up with 900 μ l FACS buffer and fluorescence intensities were measured (BD LSR II, CA USA). Relative fluorescence intensities of (A) CD4+, CD8aa+ and CD8ab+ T cell populations and (B) of activated CD4+, CD8aa+ and CD8ab+ T cells (marker CD44) were analyzed with BD FACS diva software (BD Pharmingen, CA, USA), n= 3-12 each. Two-Way ANOVA and Holm-Sidak multiple comparisons, * $p < 0.05$, ** $p < 0.01$

In spleens, CD3+ CD4+ T cell population decreased in iWT and ARE compared to WT splenocytes indicating a response to maternal inflammation and postnatal inflammation, whereas MLN CD3+CD4 T cell populations were unaffected by both types of inflammation (Figure 11A). Cytotoxic CD3+CD8aa+ T cell populations were not affected by maternal or postnatal inflammation in both organs. It has to be mentioned, that the iWT group consisted of n=3 only, which was due to technical problems during flow cytometry. However, statistical analysis revealed no lack of power for this analysis. Interestingly, cytotoxic CD3+CD8ab+ T cells in MLNs and spleen were strongly reduced during postnatal inflammation (WT versus ARE or iWT versus iARE). This is in accordance with previously published data [225]. In contrast, maternal inflammation significantly increased CD3+CD8ab+ T cell population in iWT compared to WT MLNs, but this effect was absent in spleen. Further analysis

of the activated CD4⁺ and CD8⁺ T cell clusters by using CD44 as indicative marker for effector memory T cells (Figure 11 B) showed a slight increase of CD4⁺CD44⁺ and CD8ab⁺CD44⁺ T cell subsets in ARE and iARE mice compared to their WT controls. Interestingly, maternal inflammation decreased the splenic proportion of activated cytotoxic T lymphocytes (CD8aa⁺CD44⁺ and CD8ab⁺CD44⁺) in WT offspring. The same tendency was observed in MLN residual lymphocytes. Immune suppression in response to maternal inflammation was not observed in ARE offspring where particularly CD8ab⁺CD44⁺T cell activation was increased during postnatal inflammation. Taking all findings together, maternal inflammation drove proportional increases especially in the CD3CD8ab⁺ subset with concurrently decreased lymphocyte activation in iWT compared to WT mice, but not in iARE compared to ARE offspring. This might be the reason for an absent modulatory effect of maternal inflammation on the histopathology of *Tnf*^{ARE/+} offspring.

3.2.3. Maternal inflammation influences energy homeostasis in WT and *Tnf*^{ARE/+} offspring

Besides comparable pathology and immune phenotypes of T helper cells and cytotoxic T cells between ARE and iARE mice, maternal inflammation persistently influenced the energy homeostasis in both, WT and ARE offspring. Significantly reduced body weights were observed already in 2-days old neonates lasting until 8 weeks of age (Figure 12).

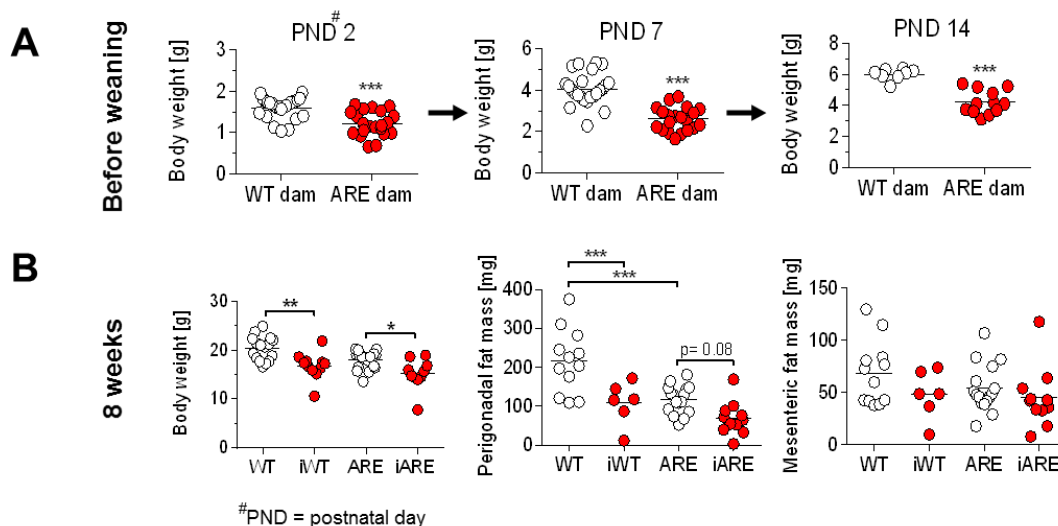


Figure 12. Offspring's body weight and fat depot masses in response to maternal inflammation. (A) Body weight was monitored weekly throughout breastfeeding period, at postnatal day (PND) 2 (n=21-26 each), 7 (n=21-24 each) and 14 (n=8-12 each) and (B) at 8 weeks of age (n=10-18 each). Body weights, perigonadal and mesenteric fat masses of 8 week-old offspring were plotted according to the genotype (WT and ARE) and according to maternal inflammation (iWT or iARE). Unpaired T-test by Welch's correction for measurements during breastfeeding; for the 8-week time point Two-Way ANOVA and Holm-Sidak multiple comparisons, *p <0.05, **p <0.01, ***p <0.001.

Both, maternal and postnatal inflammation reduced perigonadal fat masses in iWT and ARE compared to WT offspring, whereas mesenteric fat mass was unaffected.

3.2.4. Inflammation-driven shift of microbial ecology is not additionally influenced by early life exposure to maternal inflammation.

The sole fact that postnatal inflammation strongly increased caecum weight between WT and ARE (11.01±1.48mg/g BW vs. 19.73±3.96mg/g BW; $p=2.01 \times 10^{-7}$) points to a possible inflammatory impact on the microbial ecology. Therefore, it was hypothesized that postnatal inflammation might shift microbial ecology and that maternal inflammation might be a further contributor. Illumina-based inventory of 16S rRNA of caecal content bacteria from 8-week old offspring demonstrated a shift in beta diversity due to offspring's inflammation indicating a TNF-driven clustering that is related to the intestinal inflammation stage (Figure 13A+B).

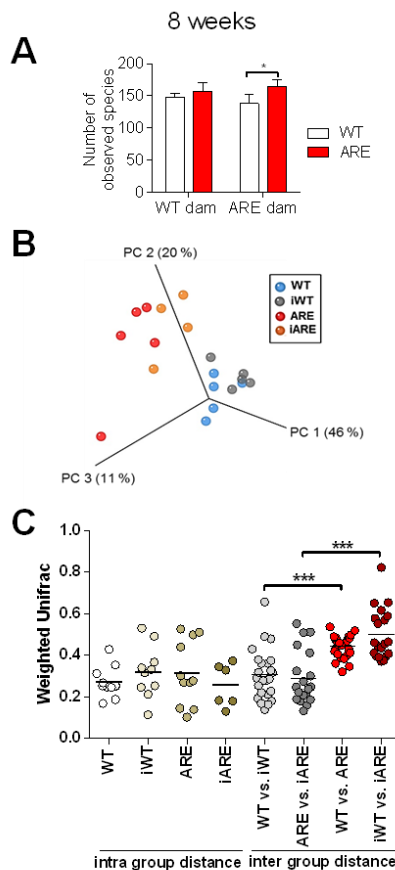


Figure 13. Microbial ecology in WT and ARE offspring after disease onset. (A) Alpha-diversity indicated as number of observed species in caecal contents from WT, iWT, ARE and iARE offspring at 8 weeks of age (right, $n=4-5$ mice each). (B) PCoA analysis revealed an inflammation-driven change in beta-diversity between 8 week-old WT, and ARE groups fed an experimental diet, which is not further influenced by maternal inflammation (WT vs.iWT or ARE vs. iARE; Two-Way ANOVA, $***p>0.0001$). (C) Comparisons of mean phylogenetic distances (weighted UniFrac) supported the PCo (Principal Coordinates) analysis. There were no significant changes between individual mice from the same group (intra-group distances, e.g. WT vs.WT) but between mice from different groups (inter-group distances, e.g. WT vs. iWT compared to WT vs. ARE). Distances that are related to the offspring's genotype were significantly higher than distances related to maternal inflammation (e.g. WT vs. iWT in comparison to WT vs. ARE Two-Way ANOVA and Holm-Sidak multiple comparisons, $***p>0.0001$).

Interestingly, maternal inflammation did not induce any clustering. UniFrac distances of the PCo analysis were significantly higher according to the offspring's genotype than according to maternal inflammation (e. g. WT vs. iWT and WT vs. ARE). Postnatal, but not maternal inflammation significantly changed the relative abundance of bacterial taxa on the phylum level (Figure 14). In detail, the phyla *Firmicutes* and *Proteobacteria* decreased, whereas the abundance of *Bacteroidetes* increased in ARE compared to WT mice. This was independently of maternal inflammation. Although maternal inflammation significantly decreased the relative sequence abundance of the taxon *Clostridia*, especially within the genus *Clostridium XIVa*, an overall influence of maternal inflammation on the phylogenetic makeup was absent. Taken all

data together, maternal inflammation elicits a marginal influence on the abundance of *Clostridia* family, especially *Clostridium XIVA*.

However, in conditions of conventional housing, the severity of CD-like ileitis and the phylogenetic make-up of the ceecal microbiota were not influenced by maternal inflammation.

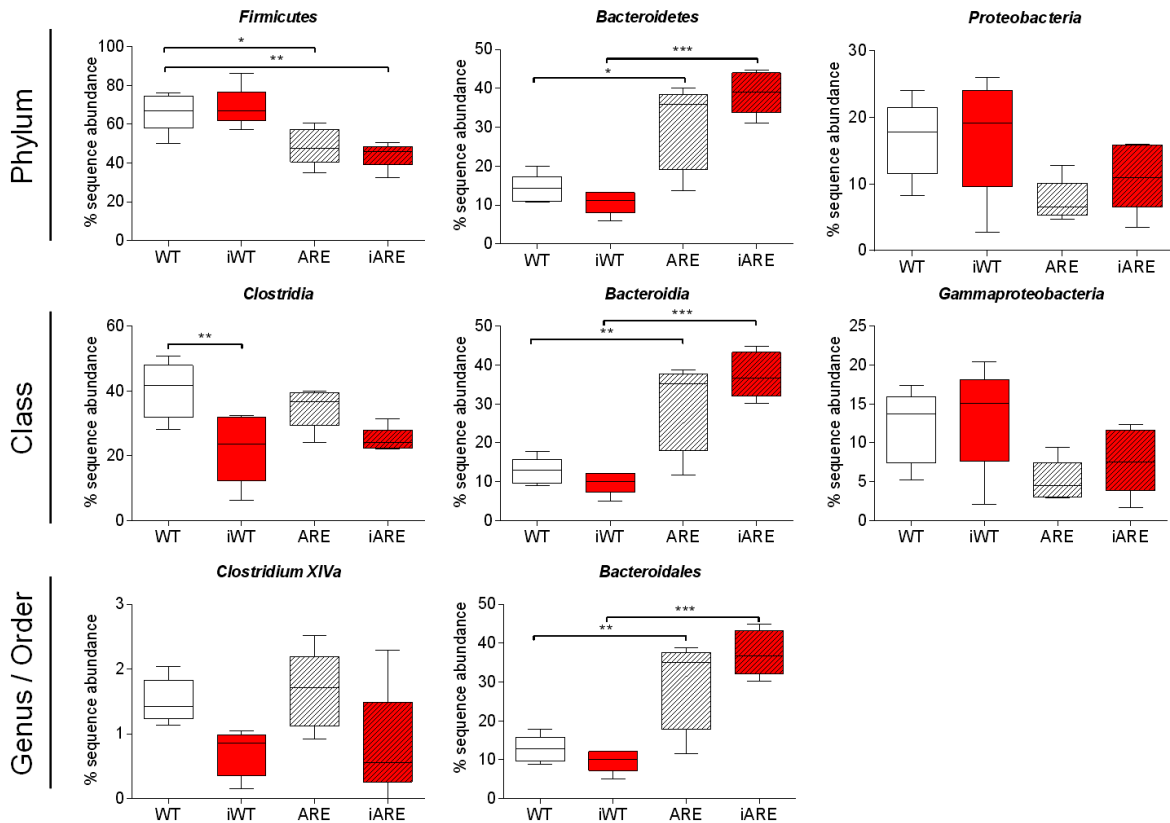


Figure 14. Inflammation-driven changes of bacterial taxa in 8 week-old offspring. Relative sequence abundance of bacterial taxa in caecal contents from WT, iWT, ARE and iARE offspring within phylum, class and order/genus level. Sequence proportions were analyzed for significant differences using F-Test followed by Benjamini-Hochberg correction for multiple testing in the R programming environment. Data were finally analyzed after adjustment for multiple testing by Two-Way ANOVA and Holm-Sidak multiple comparisons testing, * $p < 0.05$, ** $p < 0.01$, *** $p < 0.001$.

3.3. Fetal exposure to maternal diet-induced obesity and its potential to affect postnatal development of CD-like ileitis.

Breeding experiments with high-fat diet (HFD)-fed mothers were performed in order to evaluate the hypothesis whether maternal obesity initiates transcriptomic alterations in the fetal epithelium with consequences on the postnatal susceptibility to intestinal inflammation. Generated offspring were exposed to HFD at different periods of life: prenatal, pre- and perinatal and postnatal. Non-pregnant WT mice (C57/BL6) were fed either with control (12% of energy from fat) or high-fat diet (HFD: 45% of energy derives from palm oil-based fat) from 4 weeks of age on. Mating with *Tnf*^{ΔARE/+} (ARE) sires (C57/BL6) started at the age of 12 weeks. From birth on, control diet dams also received HFD, in order to equalize the HFD load in the breast-feeding period. Consequently, from birth on, all offspring were exposed to HFD. Equalization of offspring's postnatal dietary exposure enables the follow up of *in utero* effects triggered by maternal HFD during pregnancy with regard to the postnatal development of genetically-driven intestinal inflammation. All offspring were sacrificed either in the prenatal stage (17.5 dpc) or at 8 and 12 weeks postnatal.

3.3.1. The maternal diet-induced obesity environment during pregnancy and at weaning.

Dams were sacrificed at 17.5 dpc or 3 weeks after delivery (weaning) in order to analyse the progeny's grade of metabolic exposure to maternal HFD. In late gestation, HFD dams showed significantly increased body weights, mesenteric and perigonadal fat pad weights (mesenteric: 104±14.74mg vs. 343±91.23mg; perigonadal: 159.00±43.16mg vs. 871±135.30mg) as well as increased plasma leptin when compared to control dams (Figure 15A-C). Excessive energy supply by HFD dams led to increased fetal weights independent of the fetus genotype (WT vs. oWT: 0.76±0.08g vs. 0.86±0.05g and ARE vs. oARE: 0.73±0.06g vs. 0.84±0.07g (Figure 15D). However, the fetal size was unaffected indicating the same developmental stage of all fetuses (WT vs. oWT: 1.86±0.12cm vs. 1.86±0.1cm; ARE vs. oARE: 1.81±0.1cm vs. 1.91±0.12cm). Figure 15 shows the maternal metabolic stages at 17.5 dpc and at weaning. Interestingly, the dietary change in control dams at birth (control diet → HFD) equalized the offspring's metabolic conditions during breastfeeding period. HFD-fed control dams and HFD dams showed identical body weights, fat depots and plasma leptin levels at weaning indicating that both offspring groups were exposed to the same high-fat conditions in mother's milk. Equalization of metabolic conditions between dam groups was not due to exhausted fat depots upon breastfeeding, because 'unswitched' control dams (remained on control diet during breastfeeding) exhibited still less body weight, fat masses and plasma leptin compared to 'switched' control and HFD mothers.

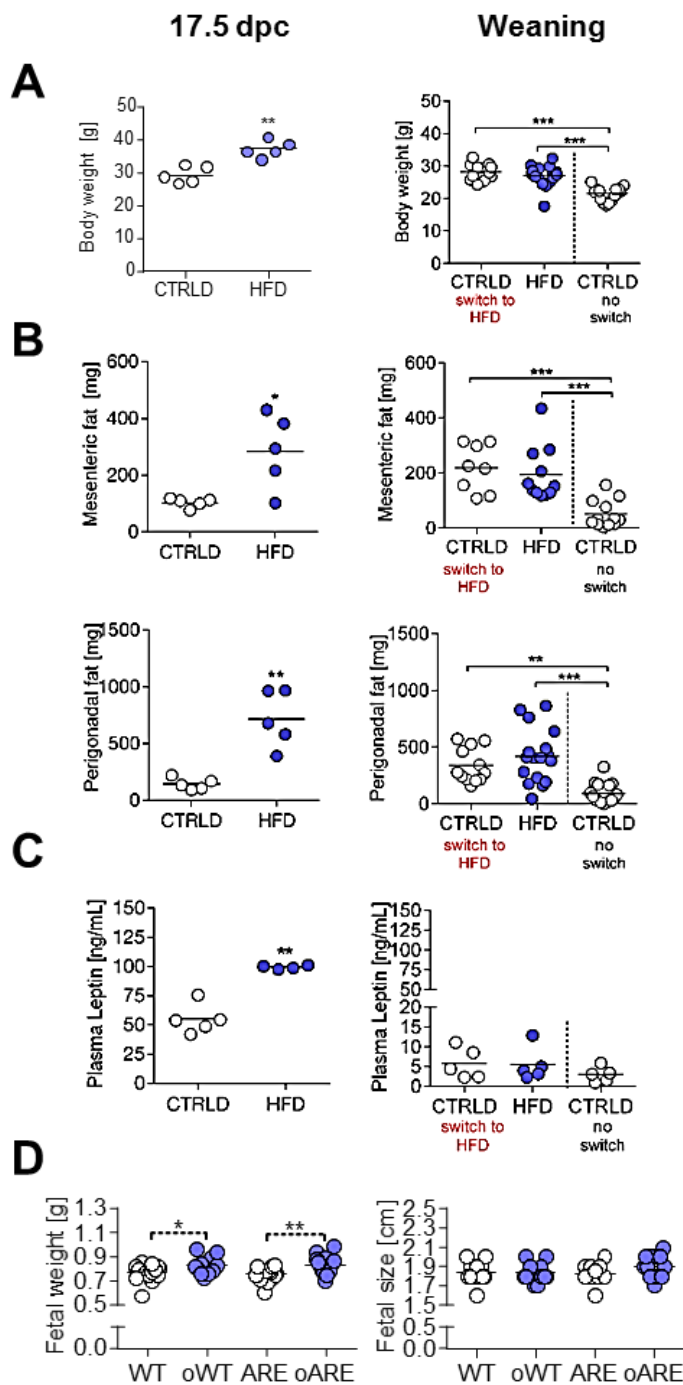


Figure 15 Metabolic differences between pregnant lean and HFD mothers equalize by postnatal HFD during breastfeeding. (A) MDIO increased maternal body weight during gestation (left) (control diet: $n=5$; HFD: $n=3-5$), but postnatal HFD-feeding equalized body weights of control dams (CTRLD) to that of HFD dams at weaning (right). $*p<0.05$, $**p<0.01$, $***p<0.001$. T-test and Two-Way ANOVA and Holm-Sidak test. **(B)** Mesenteric and perigonadal fat masses were significantly increased during gestation (left), but equalized at weaning (right) between control dams and HFD dams. $*p<0.05$, $**p<0.01$, $***p<0.001$. **(C)** Plasma leptin levels were significantly increased during gestation (left), but comparable at weaning (right) between control dams and HFD dams. $**p<0.01$ calculated by student's T-test and Two-Way ANOVA and Holm-Sidak test. **(D)** MDIO increased fetal body weight (left), but not fetal size (right) in both, WT and ARE fetuses, $*p<0.05$; $**p<0.01$, $***p<0.001$, calculated by Two-Way ANOVA and Holm-Sidak test.

From the inflammatory point of view (Figure 16), mDIO increased gene expression of proinflammatory cytokines in dam's mesenteric and perigonadal adipose tissue (mesenteric fat; *Tnf*, 4.11 ± 1.45 fold change (FC to CTRLD), *Mcp-1*, 7.97 ± 4.41 FC to CTRLD; perigonadal fat: *Il-6*, 4.96 ± 1.05 FC to CTRLD). Due to those findings, maternal HFD was suspected to drive massive inflammatory changes in the placenta, the

maternal fetal interphase. Placental gene expression of *Tnf* and *Mcp-1* were dominantly induced by the fetal genotype, but were not affected by maternal HFD (Figure 16). Low expression levels of placental *Il-6* (Ct values of 35.30 ± 0.91) around detection level was most probably responsible for inconclusive results (strong sample separation). Therefore, a statistical analysis was not meaningful. In conclusion, mDIO had a pronounced impact on the fetal metabolism, but not on the intrauterine cytokine milieu.

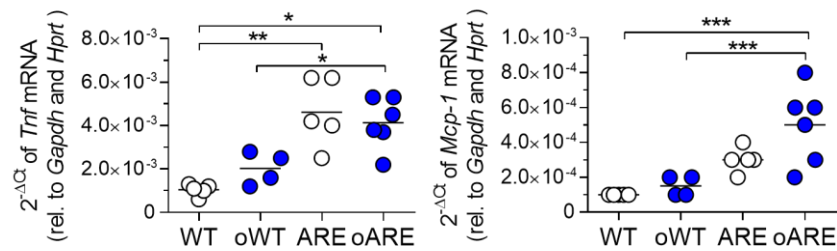


Figure 16 *Transcriptional analysis of placental cytokines.* Relative mRNA expression (pairwise comparisons) of cytokines *Tnf* and *Mcp-1* from WT, oWT, ARE and oARE placentas measured by qPCR. * $p < 0.05$; ** $p < 0.01$, *** $p < 0.001$ calculated by Two-Way ANOVA and Holm-Sidak test.

3.4. Establishment of a workflow for large scale targeted gene expression analysis from laser microdissected murine fetal intestinal epithelium.

Whether mDIO programs the fetal gut towards altered susceptibility to genetically-driven intestinal inflammation was of special interest. Since *Tnf* overexpression in the epithelium is sufficient to trigger ileitis [246] it was planned to compare the fetal transcriptome of laser microdissected (LMD) intestinal epithelial cells in WT and *Tnf^{fARE/+}* mice in response to mDIO. To address this technical issue, a workflow was established to enable the comparison of global and targeted gene expression analysis of laser microdissected fetal IEC in order to verify future microarray results by qPCR [237].

Laser microdissection with subsequent RT-qPCR, represents the most suitable investigative tool for cell-specific gene expression analysis in basic and clinical research [247-249]. However, LMD of fetal epithelium, limits RNA yields and RNA qualities making RT-qPCR often unreliable. In order to avoid misinterpretation of transcriptomic analyses due to amplification bias, validation experiments by targeted gene expression analysis (qPCR) are required. Therefore, a workflow of laser microdissection from fetal IEC, RNA-isolation, -quantification and -quality measurements complemented by the subsequent whole transcriptome amplification (WTA) procedure (NuGEN Ovation PicoSL WTA V2 with the Encore Biotin Module; NuGEN Technologies, Leek, The Netherlands) including qPCR was established. The whole transcriptome amplification is a high fidelity approach by single primer isothermal amplification (SPIA) to especially address biological samples that are limited in quantity and quality, such as laser microdissected fetal IEC. This workflow was proofed on laser microdissected IEC of the fetal ileum versus the fetal colon.

3.4.1. Single primer isothermal amplification enables large-scale targeted gene expression analysis of fetal intestinal epithelial cells

To accomplish simultaneous global and targeted gene expression, whole transcriptome amplification (WTA) on the basis of single primer isothermal amplification (SPIA) was conducted before microarray and qPCR performance of fetal IEC. In preparation, 1.5 Mio μm^2 tissue area corresponding to about 3000 murine fetal IEC were laser microdissected (Figure 17). The total RNA yield of laser microdissected fetal IEC was comparable in ileum and colon (mean 69.52 \pm 6.70ng and mean 67.80 \pm 15.40ng, respectively) with a mean RNA integrity number (RIN) of 7.2 \pm 0.4 and 7.5 \pm 0.4 in both compartments (Figure 17C+D). Simultaneous gene expression analyses required about 30ng total RNA, a minimum of 25ng total RNA for microarray analysis and 2-5ng for targeted gene expression analysis.

For global gene expression analysis total RNA was labelled using the NuGEN Ovation PicoSL WTA V2 with the Encore Biotin Module (NuGEN Technologies, Leek, The Netherlands) and hybridized to Affymetrix GeneChip Mouse Gene 1.1 ST targeting 21,187 genes (Affymetrix, Santa Clara, CA). Sample labelling; hybridization to chips and image scanning was performed according manufacturer's instructions. For targeted gene expression analysis 2-5ng RNA were applied to the whole transcriptome amplification procedure (NuGEN Ovation PicoSL WTA V2) resulting in 1.15 \pm 0.53 μg and 1.9 \pm 0.76 μg of cDNA. This was sufficient to analyse the expression of averaged 51 and 93 genes in ileum and colon, respectively, in order to validate microarray results. Stability of reference genes (*Gapdh*, *18s* and *Rpl13a*) utilized in qPCR procedure was guaranteed when using 2-5ng RNA as input material for WTA (Figure 17).

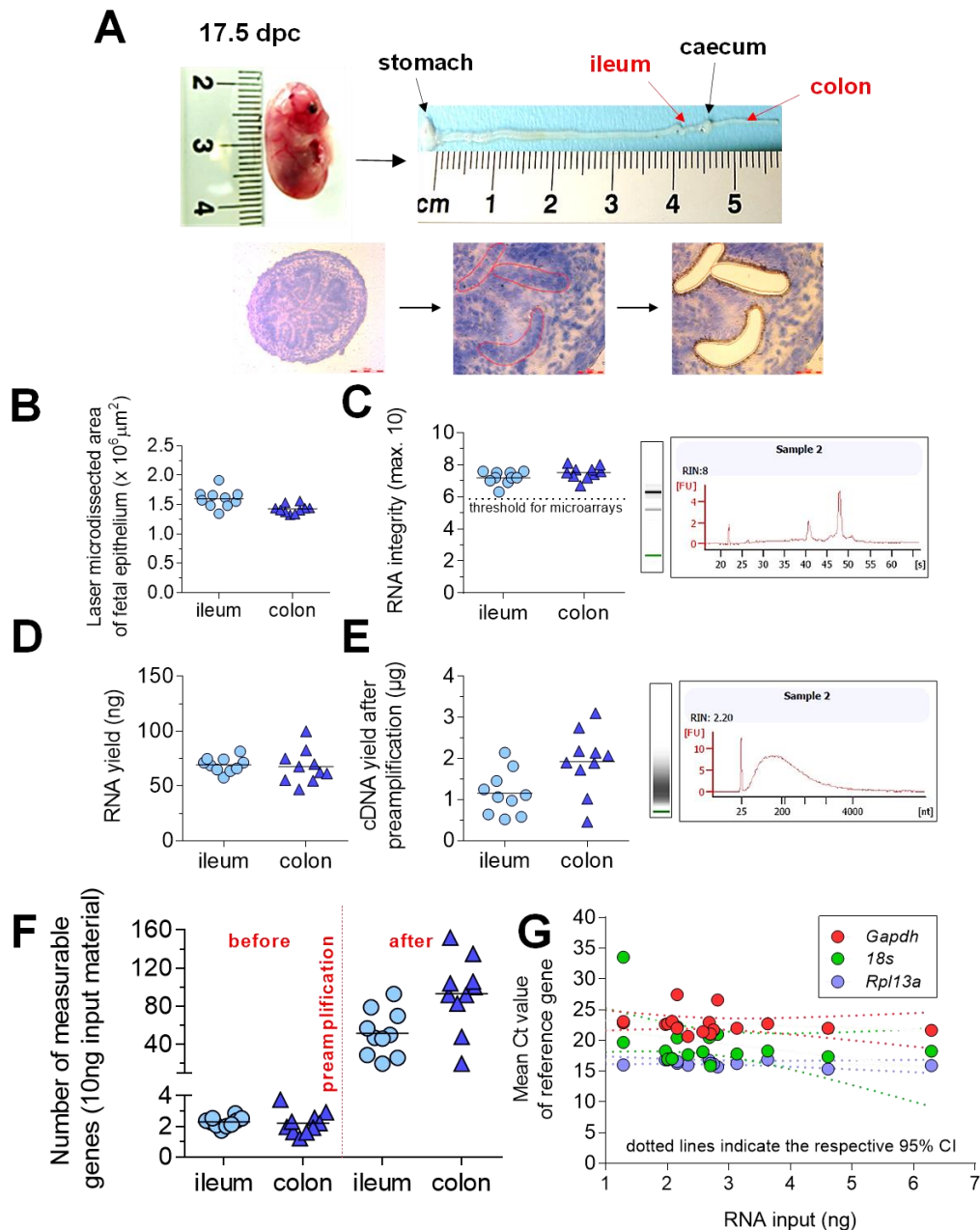


Figure 17 Laser microdissection of fetal intestinal epithelial cells from ileum and colon. (A) Randomly selected fetus corresponding 17.5 dpc (upper left), a macroscopic view of a 17.5 dpc gut (upper right) and subsequent laser microdissection procedure of fetal epithelium (panel below) are indicated. (B) Epithelial areas of $1.59 \pm 0.15 \times 10^6 \mu\text{m}^2$ (mean \pm SD) and $1.42 \pm 0.08 \times 10^6 \mu\text{m}^2$ were isolated by laser microdissection for global and targeted gene expression analysis from ileum and colon, respectively. (C) Total RNA of good quality was isolated with a mean RIN of 7.20 ± 0.40 (ileum) and 7.52 ± 0.41 (colon) with a representative electropherogram of RNA (Bioanalyzer 2100, Agilent). (D) Mean yield of ileal RNA ($69.52 \pm 6.74 \text{ ng}$) and colonic RNA ($67.80 \pm 15.42 \text{ ng}$). (E) After preamplification a SPIA cDNA yield of $1.15 \pm 0.53 \mu\text{g}$ and $1.92 \pm 0.76 \mu\text{g}$ was obtained from ileal and colonic IEC. CDNA quality (right) was confirmed by Bioanalyzer (Eukaryote Nano RNA Chip). (F) The corresponding average number of 51 and 93 measurable target genes after SPIA preamplification is depicted. (G) Stability of reference genes (*Gapdh*, *18s* and *Rpl13a*) measured by qPCR is shown relative to the RNA input amount (2-6ng) into SPIA preamplification.

3.4.2. Epithelial expression of *Muc2* and *Hoxb13* discriminates fetal ileum from colon

To further validate this protocol a comparative analysis exemplarily with *Muc2* gene and protein expression was performed. *Muc2* gene expression analysis of preamplified cDNA revealed lower expression in fetal ileum compared to colon in both methods, microarrays and qPCR. There is a moderate, but significant correlation between *Muc2*-related microarray fluorescence intensity and its $2^{-\Delta Ct}$ values in qPCR. Immunofluorescence analysis biologically confirmed this increase of MUC2 from ileum to colon at the level of protein expression. Finding appropriate (early expressed) epithelial-specific markers for either of the intestinal compartments is challenging as many expression levels were low (array spot intensity < 50, e. g. *Olfir* genes, *Pept1*). However, microarray fluorescence filtering (fold change ± 1.3 , $p < 0.05$, array spot intensity > 50) highlighted *Muc2* and *Hoxb13* genes as highly expressed epithelial markers specific for the fetal colonic epithelium, which enables a discrimination between ileum and colon (Figure 18C). *Muc2* expression significantly correlated with the expression of the colonic marker *Hoxb13* [250, 251] in both, global and targeted gene expression analysis.

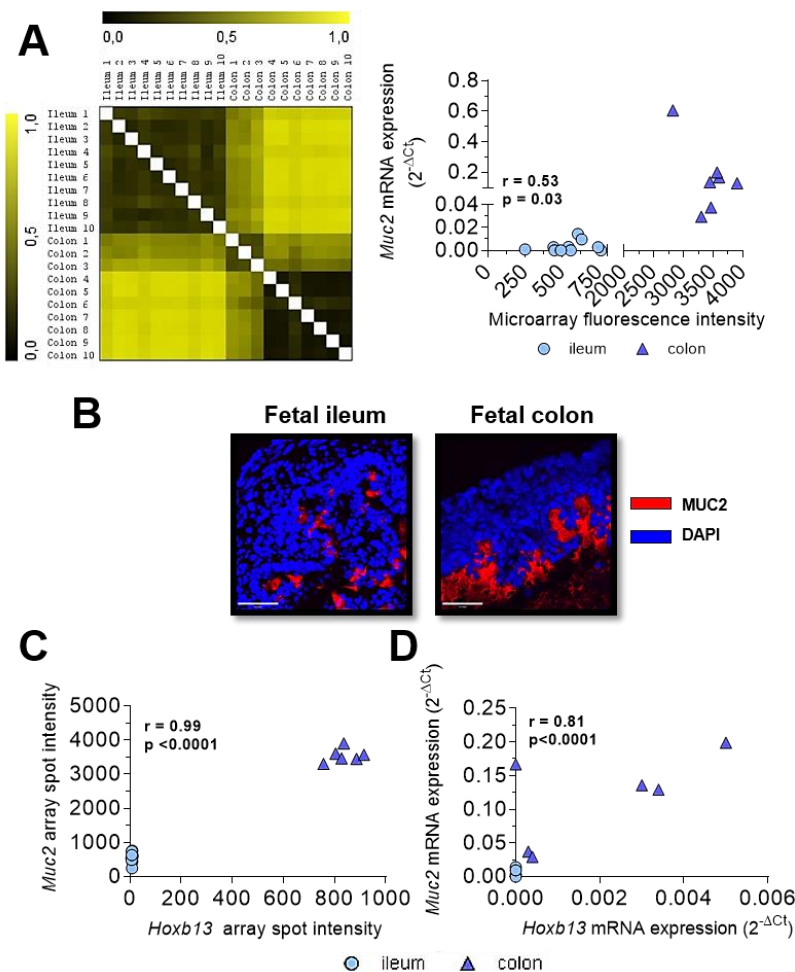
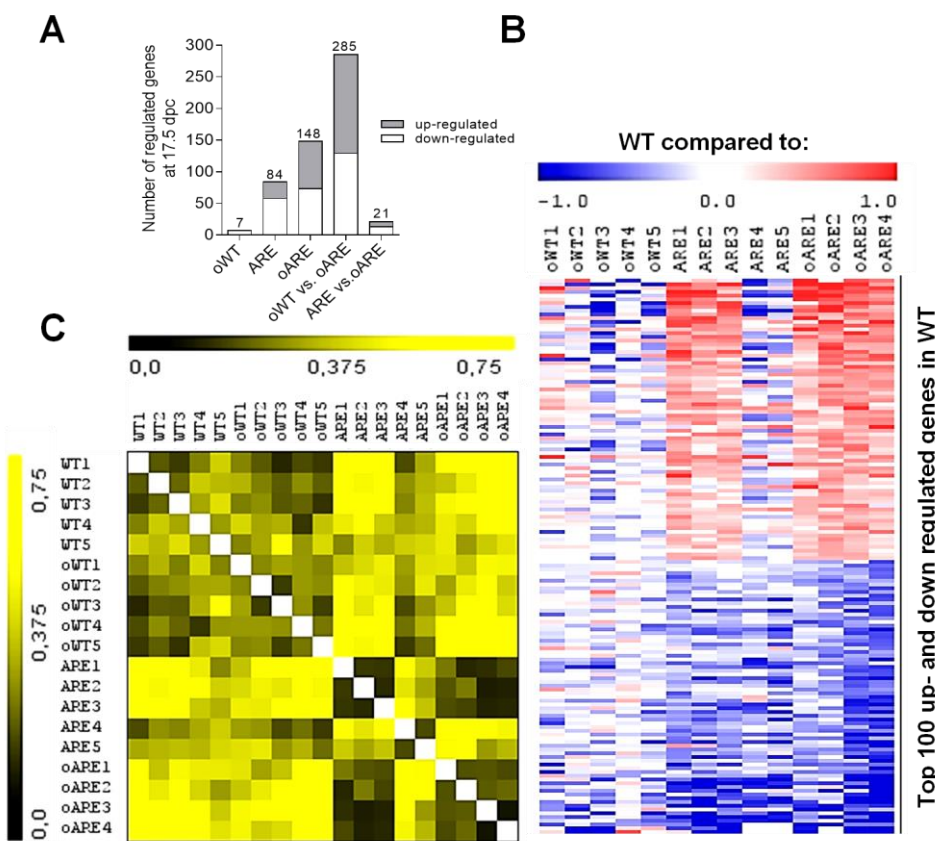


Figure 18 Proof of concept by comparative analysis of *Muc2* gene expression in fetal ileum and colon. (A) left: CDNA was hybridized to Affymetrix GeneChip Mouse Gene 1.1 ST targeting 21,187 genes. Gene distance comparisons of fetal ileum and colon show distinct gene expression patterns between ileum and colon (all genes included). Right: Microarray spot intensities of *Muc2* gene significantly correlates (Pearson correlation $r=0.53$, $p=0.03$) with $2^{-\Delta Ct}$ values of *Muc2* gene expression measured via qPCR. *Rpl13a* was chosen as housekeeping gene. (B) Representative pictures of MUC2 protein expression in the 17.5 dpc fetal ileum versus colon showed increased expression in colon compared to ileum. (C) Microarray data showed that *Muc2* array spot intensity strongly correlated with the array spot intensity of *Hoxb13*, a colonic epithelial marker (left, $r_{\text{Pearson}}=0.99$, $p<0.0001$) reflecting differences between ileal and colonic compartments. (D) QPCR analysis revealed a similar association between *Muc2* and *Hoxb13* expression. *Muc2* mRNA expression strongly correlated with *Hoxb13* mRNA expression ($r_{\text{Pearson}}=0.81$, $p<0.0001$). Those findings technically validate the workflow and the expression values from global gene expression analysis.

As a conclusion whole transcriptome preamplification in RNA samples of laser microdissected fetal epithelia enables both, global and targeted gene expression analyses to study the impact of maternal diet-induced obesity (mDIO) on the fetal transcriptome.

3.5. Maternal diet induced obesity (mDIO) hardly influenced the epithelial transcriptome of the fetal ileum in WT and *Tnf^{flARE/+}* mice

The establishment of SPIA WTA in RNA samples of laser microdissected fetal epithelia enables to study the impact of maternal diet-induced obesity (mDIO) on the fetal transcriptome. Using LMD about 50ng of good quality RNA (mean RIN=7.3) were obtained and microarrays were performed in cooperation with the University of Wageningen. Genes were defined as significantly changed with a p-value <0.05 and a log2 based fold change of ± 1.3 .



Lists of significantly regulated genes were filtered, according to the control group (WT) with expression values higher than 50. In addition, an inter quartile range (IQR) cut-off of 0.25 was used to filter out genes that showed little variation between the conditions. All microarray data are MIAME compliant.

Figure 19 Fetal transcriptional programming is hardly affected by maternal HFD. (A) The diagram depicts the number of significantly regulated genes between pairwise comparisons. Three left hand bars indicate the number of regulated genes compared to WT, the other bars compare groups as indicated. Data were filtered by $FC_{\pm 1.3}$, $p < 0.05$, array spot intensity > 50 . (B) Heat map comparisons show distinct expression patterns of the top 100 up- and downregulated genes always in comparison to WT fetuses from control diet dams ($FC_{\pm 1.3}$, $p < 0.05$, no intensity filtering). (C) The gene distance matrix shows overall similarities between groups at the level of differentially regulated genes. Black colours correspond to a high similarity score between samples and yellow colours show less similarity between samples.

The fetal epithelial transcriptome was hardly influenced by both, maternal obesity and fetal genotype (Figure 19)[252]. Interestingly, only 1.3% of all 21,187 genes were significantly regulated according to our cut-off criteria ($FC \pm 1.3$, $p < 0.05$, array spot intensity > 50). Less genes were influenced by mDIO than by the fetal ARE genotype (7 vs. 84 genes, Figure 19A). In detail, mDIO differentially regulated 7 genes between WT and oWT and 21 genes between ARE and oARE mice. However, the fetal genotype (WT vs. ARE) influenced 84 genes. In addition, the factors ARE fetus genotype and mDIO acted synergistically as even more genes were regulated between WT and oARE (148 genes). Interestingly, 285 genes were differentially regulated between oWT and oARE indicating that an mDIO-exposed *in utero* environment intensified the difference between WT and *Tnf^{ΔARE/+}* fetuses. Heat map comparisons of the top 100 up and downregulated genes illustrate similar gene expression patterns between WT and oWT, but distinct patterns between WT and ARE or WT and oARE fetuses ($FC \pm 1.3$, $p < 0.05$, no intensity filtering, Figure 19B). Furthermore, gene distance matrix (GDM) analyses indicate that transcriptomic make-ups were clustered according to the fetus genotype (low distance (black)=strong similarity between WT and oWT or ARE and oARE groups), but not in response to maternal HFD (high distance (yellow)=little similarity between WT and ARE or oWT and oARE) (Figure 19C). This led to the assumption that the transcriptional program is dominantly regulated by the fetal genotype than by mDIO.

Gene overlaps of top regulated genes between groups are shown in Figure 20A. Only 7 genes were down regulated between WT and oWT fetuses and none were up regulated. Between ARE and oARE fetuses, 21 regulated genes were identified to be differentially regulated, but they were not present in the list of regulated genes between WT and oWT comparison. This indicates that mDIO triggered different transcriptional programs in WT and ARE fetuses. The same was true for comparisons between WT and ARE or oWT and oARE. Only 18% of all regulated genes (15 genes) in the ARE expression pattern (compared to WT) could be as well identified in the oARE expression pattern (compared to oWT). This demonstrates that upon mDIO a different set of genes was regulated in *Tnf^{ΔARE/+}* compared to WT fetuses.

Microarray data were exemplarily verified by qPCR of SPIA cDNA exemplarily with *Afp* (*alpha fetoprotein*) mRNA, which was significantly increased in oARE fetal IEC compared to WT and oWT (Figure 20B). Although *I18* and *Reg3b* gene expression changes were not significantly regulated in qPCR analysis, they also display the results of microarray analysis (Figure 20C). In detail, microarray and qPCR analysis show down regulated *I18* gene expression in response to maternal HFD (WT vs. oWT). Interestingly, this was independent of the fetal genotype. *Reg3b* up-regulated gene expression in oARE IEC (compared to WT) was as well observed in qPCR analysis. Despite the upregulation of *Afp* and *Reg3b* expression in oARE compared to WT and ARE mice at the fetal stage, this pattern was not conserved in intestinal

tissue of 8- and 12-week-old offspring as observed by qPCR analysis (Figure 20C). However, there was significant downregulation of *Ii18* and *Reg3b* in the distal ileum of *Tnf^{flARE/+}* compared to WT offspring, which was most probably inflammation-driven.

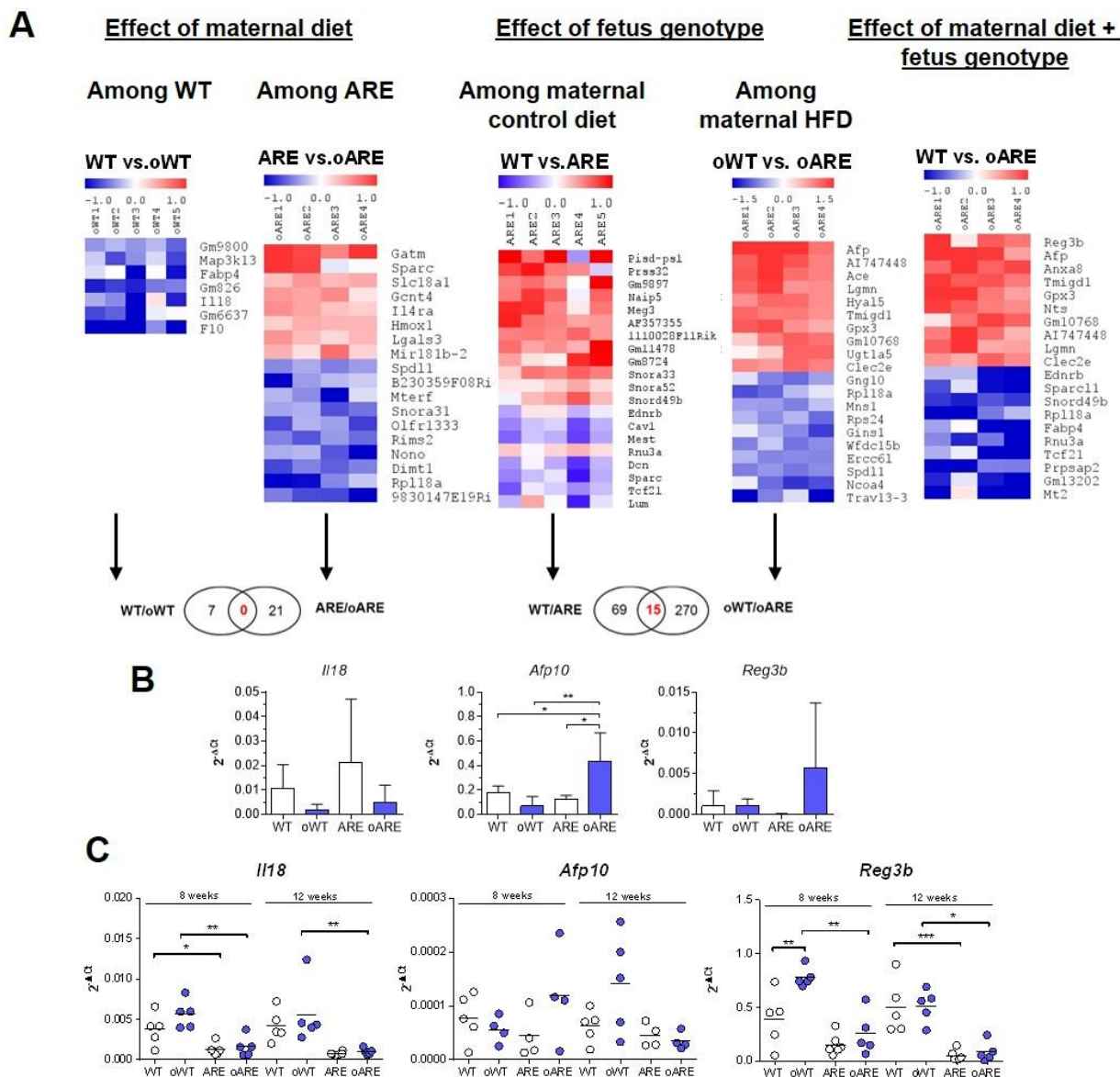
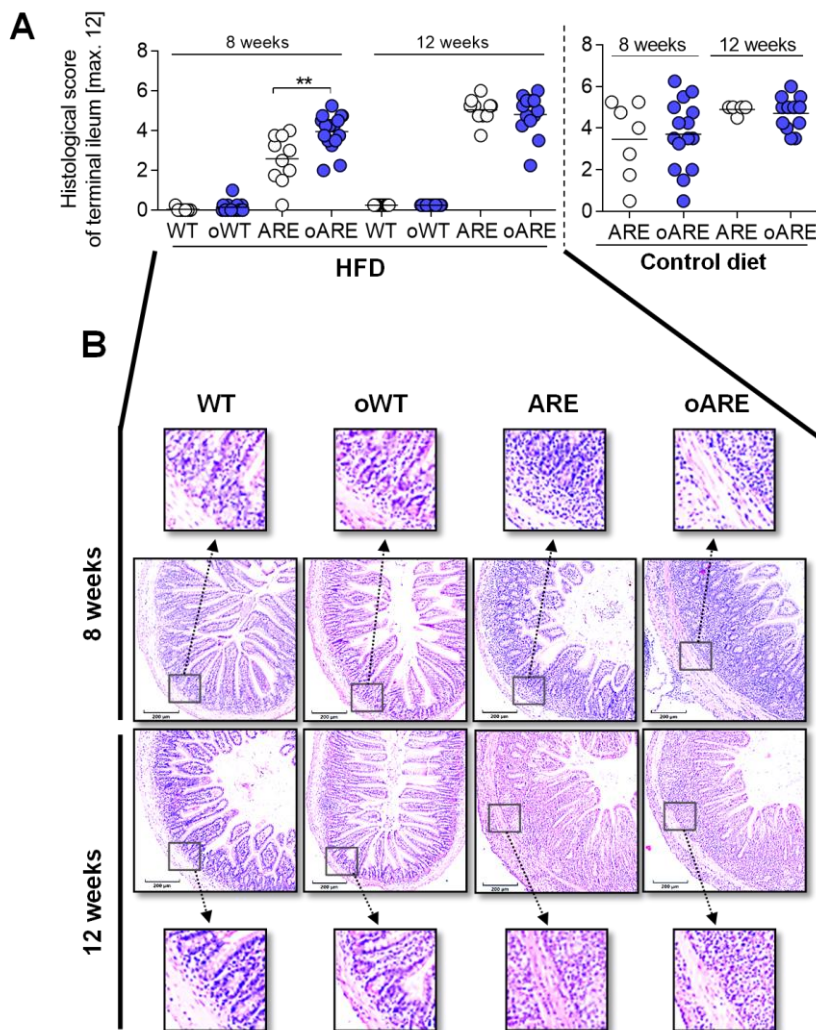


Figure 20 Overlapping and top regulated genes in fetal intestinal epithelial cells in response to mDIO or fetal genotype. (A) Numbers of shared genes (indicated in red) between different gene expression patterns. The panel above shows heat maps of the top up- and down regulated genes between indicated groups. Cut-off criteria were $FC \pm 1.3$, $p < 0.05$, array spot intensity > 50 . (B) Microarray validation of *Afp* and *Reg3b* by qPCR. * $p < 0.05$, ** $p < 0.01$, *** $p < 0.001$. Two-Way ANOVA followed by Holm-Sidak multiple comparisons. (C) Epithelial gene expression (by qPCR) of *Ii18*, *Afp10* and *Reg3b* from adult ileal cryosections ($n=5$ each) at 8 and 12 weeks of age. Results are expressed at $2^{-\Delta\Delta CT}$ values in order to compare pair-wise. * $p < 0.05$, ** $p < 0.01$, *** $p < 0.001$. Two-Way ANOVA followed by Holm-Sidak multiple comparisons.

3.6. Maternal diet induced obesity accelerates intestinal inflammation in high-fat diet-fed *Tnf^{ARE/+}* mice.

Although mDIO had no strong *in utero* effects on the fetal epithelial transcriptome, other tissue sites of the gut, e. g. submucosa might nevertheless have been existed with potential consequences on the postnatal development of CD-like ileitis in *Tnf^{ARE/+}* offspring. To address this issue, 8 and 12 week-old WT and *Tnf^{ARE/+}* offspring were generated as indicated in the breeding scheme above (Figures 5 and 6) and received a postweaning experimental control or HFD from 4 weeks of age on. Histological scoring of distal ileum sections from ARE and oARE offspring confirmed age-dependent disease progression independent of the postweaning diet (control or HFD) (Figure 21). However, mDIO effects on histological disease scores were different among the diets. ARE and oARE offspring weaned on a control diet exhibited equal histological ileitis grades at 8 and 12 weeks of age, whereas oARE offspring



weaned on a HFD showed increased inflammation (compared to ARE) at 8 weeks, but not at 12 weeks of age. WT offspring exhibited no inflammation in the distal ileum at either time point or diet.

Figure 21 Postnatal development of CD-like ileitis in *Tnf^{ARE/+}* offspring is accelerated by fetal exposure to maternal diet-induced obesity (mDIO). (A) Histological scores of H&E stained distal ileum sections from WT and ARE offspring deriving from control dams and HFD dams, respectively, was blindly ascertained resulting in a score from 0 (not inflamed) to 12 (inflamed). 8 and 12-week old offspring were fed a HFD after 4 weeks of age. (B) Representative specimens of H&E stained distal ileum sections of HFD-fed WT, oWT, ARE and oARE offspring are shown.

Further investigations of distal ileum sections from HFD-fed offspring confirmed these findings. WT and oWT offspring showed no infiltration of Ly6G-positive (Ly6G+) cells/mm² tissue (infiltrating neutrophils) into the mucosa and submucosa (Figure 22). However, ARE and oARE mice clearly exhibited increased numbers of Ly6+ cells, a hallmark for the grade of neutrophil infiltration. In detail, the numbers of Ly6G+ cells were significantly increased in 8 week-old oARE compared to ARE offspring, whereas neutrophil infiltration was comparable in 12 week-old ARE and oARE offspring. This indicates that mDIO accelerated ileitis development without affecting its severity at later ages.

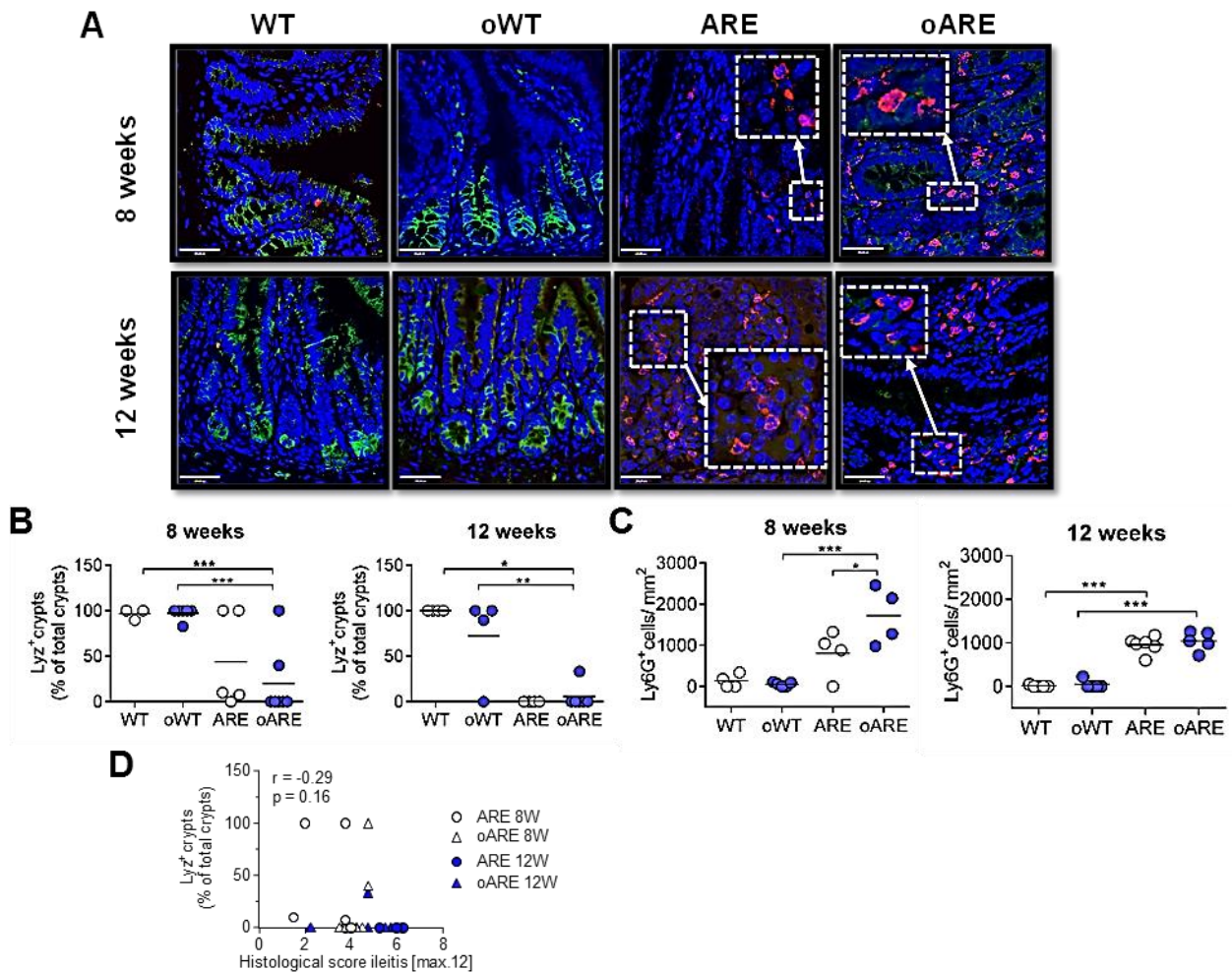


Figure 22 Neutrophil infiltration into distal ileum of $Tnf^{\Delta ARE/+}$ offspring is accelerated by maternal diet-induced obesity, without affecting loss of Lysozyme+ cells in crypts. (A) Representative microscopic immunofluorescence pictures (600x magnification) of confocal laser microscopy for Lysozyme (Lyz, green), a hallmark for Paneth cells, and Ly6G+ neutrophils (red) from distal ileum in 8- and 12-week old WT, oWT, ARE and oARE offspring on postnatal HFD. Nuclei were counterstained with DAPI (blue). **(B)** Three pictures per mouse were analyzed. The percentage of Lyz+ crypts compared to total number of crypts was ascertained per mouse (n=5-6 each). Individual data and means are shown. Two-Way ANOVA and Holm-Sidak multiple comparisons, *p<0.05, **p<0.01, ***p<0.001. **(C)** Lamina propria and submucosa were defined as regions of interest. The numbers of Ly6G+ cells per mm² from all 3 pictures per mouse were counted. Individual data and means are shown. Two-Way ANOVA and Holm-Sidak multiple comparisons, *p<0.05, **p<0.01, ***p<0.001. **(D)** Correlation analysis among ARE and oARE groups indicated no associations between histological scores and the number of Lyz+ crypts ($r_{Spearman} = -0.29$, $p = 0.16$)

Immunohistochemical measurements of the Paneth cell marker lysozyme (Lyz) revealed an inflammation-driven loss of Lyz-positive (+) crypts in $Tnf^{ARE/+}$ mice (compared to WT mice). However, this was not affected by mDIO at either time point and the number of Lyz+ crypts did not correlate with the histological ileitis score ($r_{\text{Spearman}}=-0.29$, $p=0.16$). The same was observed for inflammation-associated infiltration of Myeloperoxidase-positive (MPO+) cells into the distal ileum ($r_{\text{Spearman}}=0.22$, $p=0.28$). There was a clear infiltration of MPO+ cells into the mucosa and submucosa of $Tnf^{ARE/+}$ mice compared to WT mice, which was not further altered by mDIO indicating that MPO infiltration is a feature of genetically-driven ileitis (Figure 23).

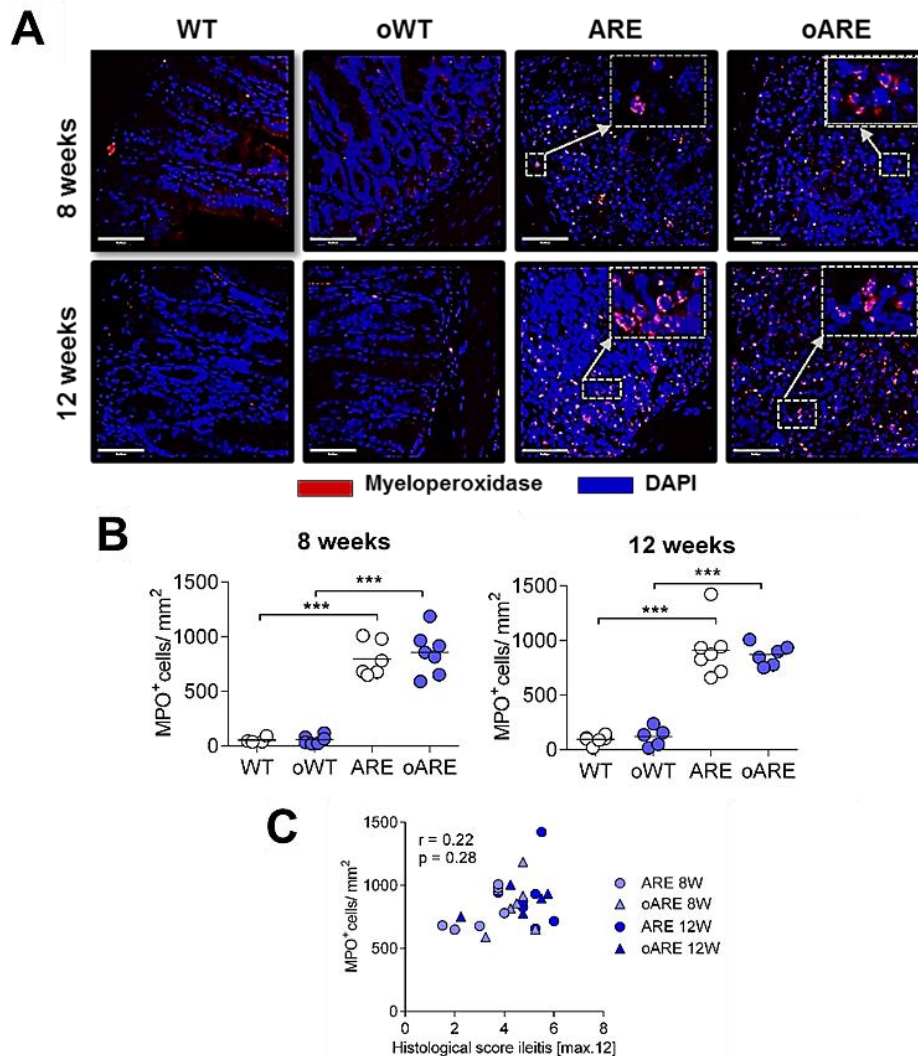


Figure 23 Myeloperoxidase (MPO)-positive cell-infiltration is not affected by maternal diet-induced obesity (mDIO). (A) Representative microscopic immunofluorescence pictures (600x magnification) of confocal laser microscopy for MPO+ cells (red) from distal ileum in 8- and 12-week old WT, oWT, ARE and oARE offspring on postnatal HFD. Nuclei were counterstained with DAPI (blue). (B) Lamina propria and submucosa were defined as regions of interest. The numbers of MPO+ cells per mm² from all 3 pictures per mouse were counted. Individual data and means are shown (Two-Way ANOVA and Holm-Sidak multiple comparisons, * $p < 0.05$, ** $p < 0.01$, *** $p < 0.001$). (C) Correlation analysis in $Tnf^{ARE/+}$ offspring indicated no associations between histopathological scores and infiltration of MPO+ cells ($r_{\text{Spearman}}=0.22$, $p=0.28$).

The mDIO-associated increase of intestinal inflammation in 8 week-old oARE mice was also observed systemically (Figure 24). TNF protein in plasma was not statistically significantly higher in 8 and 12 week-old oARE compared to ARE mice. However, the histological ileitis scores in $Tnf^{\Delta ARE/+}$ mice significantly correlated with systemic TNF levels ($r_{\text{Spearman}}=0.52$, $p=0.04$). A closer look into 8 week-old offspring indicated slightly increased portal vein endotoxin in $Tnf^{\Delta ARE/+}$ mice upon maternal HFD ($p=0.07$). Interestingly, the increase of portal vein endotoxin highly correlated with elevated plasma TNF in 8 week-old offspring ($r_{\text{Pearson}}=0.91$, $p=0.0006$). In summary, histological scoring, immunofluorescence analyses and systemic measurements revealed that, mDIO accelerated the development of CD-like ileitis in $Tnf^{\Delta ARE/+}$ offspring that were challenged with a postnatal HFD, whereas mDIO alone had no effect on tissue pathology of $Tnf^{\Delta ARE/+}$ mice.

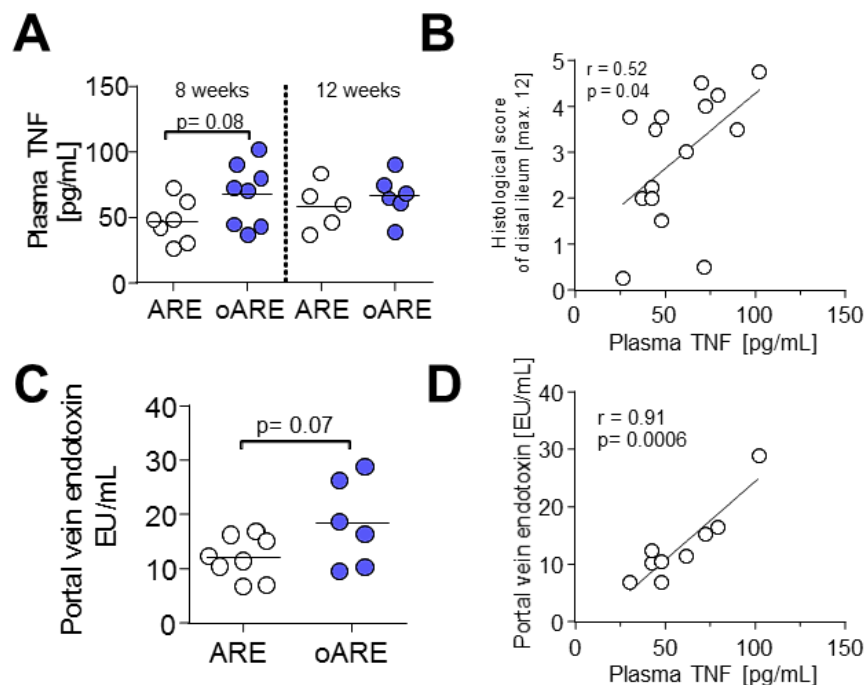


Figure 24 The development of ileitis in $Tnf^{\Delta ARE/+}$ offspring is associated with increased TNF plasma levels and elevated portal vein endotoxin. **(A)** Plasma measurements of TNF indicate a slightly, but not significantly increased inflammation in 8 week old oARE mice compared to ARE offspring. This difference is not observed anymore at 12 weeks of age. **(B)** Spearman's correlation analysis of TNF plasma levels and respective histological scores ($n=15$) indicate a significant association between tissue inflammation and protein levels of systemic TNF. **(C)** Endotoxin levels were investigated in portal vein plasma from 8 week old ARE and oARE mice. **(D)** Pearson's correlation analysis of TNF plasma levels and corresponding endotoxin concentrations in portal vein plasma ($n=10$) highlight on a strong and significant association between the two parameters ($r_{\text{Pearson}}=0.91$, $p=0.0006$).

3.7. Maternal diet-induced obesity protects WT offspring from metabolic dysfunction induced by post weaning HFD.

The fact that mDIO increased fetal weights regardless of the fetus genotype (Figure 15D) might point to metabolic changes in response to mDIO. Metabolic parameters were subsequently analyzed in WT and ARE offspring that were fed a control or HFD (Figure 25). Expectedly, an obesity phenotype was observed in WT offspring in response to postnatal HFD, which was absent in $Tnf^{\Delta ARE/+}$ offspring [60]. Body weights from ARE and oARE mice were significantly lower compared to their WT and oWT littermates. After 12 weeks of postnatal HFD-exposure, WT and oWT offspring revealed a clear obesity-like phenotype, which was not yet observed after 8 weeks of HFD-exposure. Surprisingly, mDIO protected oWT offspring from excessive body weight gain. This effect was even stronger in male than in female WT offspring (Figure 25B). The absent obesity phenotype in $Tnf^{\Delta ARE/+}$ mice was also reflected by lower mesenteric adipose fat pad weights and partially reduced plasma leptin levels in ARE and oARE mice compared to their respective WT controls, demonstrating that diet-induced obesity is restricted to WT mice (Figure 26).

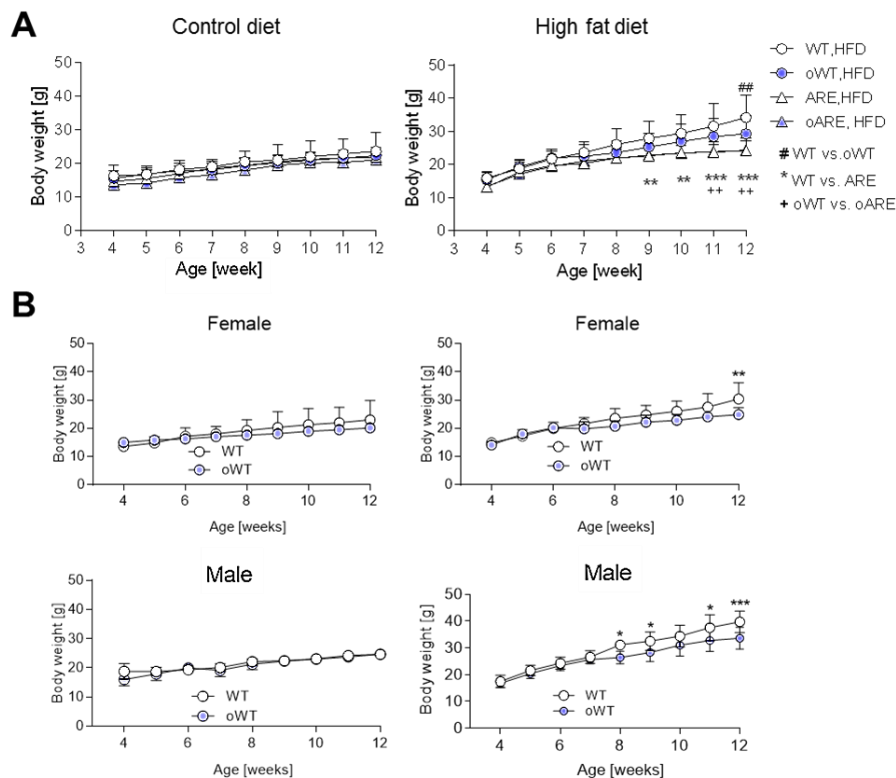


Figure 25 Body weight development in response to mDIO and postnatal HFD. All offspring were fed a control diet or HFD from 4 weeks of age on. Body weights were monitored weekly until 12 weeks of age. **(A)** Body weights of WT, oWT, ARE and oARE mice on control diet (left) and HFD (right) ($n=10-14$ each). **(B)** Gender-specific development of body weight upon exposure to control diet or HFD ($n=5-7$ each). Two-Way ANOVA and Holm-Sidak multiple comparisons, * $p<0.05$, ** $p<0.01$, *** $p<0.001$.

This might be due to genetically driven-inflammation in $Tnf^{ARE/+}$ offspring which drives fatty acid liberation from adipose tissue sites by increased TNF. Consequently, early metabolic priming by mDIO was restricted to WT offspring.

Similar to the body weight differences between 12 week-old WT and oWT offspring, mesenteric fat masses, and plasma leptin levels were significantly decreased in response to mDIO (Figure 26). The fact that control diet-fed WT offspring showed no alterations of body weight clearly indicated that a second hit by postnatal HFD is crucial for an mDIO-associated attenuation of an obesity-like phenotype.

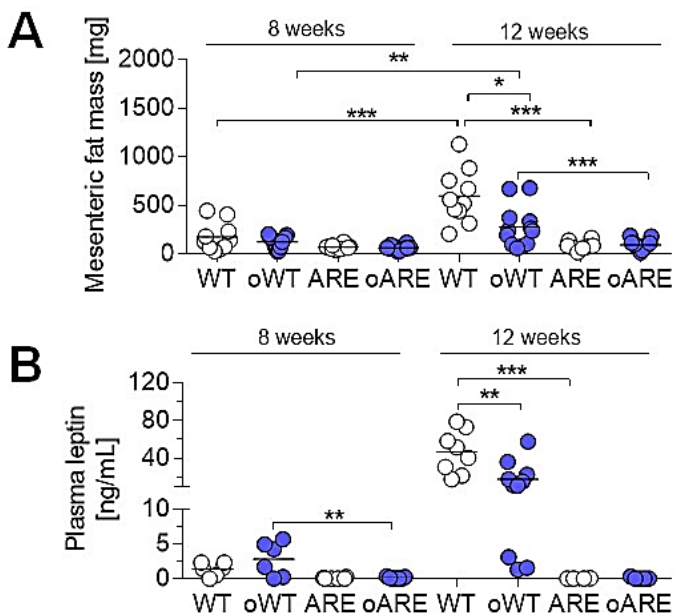


Figure 26 MDIO protects WT offspring from excessive energy storage and shows no metabolic influence on $Tnf^{ARE/+}$ offspring. (A) Mesenteric fat mass was determined in 8- and 12-week old WT, oWT, ARE and oARE offspring ($n = 8-13$ each). (B) Plasma leptin concentration was measured by ELISA (Biovendor, Czech Republic). Two-Way ANOVA and Holm-Sidak multiple comparisons, * $p < 0.05$, ** $p < 0.01$, *** $p < 0.001$.

In summary, maternal diet-induced obesity during gestation had different effects in WT compared to $Tnf^{ARE/+}$ progeny. MDIO is advantageous against the development of metabolic disease by limiting the fat storage capacity in WT offspring, whereas mDIO accelerates the development of CD-like ileitis in the genetically-susceptible $Tnf^{ARE/+}$ offspring.

3.8. Protection against DSS-induced colitis severity is attributed to maternal inflammation, but not to mDIO

Since both, the sole presence of maternal inflammation and maternal diet-induced obesity were not sufficient to alter the severity of genetically-driven ileitis in $Tnf^{ARE/+}$ offspring, this was also tested in a second model of intestinal inflammation, experimentally induced colitis of WT offspring. Therefore, 12 week-old WT offspring that derived either from healthy WT mothers and inflamed $Tnf^{ARE/+}$ mothers (maternal inflammation, WT and iWT) or from lean WT mothers and HFD-fed mothers (maternal diet-induced obesity, WT and oWT) were exposed to 1% DSS in drinking water for 7 days. As expected, water control mice did not lose body weight and showed no signs of inflammation throughout the whole period of observation (% of initial body

weight, mean range: min 99.64%-max 102.24% in WT vs. min 98.23%-max 102.83% in iWT and disease activity index, mean range: min 0-max 0.11 in WT vs. min 0-max 0.22 in iWT).

Monitoring of DSS consumption confirmed comparable cumulative DSS uptake (Day1-7) in all treatment groups (WT vs. iWT: $0.43\pm 0.06\text{g}$ vs. $0.44\pm 0.10\text{g}$ DSS and WT vs. oWT: $0.47\pm 0.10\text{g}$ vs. $0.50\pm 0.12\text{g}$ DSS) (Figure 27).

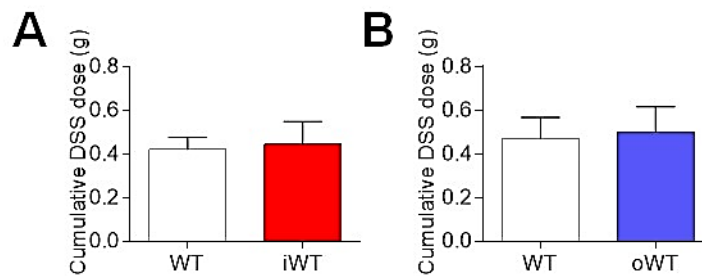


Figure 27 Cumulative DSS exposure is equal among studies in (A) WT and iWT offspring (maternal inflammation) or (B) WT and oWT offspring (maternal diet-induced obesity). WT offspring ($n=6$, no littermates within one group) were generated and fed Sniff Chow diet throughout post weaning life. At 12 weeks of age offspring were exposed to 1% DSS (w/v) for 7 days in their drinking water and were housed separately. Drinking water consumption was monitored daily and cumulatively consumed DSS dose was calculated. Unpaired, two tailed T-test was performed.

Surprisingly, maternal inflammation protected iWT offspring against DSS colitis, whereas mDIO did not alter disease course in oWT compared to WT offspring (Figure 28). In detail, during DSS exposure (day 1-7) body weights of all offspring remained stable and started to decrease during water recovery phase (days 7-11). Dropping body weights were comparable in oWT compared to WT offspring, but were less severe in iWT offspring. Thus, iWT offspring lost less body weight (day 10-12) and showed an earlier body weight recovery (at day 12) compared to WT offspring (day 14) indicating a less severe DSS colitis (Figure 28A). Furthermore, iWT offspring showed significantly attenuated clinical signs of colitis (diarrhea, weight loss and rectal bleeding) between day 10 and 13 compared to WT offspring, whereas oWT compared to WT offspring had the same disease activity throughout whole observation period (Figure 28B). The rising DAI reflects significantly more rectal bleeding, diarrhea and weight loss in WT compared to iWT between days 10-12. Maximum mean levels of DAI in iWT were 1.53 ± 0.99 and significantly increased up to 2.61 ± 0.70 in WT offspring. Although clinical signs of colitis were attenuated in iWT mice, relative spleen weights were comparable between WT and iWT after recovery (day 15). Overall, after recovery relative spleen weights were significantly increased in all DSS treated animals compared to their water control littermates, but there was no further effect of maternal inflammation or mDIO (Figure 28C). The same is true for colon lengths which showed an upward trend upon DSS treatment, but no further influence by maternal *in utero* exposure to inflammation or mDIO.

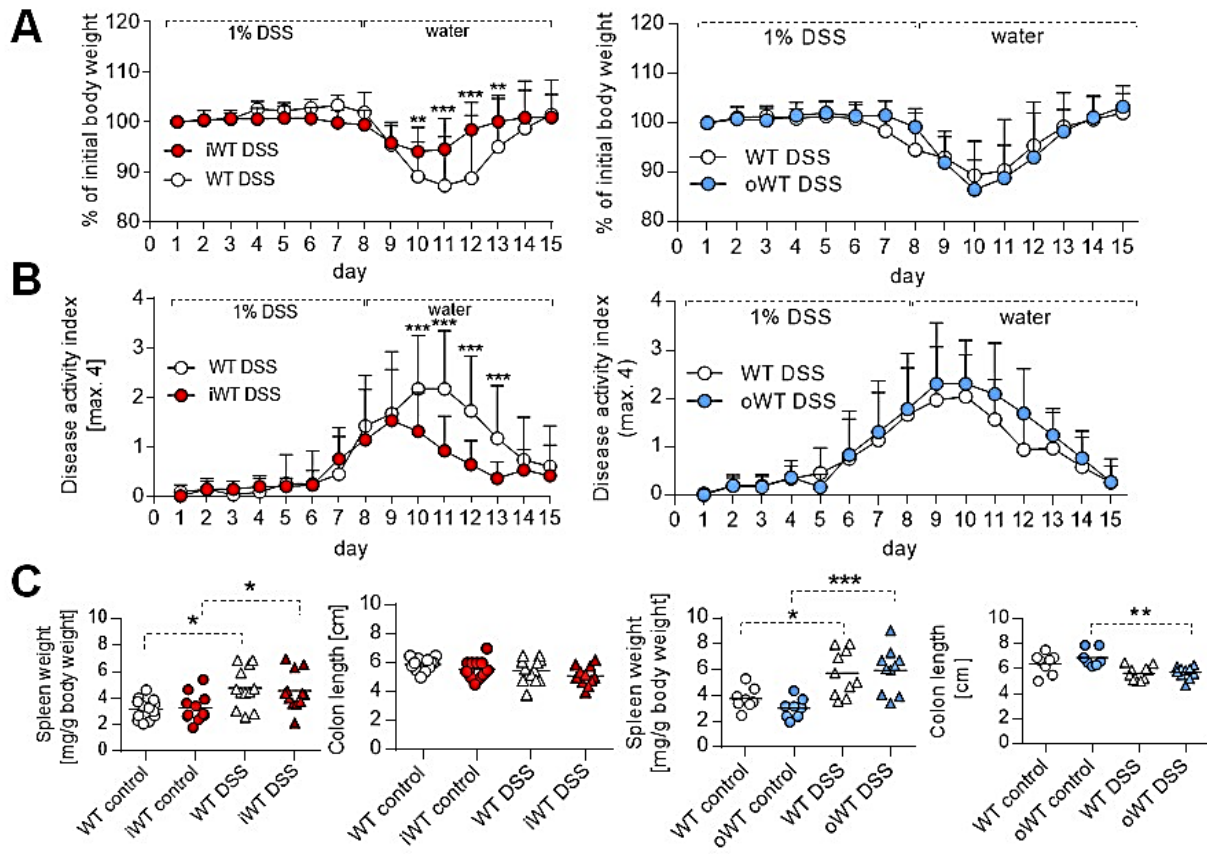


Figure 28. Maternal inflammation, but not mDIO protects offspring against DSS colitis. WT offspring ($n=12$, no littermates within one group) were fed Chow diet throughout post weaning life. At 12 weeks of age offspring were exposed to 1% DSS (w/v) for 7 days in their drinking water, followed by 8 days drinking water without DSS as recovery phase. Control animals received only drinking water throughout the whole experiment. All mice were housed separately. **(A)** Body weight was monitored daily. One-Way ANOVA was performed between WT and iWT or WT and oWT for every day and expressed as percentage of initial body weight (day1). One-Way ANOVA was performed per day. * $p<0.05$, ** $p<0.01$; *** $p<0.001$. **(B)** Disease activity index (DAI) (Cooper et.al [176]) was assessed in order to classify the severity of DSS colitis. The DAI is the mean of 3 clinical signs: stool consistency (scores: 0=normal, 2= loose and 4= diarrhea), rectal bleeding (scores: 0=negative, 2=gross bleeding, 3=bleeding>1d, 4=bleeding>2d) and weight loss, indicated as weight change in % on the basis of initial body weight at day 0 (scores: 0=none, 1=1-5%, 2=6-10%, 3=11-15%, 4>15%). Mann-Whitney Rank Sum Test, * $p<0.05$, ** $p<0.01$, *** $p<0.001$. **(C)** At the end of the experiment (day 15) all mice were sacrificed and relative spleen weights as well as absolute colon lengths were measured. Two-Way ANOVA and Holm-Sidak multiple comparisons, * $p<0.05$, ** $p<0.01$, *** $p<0.001$.

3.9. The epithelial transcriptome in the fetal colon is hardly affected in response to maternal inflammation.

Because maternal inflammation protected iWT offspring from DSS-induced colonic inflammation, it was questioned whether maternal inflammation already programmed the fetal transcriptome of the colonic epithelium. Therefore, the transcriptomes of laser microdissected IEC of 17.5 dpc WT and iWT colons were analyzed. Surprisingly, microarray analysis showed a negligible influence of maternal inflammation on fetal colonic IEC at 17.5 dpc (Figure 29). Only 0.34% of all genes (73 out of 21,187 genes, Affymetrix Exon Array ST 1.1.) were differentially regulated ($FC \pm 1.3$, $p < 0.05$, array spot intensity > 50) by maternal inflammation with 55 up and 18 downregulated genes. Top 10 up- and downregulated genes are depicted in Table 8. The fact that regulation factors did not exceed $FC \pm 2$ shows that the fetal transcriptome of the colonic epithelium was not substantially programmed by maternal inflammation. In conclusion, the altered DSS colitis susceptibility in response to maternal inflammation is not due to a profound transcriptional programming of the colonic epithelium in 17.5 dpc.

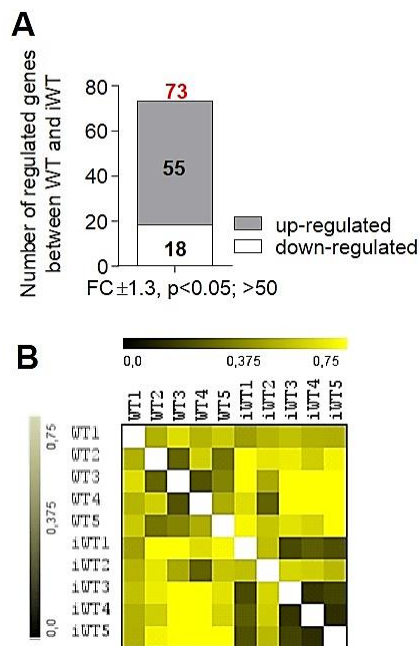


Figure 29 Fetal transcriptional programming of the colonic epithelium is hardly affected by maternal inflammation. (A) The diagram depicts the number of significantly regulated genes in iWT compared to WT fetuses. Data were filtered by $FC \pm 1.3$, $p < 0.05$, array spot intensity > 50 . **(B)** Gene distance matrix shows the overall similarities between groups at the level of differentially regulated genes. Black colours correspond to a high similarity score between samples and yellow colours show less similarity between samples.

Table 8 Top 10 up- and downregulated genes (fold change (FC) ± 1.3 , $p < 0.05$, array spot intensity > 50)

Top 10 up- and down regulated genes between WT and iWT in 17.5 dpc colonic epithelial cells		
ID	Gene	FC iWT
104307	<i>Rnu12</i>	1.90
319181	<i>Hist1h2bg</i>	1.78
69036	<i>Zg16</i>	1.68
67532	<i>Mfap1a</i>	1.67
15077	<i>Hist2h3c1</i>	1.65
665903	<i>Gm7846</i>	1.60
20383	<i>Srsf3</i>	1.51
102462	<i>Imp3</i>	1.51
22209	<i>Ube2a</i>	1.51
66488	<i>Fam136a</i>	1.47
387174	<i>Mir15a</i>	-1.44
80904	<i>Dtx3</i>	-1.45
76808	<i>Rpl18a</i>	-1.49
382551	<i>Cd300lh</i>	-1.52
19850	<i>Rnu3a</i>	-1.52
320832	<i>Sirpb1a</i>	-1.55
68690	<i>1110028F11Rik</i>	-1.56
100126777	<i>Gm20580</i>	-1.70
100302594	<i>Snord14e</i>	-1.95
19652	<i>Rbm3</i>	-1.97

4. Discussion

It is known that maternal inflammatory stimuli such as inflammation and obesity affect fetal development and consequently the susceptibility to inflammatory processes in various organs including the gut [253-255]. The present work investigated the influence of maternal stimuli, such as TNF-driven maternal inflammation or maternal diet-induced obesity (mDIO) on the offspring's risk to develop ileitis and colitis.

4.1. Maternal inflammation has no impact on genetically-driven CD-like ileitis, but protects from DSS-induced colitis

Pilot experiments of this work clearly demonstrated that both, hygienic and dietary conditions contributed to the onset of genetically driven CD-like ileitis in $Tnf^{\Delta ARE/+}$ mice. In detail, Chow diet feeding in conventional and SPF conditions revealed the same grade of ileitis in $Tnf^{\Delta ARE/+}$ mice, whereas experimental diet feeding in SPF completely protected $Tnf^{\Delta ARE/+}$ mice from chronic ileitis. The protective effect was absent under conventional conditions highlighting that the interplay of diet and hygiene drives the onset of ileitis. This is supported by the fact that the inflammation of Chow diet-fed $Tnf^{\Delta ARE/+}$ mice was abrogated in response to antibiotic treatment. Furthermore a re-establishment of the microbiota composition lead to recurrence of inflammation clearly showing that bacterial colonization of the gut plays an important role in disease development [224]. Most importantly, inflammation of $Tnf^{\Delta ARE/+}$ mice was completely absent in germ-free mice.

A certain maternal influence on the development of CD-like ileitis was already analyzed in previous mouse studies demonstrating that TNF-driven maternal inflammation substantially modulates the transcriptional profile in the fetal intestinal epithelium of the ileum [245]. However, maternal inflammation did not affect the onset or severity of chronic ileitis in $Tnf^{\Delta ARE/+}$ offspring fed a postnatal Chow diet. This implies that transcriptional fingerprints in the fetal gut were completely overwritten by signals deriving from the postnatal environment.

A possible proinflammatory postnatal factor that could have masked maternal inflammatory effects on the offspring's intestinal inflammation might be the wheat-based Chow diet. This is plausible, because gluten was identified in Chow diet as a relevant factor for the induction of chronic ileitis in $Tnf^{\Delta ARE/+}$ mice. Furthermore, a protective effect of experimental diet was associated with decreased expression of inflammation markers in ileal tissues [223]. Most importantly, gluten-fortified experimental diets again induced chronic ileitis in $Tnf^{\Delta ARE/+}$ mice indicating that gluten drives inflammation. To avoid the situation, that the severity of inflammation is not modifiable due to gluten-containing Chow diet, the present study addressed

a possible maternal inflammatory influence on the offspring's ileitis under conditions of experimental diet from week 4 on.

Maternal inflammation in *Tnf*^{ΔARE/+} dams is systemically relevant as intrinsic overexpression of *Tnf* significantly elevated TNF plasma levels and might therefore influence the fetuses indirectly via the placenta. Whether TNF is able to cross the placenta is not fully understood. However, TNF suppresses lipogenesis and promotes fatty acid liberation from dam's adipose tissues. This is biologically plausible either by direct TNF action in the fetuses or by indirect TNF effects via reduced *in utero* energy supply in inflamed (ARE) mothers. The catabolic effect of TNF might explain significantly reduced body weights in pre-, peri- and postnatal offspring. Although iWT and iARE offspring from inflamed mothers have a metabolic disadvantage compared to WT and ARE mice, the severity of CD-like ileitis in iARE offspring was not altered by maternal inflammation, since histological grades, the number of infiltrated neutrophils (Ly6G+cells/mm²) and the extent of crypt loss (% of Lyz+ crypts) in the distal ileum were comparable to ARE mice. This is also in line with the fact that the immune response at the site of inflammation was consistently unaffected by maternal inflammation in two different mouse models for genetically-driven ileitis and colitis inflammation [245]. In addition, equal proportions of CD4+ and CD8ab+ T cell subsets in MLNs and spleens from ARE compared to iARE offspring shows that maternal inflammation has no postnatal immunomodulatory effects in the offspring. Interestingly increased proportions of activated (CD44+) CD8ab+ intraepithelial lymphocytes (IEL) were associated with the development of CD-like ileitis in the *Tnf*^{ΔARE/+} mouse model [256] and were also observed in splenic lymphocytes of iARE compared to iWT mice. However, this result has to be interpreted carefully due to a lack of statistical power in the iWT group by a limited number of samples (n=3). The same is true for CD44+CD4+ cells where elevated levels were observed in MLNs of ARE mice compared to WT. The fact that CD4+ T cells were predominantly involved into the development of colitis [257] does not argue against alterations in *Tnf*^{ΔARE/+} mice, because they are able to exhibit colitis at later disease stages [60]. However, maternal inflammation had no further influence on the proportion of activated CD8ab+ T cells and CD4+ T cells.

Bacterial colonization is crucial for the establishment of the offspring's immune system. Therefore it was hypothesized whether maternal inflammation changes the microbial ecology in the offspring's gut. Previous investigations using Chow dietary conditions showed that maternally-induced changes in the fetal epithelium did not cause any shifts in diversity and composition of caecal bacterial communities at 3 and 8 weeks of age [245]. Diet might be a main confounding factor for the phylogenetic make-up of the caecal content, since wheat-based Chow diet is characterized by highly varying quality due to heterogeneity of raw products used for production. This speculation is supported by clear inflammation-driven shifts in *beta*-

diversity between WT and ARE offspring that were fed an experimental diet which were absent under Chow dietary conditions. The phylum *Firmicutes* was more abundant under postnatal inflammation, whereas *Bacteroidetes* abundance was decreased in ARE versus WT offspring. This is not in line with the dysbiosis paradigm of IBD patients where *Firmicutes* and *Bacteroidetes* were less abundant whereas the phyla *Proteobacteria* and *Actinobacteria* [28] were increased in abundance. As well, a paediatric cohort of treatment-naïve CD patients observed a high association of the disease status with increased abundance in *Enterobacteriaceae*, *Pasteurellaceae*, *Veillonellaceae* and *Fusobacteriaceae* and decreased abundance in *Erysipelotrichaceae*, *Bacteroidales* and *Clostridiales* [258]. *Faecalibacterium prausnitzii*, a butyrate producer and anti-inflammatory representative of the *Firmicutes* was less abundant in CD patients and was associated with increased risk of post resection recurrence of ileal CD [27]. Inconsistency to the literature might be explained by species differences and limited transferability from humans to mice, since coprophagy behaviour of rodents and conventional housing conditions lead to a well-mixed and extremely robust phylogenetic make-up, which might be different in humans. However, maternal inflammation does not cause any shifts in diversity and compositions of caecal bacterial communities of 8 week- old offspring that received an experimental diet, except the *Clostridia* class which was decreased in iWT compared to WT offspring. In essence, the conventional environment, which was used in this study harbours many kinds of pathogens and SFBs, fungi and worms that might manifest CD-like ileitis. This might overwrite the maternal impact.

Altogether, a conclusion from maternal inflammation studies is that maternal inflammatory fingerprints do not persist in grownup mice and are therefore not relevant for the modulation of intestinal inflammation in the genetically susceptible *Tnf^{ARE/+}* mouse. This might be because genetically-driven disease models are hard to modulate and might therefore be critical to investigate maternal inflammatory influences on the development of intestinal inflammation [245]. As a consequence, experimental colitis was induced in healthy WT and iWT offspring at 12 weeks of age. Interestingly, maternal inflammation protected iWT offspring from DSS colitis, even though the fetal colonic epithelium was hardly affected by maternal inflammation *in utero*. Only 73 genes were differentially regulated ($FC \pm 1.3$, $p < 0.05$, > 50 ,) in iWT compared to WT fetuses. This is in contrast to the fetal ileum and cannot be explained so far. It might be that the colonic epithelium is in a “precursor stage” and basically develops upon postnatal bacterial colonization in the perinatal period. However, reduced initial body weights of iWT compared to WT offspring might primarily protect against DSS-driven loss of body weight via energy saving mechanisms. Taking all findings together, offspring’s genetically-driven intestinal inflammation seems to mask maternal inflammatory fingerprints, whereas experimental colitis was clearly modifiable by maternal inflammation in non-predisposed WT offspring towards disease protection.

4.2. Maternal diet-induced obesity in the context of intestinal inflammation

Maternal diet-induced obesity (mDIO) during gestation is known to affect fetal development and disease susceptibility. Further, maternal gestational HFD feeding may initiate adverse pregnancy outcomes [259], which in terms of intestinal inflammation may be relevant to program the fetal gut towards chronic inflammatory responses. One aim of this work was to investigate whether maternal diet-induced obesity transcriptionally programs the fetal intestine and whether mDIO alters offspring's severity of genetically-driven (in *Tnf^{ΔARE/+}* offspring) and DSS-induced intestinal inflammation (in WT offspring). This was the first study that included both, programming of the fetal epithelial transcriptome by mDIO and postnatal outcomes of intestinal inflammation using two different models, genetically-driven ileitis and DSS-induced colitis, challenged with mDIO.

4.2.1. Fetal exposure to maternal-diet induced obesity has marginal effects on the epithelial transcriptome

To investigate the influence of mDIO on the intestine WT dams were fed a control (control dams) or high-fat diet (mDIO dams) and mated with *Tnf^{ΔARE/+}* (ARE) sires. During late gestation mDIO dams showed significantly increased body weights, mesenteric and perigonadal fat pad weights and elevated plasma leptin levels when compared to control dams. As well, fetal progeny of both genotypes exhibited increased body weight under the influence of mDIO. Studies in C57BL6 mice [260], Sprague–Dawley rats [261] and Albino Wistar rats [262] also reported a marked increase in fetal weight associated with maternal gestational HFD, possibly related to increased trans-placental transport of glucose and amino acids, upregulated anabolic pathways and adipogenic differentiation in the offspring [260-263]. Interestingly, upregulation of specific placental amino acid transporter isoforms have also been reported in obese women giving birth to large babies [264]. While there is an ongoing debate on how maternal obesity and/or overnutrition in humans affects fetal growth and weight development [265-267], there is evidence for increased susceptibility to obesity and metabolic disorders for the offspring in later life [265, 266, 268, 269]. In addition, literature indicates that these effects of maternal HFD are further potentiated by post weaning HFD-feeding [112].

From the inflammatory point of view, mDIO increased gene expression of proinflammatory cytokines in dam's mesenteric and perigonadal adipose tissue and was therefore suspected to drive massive inflammatory changes in the placenta. However, placental inflammatory activators (*Il-6*, *Tnf* and *Mcp-1* gene expression) were more affected by the fetal genotype than by mDIO per se. In conclusion, mDIO might have a more pronounced impact on the fetal metabolism, than on the *in utero* cytokine milieu.

To get insights into the transcriptional programming effect of mDIO fetal IEC were transcriptionally profiled. There are two reasons to investigate the fetal transcriptome specifically in IEC. Firstly, barrier-degrading effects of HFD [60] were considered in the fetuses of mDIO dams since fatty acids pass the placenta and are consequently present in the fetal blood. Secondly, *Tnf* overexpression in the adult epithelium is sufficient to trigger ileitis [246] and highlights on the strong involvement of the intestinal epithelium in the development of CD-like ileitis. Microarray analysis of the fetal transcriptome from laser microdissected IEC revealed that mDIO does not program the ileal epithelium. Less genes were significantly regulated by mDIO (7 genes) than by the fetal ARE genotype (84 genes). This cannot be explained so far since the *Tnf* overexpression in the ARE genotype is not present in the epithelium at that stage. If this is also true for other fetal tissues needs to be investigated. The fact that *Tnf* expression levels in placentas from the same *in utero* environment (e. g. WT dam) are different between WT and ARE fetuses points to further ARE genotype-dependent inflammatory mechanisms beyond the intestinal epithelium. Interestingly, the mDIO-driven *in utero* environment intensifies the genotype effect between WT and ARE fetuses as 285 genes were differentially regulated between oWT and oARE fetuses. There seems to be an additive effect of the fetus genotype and the exposure to mDIO on the transcriptome of fetal IEC, because more genes were differentially regulated between WT and oARE (148 genes) than between WT and ARE (84 genes). In summary, heatmap and gene distance matrix (GDM) comparisons indicate that mDIO does not influence global gene expression patterns (WT vs. oWT and ARE vs. oARE are very similar), whereas gene patterns are different according to the fetal genotype (WT vs. ARE and oWT vs. oARE).

Despite missing transcriptional programming of the fetal gut epithelium, previous publications have been shown that inflammatory features of fetal intestines from rats and sheep are vulnerable to mDIO resulting in increased intestinal inflammation and barrier permeability. In sheep, mDIO increased gene expressions of pro-inflammatory cytokines *Tnf*, *Il-1 α* , *Il-1 β* , *Il-6*, *Il-8*, *Mcp-1* and macrophage markers *Cd11b*, *Cd14* and *Cd68* in the fetal and offspring's large intestine [74]. Further, increased *Tlr2* and *Tlr4* expressions with corresponding NF- κ B and Jak signalling points to activated innate immune responses upon mDIO. Another publication showed that mDIO drives T_H17 differentiation from naïve T cells via TGF β and IL-6 [93], the same mechanism as in a CD-like inflammatory phenotype. However, all these hallmarks were not observed in the murine epithelium of fetuses from mDIO dams. This is not contradictory since this work, unlike previously published work, focussed on the fetal epithelium. The main part of immune cells resides in gut-associated lymphoid tissue (GALT), which was not focus of this work and might explain absent inflammatory modulation by mDIO. Further, species differences might be relevant.

A closer look into the regulated gene patterns of fetal IEC revealed that mDIO influenced different genes in WT and ARE fetuses, respectively. None of the genes that were regulated between WT and oWT were regulated between ARE and oARE. The same is reflected when comparing regulated genes between WT and ARE or oWT and oARE. Only 18% of the regulated genes between WT versus ARE (=15 genes) were also identified among genes that were regulated between oWT and oARE. This demonstrates that mDIO affects the ARE fetus genotype differently to the maternal control diet. As an example, alpha fetoprotein 10 (*Afp10*) was the top up-regulated gene between oWT and oARE, but was not regulated between WT and ARE. Verifications of *Afp10* mRNA expression in laser microdissected fetal IEC by qPCR confirmed these results. *Afp* is known to be highly expressed in yolk sac visceral endoderm, fetal liver, gut and kidney [270]. Its expression declines during perinatal period and is re-expressed in response to malignant transformations into neoplastic tissues (e. g. liver, gut, and pancreas) [10, 11]. In this context, mDIO did not affect the *Afp10* mRNA expression in adult ileum of WT and ARE offspring indicating that *Afp10* is not involved in the pathogenesis of CD-like ileitis of *Tnf^{flARE/+}* mice.

In addition, gene regulation of *Reg3b* which was the top regulated gene between WT and oARE was in tendency verified by qPCR. The general success of microarray elaboration is fragile as many factors can influence both methodologies [271]. In essence, low array spot intensities for *Reg3b* (~10-300) might explain discrepancies of results between microarray and qPCR results. The antimicrobial peptide REG3B is expressed by Paneth cells and by the absorptive part of the epithelium. It drives host bacterial segregation and protects from bacterial translocation of Gram-negative species, such as *Salmonella ssp.* across the epithelial interface. Thus, elevated *Reg3b* expression in ARE fetuses upon mDIO might point to a maternal shift in microbial ecology upon HFD. But, the fact that *Reg3b* was as well highly upregulated in fetal IEC under maternal inflammation without resulting in any maternally driven-shifts of the offspring's microbial ecology in the perinatal period (3 weeks after birth) argues against it [245]. *Reg3b* mRNA in the distal ileum of 8 and 12 week-old WT and ARE offspring confirmed previous findings that its downregulation is basically associated with intestinal inflammation and not with prenatal exposure to mDIO leading to the conclusion that transcriptional fingerprints by mDIO do not persist in postnatal life.

The same is true for interleukin 18 (*Il-18*) gene expression. IL-18 together with IL-12 induces cell-mediated immunity upon infection with microbial products like lipopolysaccharide. In fetal IEC *Il-18* was identified under the top down-regulated genes between WT and oWT. However, the influence of mDIO was not observed in intestinal tissue of 8 and 12 week-old offspring. Here, *Il18* was downregulated in response to the offspring's genotype (ARE compared to WT offspring) independently of mDIO. Interestingly and in contrast to this, a NAFLD model of mDIO

showed induced hepatic expression of *Il-18* [272]. Nevertheless, the weakness of the study lies in comparing influences of Chow diet dams with dams that received a semisynthetic energy-enriched HFD. Furthermore, they observed not only prenatal, but also perinatal programming effects, since offspring were exposed to mothers control or HFD until weaning. These facts might complicate comparisons. It was shown in another mouse model of Type 1 diabetes (T1D, NOD/ShiLtJ mice) that mDIO (60% energy derives from HFD) induced gut inflammation and induces *Il-18* mRNA expression in non-obese diabetic mice [273]. Because of the combination of mDIO with mT1D (mT1DmDIO) it is not possible to extract the pure effect of mDIO on the offspring's intestinal inflammation. As seen in this work, a different set of genes in fetal IEC was influenced by mDIO between WT and ARE than between oWT and oARE. Additionally, in T1D mice a novel role for IL-18 in expanding the pool of islet-destructive T cells during pre-diabetes was assigned [274] and might be responsible for increased *Il-18* mRNA expression in offspring from mT1DmDIO mothers. Since in the mT1DmDIO model there is nothing known about fetal *Il-18* expression a disturbed glucose homeostasis during gestation might reveal complete different outcomes according to intestinal inflammation compared to studies of this work. Placentas might be additionally challenged by hyperglycaemia and the presence of inflammatory mediators might influence the developmental programming. However, this needs further investigations of placental tissues at different developmental stages.

In summary, mDIO during gestation did not transcriptionally program fetal IEC in both, WT and *Tnf^{flARE/+}* mice. Single transcriptional fingerprints that were induced by mDIO in the prenatal intestine (e. g. *Afp10*, *Il-18* or *Reg3b*) were not sustained in postnatal period. However, even though that there were no effects of mDIO on fetal IEC, there were mDIO-driven significant metabolic changes in the fetuses independent of the fetus genotype suggesting a certain role of mDIO in developmental programming occurring on sites beyond the intestinal epithelium. To test whether mDIO during gestation influences the susceptibility to intestinal inflammation, offspring were further analyzed at 8 and 12 weeks after birth.

4.2.2. Changing control dams diet to HFD at birth equalized the offspring's metabolic conditions during breastfeeding

The change of control diet to HFD in control dams at birth is sufficient to equalize metabolic parameters between lean and obese mothers at weaning.

At birth, half of the control diet dam group was fed a HFD ('switched dams'), in order to equalize the energy supply and fatty acid content of breast milk to that of mDIO mothers. Consequently, offspring from 'switched dams' and mDIO dams were exposed to HFD from birth on. Equalization of offspring's postnatal dietary exposure enables the follow-up of *in utero* effects

triggered by maternal HFD during pregnancy with regard to the postnatal development of genetically-driven intestinal inflammation. Offspring were sacrificed at 8 and 12 weeks of age. Interestingly, the dietary change to HFD in control dams upon date of delivery equalized the offspring's metabolic conditions during breastfeeding period. Both dam groups showed identical body weights, fat depots and plasma leptin levels at weaning which might suggest that all offspring were exposed to the same energetic conditions during lactation. The equalized metabolic parameters between dam groups were not due to exhausted fat depots upon breastfeeding since 'unswitched' control mothers exhibit less body weight, fat masses and plasma leptin compared to 'switched control' and HFD dams.

4.2.3. Maternal diet-induced obesity combined with postnatal HFD accelerates TNF-driven intestinal inflammation in *Tnf^{ΔARE/+}* mice.

Although mDIO during gestation does not profoundly influence the fetal epithelial transcriptome, postnatal development of CD-like ileitis was altered by mDIO.

Switching control mothers at date of delivery to a HFD enables the investigation of the mDIO effect that is restricted to the prenatal period. After weaning, WT and ARE offspring were fed a control or HFD until 8 or 12 weeks of age. As a result, 8 and 12 week-old ARE and oARE offspring that were housed on experimental control diet exhibited the same ileitis scores indicating that mDIO alone was not sufficient to alter genetically-driven ileitis in *Tnf^{ΔARE/+}* mice. Interestingly, CD-like ileitis (histological ileitis score and number of Ly6G+ cells/mm²) was increased in 8 week-old oARE offspring (compared to ARE) housed on a postnatal HFD, whereas intestinal inflammation was comparable between 12 week-old ARE and oARE offspring. As a conclusion, the combination of mDIO and the second hit of postweaning HFD accelerates CD-like ileitis, without affecting disease severity at later stages. In essence, neutrophil infiltration (indicated by Ly6G) was increased in the same manner as the histological ileitis scores, whereas MPO+ cell infiltration did not represent the mDIO effect in 8 week-old oARE mice. Ly6 proteins have been implicated in leukocyte differentiation, cell adhesion, cell migration, and cytokine production representing its strong involvement in inflammatory processes [275]. Ly6G expression is higher in circulating neutrophils than in bone marrow neutrophils and higher in cells recruited to inflamed sites. This is in line with the observation that neutrophil number (Ly6G+ cells) is higher in *Tnf^{ΔARE/+}* mice compared to WT mice. MPO is a key enzyme in innate immunity and defence against pathogens. It is the major protein of neutrophils, but it is also present in monocytes [276]. This might explain different outcomes between Ly6G+ cells and MPO+ cells ARE mice. Unlike Ly6G+ cell number, MPO+ cell number is not associated with intestinal inflammation in *Tnf^{ΔARE/+}* mice. However, the effect of mDIO on offspring's intestinal inflammation is clearer at local than systemic sites of inflammation. For instance, only slightly increased portal vein endotoxin and plasma TNF in

oARE offspring (compared to ARE) reflect that mDIO effects are present to a lesser extent beyond intestinal tissues. Significant correlation ($r=0.91$, $p=0.0006$) between portal vein endotoxin and plasma TNF in genetically-driven intestinal inflammation demonstrates interconnection of intestinal permeability with systemic inflammation in CD-like ileitis. Whether intestinal permeability is a cause or consequence of intestinal inflammation remains to be elucidated. Nevertheless, the level of TNF is a hallmark for the disease severity, since there is a significant correlation between plasma TNF levels and the histological ileitis score in $Tnf^{\Delta ARE/+}$ mice. In summary, kinetic experiments reveal that only the combination of mDIO with post weaning HFD accelerates the development of CD-like ileitis, whereas mDIO alone had no effect on tissue pathology. The proinflammatory effect of postweaning HFD is obviously uncoupled of offspring's obesity since $Tnf^{\Delta ARE/+}$ mice were protected against HFD-induced weight gain. Further, genetically-driven models of obesity indicated no increased intestinal permeability [277]. Consequently, HFD per se accelerates disease onset by increased intestinal permeability and immune activation (DC recruitment and T_H17 -response) [60]. This pro-inflammatory trait of HFD seems to be further accelerated in $Tnf^{\Delta ARE/+}$ offspring deriving from mDIO dams.

Fetal programming studies of this work were performed in order to investigate a possible influence of mDIO on the fetal gut epithelium. Consequently any influence of mDIO during gestation on immune cells in the fetal gut was not directly assessed. However, due to a limited exposure to antigens *in utero*, the germfree fetal small intestine is hardly populated with educated lymphocytes [152, 153]. Furthermore, cryptopatches and isolated lymphoid follicles are developing postnatally in mice [278]. The neonate lymphocytes have to undergo immune maturation upon bacterial colonization of the gastrointestinal tract and the first contacts with a huge variety of antigens. In contrast to the lymphocytes, enterocytes play a major role in innate immunity during the fetal stage, because they express a variety of defensins and pathogen sensing receptors [73]. Selective overexpression of TNF in the intestinal epithelium seems to be sufficient to trigger CD-like ileitis [246] and therefore the epithelium was suggested to play an important role in the pathogenesis of chronic intestinal inflammation. Therefore it was hypothesized that transcriptional programming might be a potential factor for the observed acceleration of disease onset. As a result, this work reported that mDIO hardly influenced the gene expression pattern in fetal IEC. A very low number of genes were regulated by mDIO overall. Of note, *Afp* and *Reg3b* were upregulated in oARE compared to WT and ARE fetuses. However, qPCR analysis of intestinal tissue of 8 and 12 week- old offspring showed that this pattern was not conserved. It was therefore considered as unlikely that even the main regulated genes in the fetal stage profoundly influenced the intestinal health in the grown up offspring.

Since HFD prolongs and aggravates chronic DSS-induced inflammatory manifestations in the colon [279] it was also suggested that mDIO alters the susceptibility to offspring's DSS-induced colitis. However, mDIO alone had no influence on the susceptibility to DSS colitis (no alterations in body weight development and disease activity) in genetically non-predisposed WT offspring from lean and obese mothers. This is in line with the fact that mDIO alone had also no influence on disease severity of *Tnf^{ARE/+}* offspring. Most probably, a second hit, i.e. a postweaning HFD as additional pro-inflammatory trigger might shift the susceptibility to intestinal inflammation.

Another aspect of an indirect pro-inflammatory feature of mDIO is the potential of maternal diet in shaping commensal microbiome communities and maturation of the intestinal immune system. Since it is clinically evident that maternal weight gain during pregnancy results in faecal microbiota acquisitions of the infants favouring *Bacteroides*, *Clostridium* and *Staphylococcus* abundance on the expense of *Bifidobacterium* group in early life [280], it might explain the accelerated intestinal inflammation in oARE offspring. A recent study showed that HFD (maternal or postnatal), but not obesity per se, structures the offspring's intestinal microbiome in *Macaca fuscata* (Japanese macaque) towards dysbiosis [96]. The fact that *Tnf^{ARE/+}* offspring were protected against DIO might support the hypothesis of a HFD-driven rather than obesity-driven dysbiosis. Whether an mDIO-driven shift in offspring's microbial ecology is responsible for accelerated intestinal inflammation in HFD fed oARE offspring remains to be elucidated. However, a sole possible influence of mDIO on the offspring's intestinal microbiome is obviously not sufficient to alter the susceptibility to intestinal inflammation, since ARE and oARE offspring showed the same disease severity. A disease relevant shift of microbial ecology might only result from the combined exposure to maternal and postnatal HFD.

In conclusion, mDIO only mildly impacts on the fetal transcriptome of laser dissected intestinal epithelial cells. The fact that mDIO alone does not trigger genetically-driven ileitis and experimentally induced colitis suggests that fetal intestinal programming by mDIO alone is not sufficient to alter disease course. Most importantly, a second hit induced by a post weaning HFD accelerates the disease onset. This clearly highlights that the fetal intestine is programmed towards accelerated disease onset when certain environmental factors accrue.

4.2.4. Maternal-diet induced obesity protects from metabolic dysfunction

Increased body weights from fetuses of mDIO dams, regardless of the fetal genotype, suggest a possible metabolic programming. Interestingly, this early metabolic programming did not persist until adulthood in control diet fed *Tnf^{+/+}* and *Tnf^{ARE/+}* offspring indicating the strong influence of the postnatal environment on metabolic mechanisms e. g. by diet and microbial

exposure (see Figure 25 A). Instead, a postnatal metabolic challenge of the offspring (by feeding HFD) showed a clear obesity-like phenotype in WT offspring, but not in $Tnf^{\Delta ARE/+}$ offspring. This is in accordance to previously published work, where $Tnf^{\Delta ARE/+}$, but not WT mice were protected against DIO [60]. This was most likely due to the catabolic effects of both TNF overexpression and an increasing degree of inflammation. Because of this it is biologically plausible that maternal HFD was not able to increase postnatal body weight or adipose tissue mass in this mouse model. Since no changes in body weight, adipose tissue weight, or plasma leptin levels were detected it was unlikely that metabolic disturbances were responsible for the disease aggravation in oARE mice compared to ARE mice.

Interestingly, decreased body weights, mesenteric fat masses and plasma leptin levels in oWT compared to WT offspring indicate that postnatal HFD in addition to mDIO during gestation attenuate metabolic features of offspring's DIO, even though the exposure time to HFD was far longer (3 weeks) as in WT offspring. This effect was even more prominent in male than female offspring and shows a metabolic adaptation in response to maternal HFD exposure *in utero*.

The considerable effect of maternal overnutrition or obesity on metabolic programming is not limited to the *in utero* environment because physiological systems develop after birth. Results from the fetal body weights of this work are in accordance to the 'thrifty phenotype' hypothesis [281, 282]. Fetuses from lean mothers showed significantly decreased body weights at 17.5 dpc and were adapted to poor energy conditions before birth. Excessive metabolic responses to postnatal HFD in WT offspring born by a control diet mother revealed that the early perinatal time is a critical period where dramatic dietary changes might have long term consequences on offspring's health later in life. Many studies have been reviewed by Alfaradhi and Ozanne [98] restricting the onset of obesity to early life, either pre- or postnatal. Despite this, only a few studies showed mDIO effects that were restricted to gestation and not throughout breastfeeding. Studies being limited to prenatal mDIO effects like crossfostering experiments somehow confirmed the metabolic outcome of this study. They highlight potential effects of postnatal overnutrition in contributing to an obese phenotype later in life.

Discrepancies of obesity outcomes in offspring among prenatal and perinatal exposure to maternal obesity emphasize on adaptive outcomes of early life exposure to HFD during critical developmental windows [98]. For instance, control rat offspring cross-fostered to a HFD dam developed hypertension and endothelial dysfunction similarly to HFD rat offspring. However, maintaining energy rich diet after weaning, resulted in an exacerbated onset of metabolic syndrome features [116, 119, 123] as seen in this study. Interestingly, cross-fostering of HFD rat offspring to lean foster dams showed no altered body weight, but increased serum insulin and leptin levels indicating that mDIO-driven alterations in the hormonal regulation of food

intake are robust until postnatal period. Long term feeding of HFD might cause a dysregulation of feeding/appetite-controlling pathways in the brain. In obesity phenotypes orexigenic neuropeptides agouti-related peptide (AgRP) and neuropeptide Y (NPY) are increased, whereas anorectic pro-opiomelanocortin (POMC) is decreased [283]. This might be due to disturbances in leptin and insulin that regulate their production and release [284]. Inappropriate levels or alterations in these hormones during a critical developmental phase might have permanent metabolic consequences. Neurodevelopmental effects of leptin are limited to the neonatal period as leptin treatment reversed the abnormalities in ARC connectivity in *ob/ob* mice in neonates, but not in adults [285]. Other studies demonstrate that exogenous leptin treatment during early postnatal life causes abnormal expressions of NPY, AgRP and POMC [286]. Such an inappropriate shift might have occurred in WT offspring from control diet dams that were switched to a HFD after date of delivery. In this work, WT fetuses from lean dams were exposed to low maternal leptin and HFD during prenatal development, but experienced a dramatic energetic change in the neonatal period. This might have led to an overproduction of leptin in order to decrease food intake. Whether this is true in WT and oWT neonates of this work remains to be investigated. However, leptin overproduction in WT offspring compared to oWT offspring was confirmed at 12 weeks of age and might be the consequence of HFD-induced weight gain and mesenteric fat mass.

In conclusion, both maternal inflammation and maternal diet-induced obesity do hardly influence the fetal epithelial gene programme, but show differences in programming the offspring's susceptibility to intestinal inflammation. Maternal inflammation protects offspring from DSS-induced colitis, whereas mDIO had no influence on colitis susceptibility. The development of postnatal CD-like ileitis was not affected by both maternal stimuli alone, indicating that the postnatal environment is a robust modulator for intestinal inflammation, consequently overwriting maternal fingerprints. But, the combination of mDIO with postnatal HFD clearly demonstrates that mDIO ambiguously programs the offspring's health later in life. Upon HFD, WT offspring were protected against the development of metabolic disorders, whereas genetically-predisposed offspring showed accelerated development of CD-like ileitis. The disease-accelerating potential of mDIO in combination with a postnatal HFD that were observed in the *Tnf*^{ΔARE/+} mouse model might be of high human relevance. In humans, the development of IBD might be accelerated in predisposed children who are born and breastfed from obese mothers with a subsequent hyper caloric diet throughout life.

5. References

1. Sartor, R.B., *Mechanisms of disease: pathogenesis of Crohn's disease and ulcerative colitis*. Nat Clin Pract Gastroenterol Hepatol, 2006. **3**(7): p. 390-407.
2. Strober, W. and I.J. Fuss, *Proinflammatory cytokines in the pathogenesis of inflammatory bowel diseases*. Gastroenterology, 2011. **140**(6): p. 1756-67.
3. Vos, T., et al., *Global, regional, and national incidence, prevalence, and years lived with disability for 301 acute and chronic diseases and injuries in 188 countries, 1990-2013: a systematic analysis for the Global Burden of Disease Study 2013*. Lancet, 2015.
4. Ananthakrishnan, A.N., *Epidemiology and risk factors for IBD*. Nat Rev Gastroenterol Hepatol, 2015. **12**(4): p. 205-17.
5. Khalili, H., et al., *Geographical variation and incidence of inflammatory bowel disease among US women*. Gut, 2012. **61**(12): p. 1686-92.
6. Baumgart, D.C. and W.J. Sandborn, *Crohn's disease*. Lancet, 2012. **380**(9853): p. 1590-605.
7. Liu, J.Z., et al., *Association analyses identify 38 susceptibility loci for inflammatory bowel disease and highlight shared genetic risk across populations*. Nat Genet, 2015. **47**(9): p. 979-986.
8. Jostins, L., et al., *Host-microbe interactions have shaped the genetic architecture of inflammatory bowel disease*. Nature, 2012. **491**(7422): p. 119-24.
9. Spehlmann, M.E., et al., *Epidemiology of inflammatory bowel disease in a German twin cohort: results of a nationwide study*. Inflamm Bowel Dis, 2008. **14**(7): p. 968-76.
10. Ventham, N.T., et al., *Beyond gene discovery in inflammatory bowel disease: the emerging role of epigenetics*. Gastroenterology, 2013. **145**(2): p. 293-308.
11. Lin, Z., et al., *Identification of disease-associated DNA methylation in intestinal tissues from patients with inflammatory bowel disease*. Clin Genet, 2011. **80**(1): p. 59-67.
12. Lin, Z., et al., *Identification of disease-associated DNA methylation in B cells from Crohn's disease and ulcerative colitis patients*. Dig Dis Sci, 2012. **57**(12): p. 3145-53.
13. Cooke, J., et al., *Mucosal genome-wide methylation changes in inflammatory bowel disease*. Inflamm Bowel Dis, 2012. **18**(11): p. 2128-37.
14. Hasler, R., et al., *A functional methylome map of ulcerative colitis*. Genome Res, 2012. **22**(11): p. 2130-7.
15. Harris, R.A., et al., *Genome-wide peripheral blood leukocyte DNA methylation microarrays identified a single association with inflammatory bowel diseases*. Inflamm Bowel Dis, 2012. **18**(12): p. 2334-41.
16. Azarschab, P., et al., *Epigenetic control of the E-cadherin gene (CDH1) by CpG methylation in colectomy samples of patients with ulcerative colitis*. Genes Chromosomes Cancer, 2002. **35**(2): p. 121-6.
17. Yi, J.M. and T.O. Kim, *Epigenetic alterations in inflammatory bowel disease and cancer*. Intest Res, 2015. **13**(2): p. 112-21.
18. Ng, S.C., et al., *Geographical variability and environmental risk factors in inflammatory bowel disease*. Gut, 2013. **62**(4): p. 630-49.
19. Baron, S., et al., *Environmental risk factors in paediatric inflammatory bowel diseases: a population based case control study*. Gut, 2005. **54**(3): p. 357-363.

20. Ponder, A. and M.D. Long, *A clinical review of recent findings in the epidemiology of inflammatory bowel disease*. *Clinical Epidemiology*, 2013. **5**: p. 237-247.
21. Kinross, J.M., A.W. Darzi, and J.K. Nicholson, *Gut microbiome-host interactions in health and disease*. *Genome Med*, 2011. **3**(3): p. 14.
22. Kiely, E.M., et al., *Diversion procto-colitis: response to treatment with short-chain fatty acids*. *J Pediatr Surg*, 2001. **36**(10): p. 1514-7.
23. Fujiwara, D., et al., *Systemic control of plasmacytoid dendritic cells by CD8+ T cells and commensal microbiota*. *J Immunol*, 2008. **180**(9): p. 5843-52.
24. Craven, M., et al., *Inflammation Drives Dysbiosis and Bacterial Invasion in Murine Models of Ileal Crohn's Disease*. *PLoS ONE*, 2012. **7**(7): p. e41594.
25. He, Q., et al., *Microbial fingerprinting detects intestinal microbiota dysbiosis in Zebrafish models with chemically-induced enterocolitis*. *BMC Microbiology*, 2013. **13**: p. 289-289.
26. Buffie, C.G., et al., *Profound alterations of intestinal microbiota following a single dose of clindamycin results in sustained susceptibility to Clostridium difficile-induced colitis*. *Infect Immun*, 2012. **80**(1): p. 62-73.
27. Sokol, H., et al., *Faecalibacterium prausnitzii is an anti-inflammatory commensal bacterium identified by gut microbiota analysis of Crohn disease patients*. *Proc Natl Acad Sci U S A*, 2008. **105**(43): p. 16731-6.
28. Frank, D.N., et al., *Molecular-phylogenetic characterization of microbial community imbalances in human inflammatory bowel diseases*. *Proc Natl Acad Sci U S A*, 2007. **104**(34): p. 13780-5.
29. Lapaquette, P., et al., *Crohn's disease-associated adherent-invasive E. coli are selectively favoured by impaired autophagy to replicate intracellularly*. *Cell Microbiol*, 2010. **12**(1): p. 99-113.
30. Png, C.W., et al., *Mucolytic bacteria with increased prevalence in IBD mucosa augment in vitro utilization of mucin by other bacteria*. *Am J Gastroenterol*, 2010. **105**(11): p. 2420-8.
31. Gill, C.O., L. Saucier, and W.J. Meadus, *Mycobacterium avium subsp. paratuberculosis in dairy products, meat, and drinking water*. *J Food Prot*, 2011. **74**(3): p. 480-99.
32. Zeissig, S., et al., *Changes in expression and distribution of claudin 2, 5 and 8 lead to discontinuous tight junctions and barrier dysfunction in active Crohn's disease*. *Gut*, 2007. **56**(1): p. 61-72.
33. Keita, A.V., et al., *Increased uptake of non-pathogenic E. coli via the follicle-associated epithelium in longstanding ileal Crohn's disease*. *J Pathol*, 2008. **215**(2): p. 135-44.
34. Braun, A., et al., *Alterations of phospholipid concentration and species composition of the intestinal mucus barrier in ulcerative colitis: a clue to pathogenesis*. *Inflamm Bowel Dis*, 2009. **15**(11): p. 1705-20.
35. Aldhous, M.C., C.L. Noble, and J. Satsangi, *Dysregulation of human beta-defensin-2 protein in inflammatory bowel disease*. *PLoS One*, 2009. **4**(7): p. e6285.
36. Nuding, S., et al., *Reduced mucosal antimicrobial activity in Crohn's disease of the colon*. *Gut*, 2007. **56**(9): p. 1240-7.
37. Wehkamp, J., et al., *Reduced Paneth cell alpha-defensins in ileal Crohn's disease*. *Proc Natl Acad Sci U S A*, 2005. **102**(50): p. 18129-34.
38. Cash, H.L., et al., *Symbiotic bacteria direct expression of an intestinal bactericidal lectin*. *Science*, 2006. **313**(5790): p. 1126-30.

39. Hooper, L.V., et al., *Angiogenins: a new class of microbicidal proteins involved in innate immunity*. Nat Immunol, 2003. **4**(3): p. 269-73.
40. Amre, D.K., et al., *Imbalances in dietary consumption of fatty acids, vegetables, and fruits are associated with risk for Crohn's disease in children*. Am J Gastroenterol, 2007. **102**(9): p. 2016-25.
41. Ananthakrishnan, A.N., et al., *A prospective study of long-term intake of dietary fiber and risk of Crohn's disease and ulcerative colitis*. Gastroenterology, 2013. **145**(5): p. 970-7.
42. Roberts, C.L., et al., *Translocation of Crohn's disease Escherichia coli across M-cells: contrasting effects of soluble plant fibres and emulsifiers*. Gut, 2010. **59**(10): p. 1331-9.
43. Ooi, J.H., et al., *Vitamin D regulates the gut microbiome and protects mice from dextran sodium sulfate-induced colitis*. J Nutr, 2013. **143**(10): p. 1679-86.
44. Ananthakrishnan, A.N., et al., *Higher predicted vitamin D status is associated with reduced risk of Crohn's disease*. Gastroenterology, 2012. **142**(3): p. 482-9.
45. Guilbert, J.J., *The world health report 2002 - reducing risks, promoting healthy life*. Educ Health (Abingdon), 2003. **16**(2): p. 230.
46. Ananthakrishnan, A.N., et al., *Long-term intake of dietary fat and risk of ulcerative colitis and Crohn's disease*. Gut, 2014. **63**(5): p. 776-84.
47. de Silva, P.S., et al., *An association between dietary arachidonic acid, measured in adipose tissue, and ulcerative colitis*. Gastroenterology, 2010. **139**(6): p. 1912-7.
48. Wellen, K.E. and G.S. Hotamisligil, *Inflammation, stress, and diabetes*. J Clin Invest, 2005. **115**(5): p. 1111-9.
49. Chandalia, M. and N. Abate, *Metabolic complications of obesity: inflated or inflamed?* J Diabetes Complications, 2007. **21**(2): p. 128-36.
50. Xu, H., et al., *Chronic inflammation in fat plays a crucial role in the development of obesity-related insulin resistance*. J Clin Invest, 2003. **112**(12): p. 1821-30.
51. Pendyala, S., et al., *Diet-induced weight loss reduces colorectal inflammation: implications for colorectal carcinogenesis*. Am J Clin Nutr, 2011. **93**(2): p. 234-42.
52. Weisberg, S.P., et al., *Obesity is associated with macrophage accumulation in adipose tissue*. J Clin Invest, 2003. **112**(12): p. 1796-808.
53. Yuan, M., et al., *Reversal of obesity- and diet-induced insulin resistance with salicylates or targeted disruption of Ikkbeta*. Science, 2001. **293**(5535): p. 1673-7.
54. Ding, S., et al., *High-fat diet: bacteria interactions promote intestinal inflammation which precedes and correlates with obesity and insulin resistance in mouse*. PLoS One, 2010. **5**(8): p. e12191.
55. Fink, C., et al., *Adipose tissue and inflammatory bowel disease pathogenesis*. Inflamm Bowel Dis, 2012. **18**(8): p. 1550-7.
56. Peyrin-Biroulet, L., et al., *Mesenteric fat in Crohn's disease: a pathogenetic hallmark or an innocent bystander?* Gut, 2007. **56**(4): p. 577-83.
57. Weakley, F.L. and R.B. Turnbull, *Recognition of regional ileitis in the operating room*. Dis Colon Rectum, 1971. **14**(1): p. 17-23.
58. Solem, C.A., et al., *Correlation of C-reactive protein with clinical, endoscopic, histologic, and radiographic activity in inflammatory bowel disease*. Inflamm Bowel Dis, 2005. **11**(8): p. 707-12.
59. de La Serre, C.B., et al., *Propensity to high-fat diet-induced obesity in rats is associated with changes in the gut microbiota and gut inflammation*. Am J Physiol Gastrointest Liver Physiol, 2010. **299**(2): p. G440-8.

60. Gruber, L., et al., *High fat diet accelerates pathogenesis of murine Crohn's disease-like ileitis independently of obesity*. PLoS One, 2013. **8**(8): p. e71661.
61. Musso, G., R. Gambino, and M. Cassader, *Interactions between gut microbiota and host metabolism predisposing to obesity and diabetes*. Annu Rev Med, 2011. **62**: p. 361-80.
62. Turnbaugh, P.J., et al., *An obesity-associated gut microbiome with increased capacity for energy harvest*. Nature, 2006. **444**(7122): p. 1027-31.
63. Ghoshal, S., et al., *Chylomicrons promote intestinal absorption of lipopolysaccharides*. J Lipid Res, 2009. **50**(1): p. 90-7.
64. Fowden, A.L., D.A. Giussani, and A.J. Forhead, *Intrauterine programming of physiological systems: causes and consequences*. Physiology (Bethesda), 2006. **21**: p. 29-37.
65. Roseboom, T., S. de Rooij, and R. Painter, *The Dutch famine and its long-term consequences for adult health*. Early Hum Dev, 2006. **82**(8): p. 485-91.
66. Hales, C.N. and D.J. Barker, *The thrifty phenotype hypothesis*. Br Med Bull, 2001. **60**: p. 5-20.
67. Dominitz, J.A., J.C. Young, and E.J. Boyko, *Outcomes of infants born to mothers with inflammatory bowel disease: a population-based cohort study*. Am J Gastroenterol, 2002. **97**(3): p. 641-8.
68. Morales, M., et al., *Crohn's disease as a risk factor for the outcome of pregnancy*. Hepatogastroenterology, 2000. **47**(36): p. 1595-8.
69. Getahun, D., et al., *Association between maternal inflammatory bowel disease and adverse perinatal outcomes*. J Perinatol, 2014. **34**(6): p. 435-40.
70. Ajslev, T.A., T.I. Sorensen, and T. Jess, *Maternal inflammatory bowel disease and offspring body size: a prospective cohort study*. Inflamm Bowel Dis, 2012. **18**(4): p. 709-17.
71. Stoehr L. et al. Ecco Poster Presentation 2014, P115
72. Ban, L., et al., *Limited risks of major congenital anomalies in children of mothers with IBD and effects of medications*. Gastroenterology, 2014. **146**(1): p. 76-84.
73. Renz, H., P. Brandtzaeg, and M. Hornef, *The impact of perinatal immune development on mucosal homeostasis and chronic inflammation*. Nat Rev Immunol, 2012. **12**(1): p. 9-23.
74. Yan, X., et al., *Maternal obesity induces sustained inflammation in both fetal and offspring large intestine of sheep*. Inflamm Bowel Dis, 2011. **17**(7): p. 1513-22.
75. Sykes, L., et al., *The Th1:th2 dichotomy of pregnancy and preterm labour*. Mediators Inflamm, 2012. **2012**: p. 967629.
76. Rowe, J.H., et al., *Regulatory T cells and the immune pathogenesis of prenatal infection*. Reproduction, 2013. **146**(6): p. R191-203.
77. Sasaki, Y., et al., *Decidual and peripheral blood CD4+CD25+ regulatory T cells in early pregnancy subjects and spontaneous abortion cases*. Mol Hum Reprod, 2004. **10**(5): p. 347-53.
78. Somerset, D.A., et al., *Normal human pregnancy is associated with an elevation in the immune suppressive CD25+ CD4+ regulatory T-cell subset*. Immunology, 2004. **112**(1): p. 38-43.
79. Mor, G., et al., *Inflammation and pregnancy: the role of the immune system at the implantation site*. Ann N Y Acad Sci, 2011. **1221**: p. 80-7.
80. Holmlund, U., et al., *Expression and regulation of the pattern recognition receptors Toll-like receptor-2 and Toll-like receptor-4 in the human placenta*. Immunology, 2002. **107**(1): p. 145-51.

81. Crainie, M., L. Guilbert, and T.G. Wegmann, *Expression of novel cytokine transcripts in the murine placenta*. Biol Reprod, 1990. **43**(6): p. 999-1005.
82. Bennett, W.A., et al., *First-trimester human chorionic villi express both immunoregulatory and inflammatory cytokines: a role for interleukin-10 in regulating the cytokine network of pregnancy*. Am J Reprod Immunol, 1999. **41**(1): p. 70-8.
83. Samstein, R.M., et al., *Extrathymic generation of regulatory T cells in placental mammals mitigates maternal-fetal conflict*. Cell, 2012. **150**(1): p. 29-38.
84. Malek, A., R. Sager, and H. Schneider, *Effect of hypoxia, oxidative stress and lipopolysaccharides on the release of prostaglandins and cytokines from human term placental explants*. Placenta, 2001. **22 Suppl A**: p. S45-50.
85. Wolfs, T.G., et al., *Endotoxin induced chorioamnionitis prevents intestinal development during gestation in fetal sheep*. PLoS One, 2009. **4**(6): p. e5837.
86. Carpentier, P.A., A.L. Dingman, and T.D. Palmer, *Placental TNF-alpha signaling in illness-induced complications of pregnancy*. Am J Pathol, 2011. **178**(6): p. 2802-10.
87. Gendron, R.L., et al., *Lipopolysaccharide-induced fetal resorption in mice is associated with the intrauterine production of tumour necrosis factor-alpha*. J Reprod Fertil, 1990. **90**(2): p. 395-402.
88. Silen, M.L., et al., *Interleukin-1 alpha and tumor necrosis factor alpha cause placental injury in the rat*. Am J Pathol, 1989. **135**(2): p. 239-44.
89. Silver, R.M., et al., *Lipopolysaccharide-induced fetal death: the role of tumor-necrosis factor alpha*. Biol Reprod, 1994. **50**(5): p. 1108-12.
90. Fraccaroli, L., et al., *Immunomodulatory effects of chemokines during the early implantation window*. Front Biosci (Elite Ed), 2009. **1**: p. 288-98.
91. Halaas, J.L., et al., *Weight-reducing effects of the plasma protein encoded by the obese gene*. Science, 1995. **269**(5223): p. 543-6.
92. Pelleymounter, M.A., et al., *Effects of the obese gene product on body weight regulation in ob/ob mice*. Science, 1995. **269**(5223): p. 540-3.
93. Qin, H., et al., *TGF-beta promotes Th17 cell development through inhibition of SOCS3*. J Immunol, 2009. **183**(1): p. 97-105.
94. Collado, M.C., et al., *Microbial ecology and host-microbiota interactions during early life stages*. Gut Microbes, 2012. **3**(4): p. 352-65.
95. Santacruz, A., et al., *Gut microbiota composition is associated with body weight, weight gain and biochemical parameters in pregnant women*. Br J Nutr, 2010. **104**(1): p. 83-92.
96. Ma, J., et al., *High-fat maternal diet during pregnancy persistently alters the offspring microbiome in a primate model*. Nat Commun, 2014. **5**: p. 3889.
97. Segovia, S.A., M.H. Vickers, and C. Gray, *Maternal obesity, inflammation, and developmental programming*. 2014. **2014**: p. 418975.
98. Alfaradhi, M.Z. and S.E. Ozanne, *Developmental programming in response to maternal overnutrition*. Front Genet, 2011. **2**: p. 27.
99. Forsdahl, A., *Are poor living conditions in childhood and adolescence an important risk factor for arteriosclerotic heart disease?* Br J Prev Soc Med, 1977. **31**(2): p. 91-5.
100. Barker, D.J., et al., *Growth in utero and serum cholesterol concentrations in adult life*. Bmj, 1993. **307**(6918): p. 1524-7.
101. Barker, D.J. and C. Osmond, *Infant mortality, childhood nutrition, and ischaemic heart disease in England and Wales*. Lancet, 1986. **1**(8489): p. 1077-81.
102. Hales, C.N., et al., *Fetal and infant growth and impaired glucose tolerance at age 64*. Bmj, 1991. **303**(6809): p. 1019-22.

103. Dabelea, D., et al., *Intrauterine exposure to diabetes conveys risks for type 2 diabetes and obesity: a study of discordant sibships*. *Diabetes*, 2000. **49**(12): p. 2208-11.
104. Akyol, A., S.C. Langley-Evans, and S. McMullen, *Obesity induced by cafeteria feeding and pregnancy outcome in the rat*. *Br J Nutr*, 2009. **102**(11): p. 1601-10.
105. Howie, G.J., et al., *Maternal nutritional history predicts obesity in adult offspring independent of postnatal diet*. *J Physiol*, 2009. **587**(Pt 4): p. 905-15.
106. White, C.L., et al., *Effects of high fat diet on Morris maze performance, oxidative stress, and inflammation in rats: contributions of maternal diet*. *Neurobiol Dis*, 2009. **35**(1): p. 3-13.
107. Lewis, D.S., A.M. Coelho, Jr., and E.M. Jackson, *Maternal weight and sire group, not caloric intake, influence adipocyte volume in infant female baboons*. *Pediatr Res*, 1991. **30**(6): p. 534-40.
108. Zhu, M.J., et al., *Maternal obesity markedly increases placental fatty acid transporter expression and fetal blood triglycerides at midgestation in the ewe*. *Am J Physiol Regul Integr Comp Physiol*, 2010. **299**(5): p. R1224-31.
109. McCurdy, C.E., et al., *Maternal high-fat diet triggers lipotoxicity in the fetal livers of nonhuman primates*. *J Clin Invest*, 2009. **119**(2): p. 323-35.
110. Buckley, A.J., et al., *Altered body composition and metabolism in the male offspring of high fat-fed rats*. *Metabolism*, 2005. **54**(4): p. 500-7.
111. Khan, I.Y., et al., *A high-fat diet during rat pregnancy or suckling induces cardiovascular dysfunction in adult offspring*. *Am J Physiol Regul Integr Comp Physiol*, 2005. **288**(1): p. R127-33.
112. Shankar, K., et al., *Maternal obesity at conception programs obesity in the offspring*. *Am J Physiol Regul Integr Comp Physiol*, 2008. **294**(2): p. R528-38.
113. Shankar, K., et al., *Maternal overweight programs insulin and adiponectin signaling in the offspring*. *Endocrinology*, 2010. **151**(6): p. 2577-89.
114. Nivoit, P., et al., *Established diet-induced obesity in female rats leads to offspring hyperphagia, adiposity and insulin resistance*. *Diabetologia*, 2009. **52**(6): p. 1133-42.
115. Samuelsson, A.M., et al., *Diet-induced obesity in female mice leads to offspring hyperphagia, adiposity, hypertension, and insulin resistance: a novel murine model of developmental programming*. *Hypertension*, 2008. **51**(2): p. 383-92.
116. Bayol, S.A., S.J. Farrington, and N.C. Stickland, *A maternal 'junk food' diet in pregnancy and lactation promotes an exacerbated taste for 'junk food' and a greater propensity for obesity in rat offspring*. *Br J Nutr*, 2007. **98**(4): p. 843-51.
117. Bayol, S.A., B.H. Simbi, and N.C. Stickland, *A maternal cafeteria diet during gestation and lactation promotes adiposity and impairs skeletal muscle development and metabolism in rat offspring at weaning*. *J Physiol*, 2005. **567**(Pt 3): p. 951-61.
118. King, V., et al., *Post-weaning diet determines metabolic risk in mice exposed to overnutrition in early life*. *Reprod Biol Endocrinol*, 2014. **12**: p. 73.
119. Page, K.C., et al., *Maternal and postweaning diet interaction alters hypothalamic gene expression and modulates response to a high-fat diet in male offspring*. *Am J Physiol Regul Integr Comp Physiol*, 2009. **297**(4): p. R1049-57.
120. Song, Y., et al., *Maternal high-fat diet feeding during pregnancy and lactation augments lung inflammation and remodeling in the offspring*. *Respir Physiol Neurobiol*, 2014. **207c**: p. 1-6.

121. Hawkes, C.A., et al., *Prenatal high fat diet alters the cerebrovasculature and clearance of beta-amyloid in adult offspring*. J Pathol, 2014.
122. Gorski, J.N., et al., *Postnatal environment overrides genetic and prenatal factors influencing offspring obesity and insulin resistance*. Am J Physiol Regul Integr Comp Physiol, 2006. **291**(3): p. R768-78.
123. Mitra, A., et al., *Effect of high-fat diet during gestation, lactation, or postweaning on physiological and behavioral indexes in borderline hypertensive rats*. Am J Physiol Regul Integr Comp Physiol, 2009. **296**(1): p. R20-8.
124. Umekawa, T., et al., *A maternal mouse diet with moderately high-fat levels does not lead to maternal obesity but causes mesenteric adipose tissue dysfunction in male offspring*. J Nutr Biochem, 2014.
125. Dominguez-Bello, M.G., et al., *Delivery mode shapes the acquisition and structure of the initial microbiota across multiple body habitats in newborns*. Proc Natl Acad Sci U S A, 2010. **107**(26): p. 11971-5.
126. Favier, C.F., W.M. de Vos, and A.D. Akkermans, *Development of bacterial and bifidobacterial communities in feces of newborn babies*. Anaerobe, 2003. **9**(5): p. 219-29.
127. Mackie, R.I., A. Sghir, and H.R. Gaskins, *Developmental microbial ecology of the neonatal gastrointestinal tract*. Am J Clin Nutr, 1999. **69**(5): p. 1035s-1045s.
128. Azad, M.B., et al., *Gut microbiota of healthy Canadian infants: profiles by mode of delivery and infant diet at 4 months*. Cmaj, 2013. **185**(5): p. 385-94.
129. Barros, F.C., et al., *Cesarean section and risk of obesity in childhood, adolescence, and early adulthood: evidence from 3 Brazilian birth cohorts*. Am J Clin Nutr, 2012. **95**(2): p. 465-70.
130. Goldani, H.A., et al., *Cesarean delivery is associated with an increased risk of obesity in adulthood in a Brazilian birth cohort study*. Am J Clin Nutr, 2011. **93**(6): p. 1344-7.
131. Neu, J. and J. Rushing, *Cesarean versus vaginal delivery: long-term infant outcomes and the hygiene hypothesis*. Clin Perinatol, 2011. **38**(2): p. 321-31.
132. Favier, C.F., et al., *Molecular monitoring of succession of bacterial communities in human neonates*. Appl Environ Microbiol, 2002. **68**(1): p. 219-26.
133. Penders, J., et al., *Factors influencing the composition of the intestinal microbiota in early infancy*. Pediatrics, 2006. **118**(2): p. 511-21.
134. Stout, M.J., et al., *Identification of intracellular bacteria in the basal plate of the human placenta in term and preterm gestations*. Am J Obstet Gynecol, 2013. **208**(3): p. 226.e1-7.
135. Garrett, W.S., et al., *Enterobacteriaceae act in concert with the gut microbiota to induce spontaneous and maternally transmitted colitis*. Cell Host Microbe, 2010. **8**(3): p. 292-300.
136. Noah, T.K., B. Donahue, and N.F. Shroyer, *Intestinal development and differentiation*. Exp Cell Res, 2011. **317**(19): p. 2702-10.
137. Grosse, A.S., et al., *Cell dynamics in fetal intestinal epithelium: implications for intestinal growth and morphogenesis*. Development, 2011. **138**(20): p. 4423-32.
138. Dauca, M., et al., *Development of the vertebrate small intestine and mechanisms of cell differentiation*. Int J Dev Biol, 1990. **34**(1): p. 205-18.
139. Hashimoto, H., H. Ishikawa, and M. Kusakabe, *Development of vascular networks during the morphogenesis of intestinal villi in the fetal mouse*. Kaibogaku Zasshi, 1999. **74**(5): p. 567-76.
140. Karlsson, L., et al., *Abnormal gastrointestinal development in PDGF-A and PDGFR-(alpha) deficient mice implicates a novel mesenchymal structure with*

- putative instructive properties in villus morphogenesis*. *Development*, 2000. **127**(16): p. 3457-66.
141. McLin, V.A., S.J. Henning, and M. Jamrich, *The role of the visceral mesoderm in the development of the gastrointestinal tract*. *Gastroenterology*, 2009. **136**(7): p. 2074-91.
 142. van den Brink, G.R., *Hedgehog signaling in development and homeostasis of the gastrointestinal tract*. *Physiol Rev*, 2007. **87**(4): p. 1343-75.
 143. Kim, B.M., et al., *Phases of canonical Wnt signaling during the development of mouse intestinal epithelium*. *Gastroenterology*, 2007. **133**(2): p. 529-38.
 144. Jensen, J., et al., *Control of endodermal endocrine development by Hes-1*. *Nat Genet*, 2000. **24**(1): p. 36-44.
 145. VanDussen, K.L. and L.C. Samuelson, *Mouse atonal homolog 1 directs intestinal progenitors to secretory cell rather than absorptive cell fate*. *Dev Biol*, 2010. **346**(2): p. 215-23.
 146. Kazanjian, A., et al., *Atonal homolog 1 is required for growth and differentiation effects of notch/gamma-secretase inhibitors on normal and cancerous intestinal epithelial cells*. *Gastroenterology*, 2010. **139**(3): p. 918-28, 928.e1-6.
 147. Kim, T.H. and R.A. Shivdasani, *Genetic evidence that intestinal Notch functions vary regionally and operate through a common mechanism of Math1 repression*. *J Biol Chem*, 2011. **286**(13): p. 11427-33.
 148. Tulic, M.K., et al., *Changes in thymic regulatory T-cell maturation from birth to puberty: differences in atopic children*. *J Allergy Clin Immunol*, 2012. **129**(1): p. 199-206.e1-4.
 149. Prescott, S.L. and V. Clifton, *Asthma and pregnancy: emerging evidence of epigenetic interactions in utero*. *Curr Opin Allergy Clin Immunol*, 2009. **9**(5): p. 417-26.
 150. Haddeland, U., et al., *Putative regulatory T cells are impaired in cord blood from neonates with hereditary allergy risk*. *Pediatr Allergy Immunol*, 2005. **16**(2): p. 104-12.
 151. Harper, J., et al., *The transcriptional repressor Blimp1/Prdm1 regulates postnatal reprogramming of intestinal enterocytes*. *Proc Natl Acad Sci U S A*, 2011. **108**(26): p. 10585-90.
 152. Brandtzaeg, P., *Function of mucosa-associated lymphoid tissue in antibody formation*. *Immunol Invest*, 2010. **39**(4-5): p. 303-55.
 153. van de Pavert, S.A. and R.E. Mebius, *New insights into the development of lymphoid tissues*. *Nat Rev Immunol*, 2010. **10**(9): p. 664-74.
 154. Salzman, N.H., et al., *Enteric defensins are essential regulators of intestinal microbial ecology*. *Nat Immunol*, 2010. **11**(1): p. 76-83.
 155. Kai-Larsen, Y., et al., *Antimicrobial components of the neonatal gut affected upon colonization*. *Pediatr Res*, 2007. **61**(5 Pt 1): p. 530-6.
 156. Keilbaugh, S.A., et al., *Activation of RegIIIbeta/gamma and interferon gamma expression in the intestinal tract of SCID mice: an innate response to bacterial colonisation of the gut*. *Gut*, 2005. **54**(5): p. 623-9.
 157. Mortha, A., et al., *Microbiota-dependent crosstalk between macrophages and ILC3 promotes intestinal homeostasis*. *Science*, 2014. **343**(6178): p. 1249288.
 158. Wang, G., et al., *"Default" generation of neonatal regulatory T cells*. *J Immunol*, 2010. **185**(1): p. 71-8.
 159. O'Mahony, C., et al., *Commensal-induced regulatory T cells mediate protection against pathogen-stimulated NF-kappaB activation*. *PLoS Pathog*, 2008. **4**(8): p. e1000112.

160. Atarashi, K., et al., *Induction of colonic regulatory T cells by indigenous Clostridium species*. Science, 2011. **331**(6015): p. 337-41.
161. Gaboriau-Routhiau, V., et al., *The key role of segmented filamentous bacteria in the coordinated maturation of gut helper T cell responses*. Immunity, 2009. **31**(4): p. 677-89.
162. Jiang, H.Q., N.A. Bos, and J.J. Cebra, *Timing, localization, and persistence of colonization by segmented filamentous bacteria in the neonatal mouse gut depend on immune status of mothers and pups*. Infect Immun, 2001. **69**(6): p. 3611-7.
163. Wijburg, O.L., et al., *Innate secretory antibodies protect against natural Salmonella typhimurium infection*. J Exp Med, 2006. **203**(1): p. 21-6.
164. Hanson, L.A., *Session 1: Feeding and infant development breast-feeding and immune function*. Proc Nutr Soc, 2007. **66**(3): p. 384-96.
165. Hapfelmeier, S., et al., *Reversible microbial colonization of germ-free mice reveals the dynamics of IgA immune responses*. Science, 2010. **328**(5986): p. 1705-9.
166. Shroff, K.E., K. Meslin, and J.J. Cebra, *Commensal enteric bacteria engender a self-limiting humoral mucosal immune response while permanently colonizing the gut*. Infect Immun, 1995. **63**(10): p. 3904-13.
167. Mabbott, N.A., et al., *Microfold (M) cells: important immunosurveillance posts in the intestinal epithelium*. Mucosal immunology, 2013. **6**(4): p. 666-677.
168. Gallo, R.L. and L.V. Hooper, *Epithelial antimicrobial defence of the skin and intestine*. Nature reviews. Immunology, 2012. **12**(7): p. 503-516.
169. Artis, D., et al., *RELM β /FIZZ2 is a goblet cell-specific immune-effector molecule in the gastrointestinal tract*. Proceedings of the National Academy of Sciences of the United States of America, 2004. **101**(37): p. 13596-13600.
170. Nair, M.G., et al., *Goblet Cell-Derived Resistin-Like Molecule β Augments CD4(+) T Cell Production of IFN- γ and Infection-Induced Intestinal Inflammation*. Journal of immunology (Baltimore, Md. : 1950), 2008. **181**(7): p. 4709.
171. Vaishnava, S., et al., *The antibacterial lectin RegIII γ promotes the spatial segregation of microbiota and host in the intestine*. Science (New York, N.Y.), 2011. **334**(6053): p. 255-258.
172. Johansson, M.E.V., et al., *The inner of the two Muc2 mucin-dependent mucus layers in colon is devoid of bacteria*. Proceedings of the National Academy of Sciences of the United States of America, 2008. **105**(39): p. 15064-15069.
173. Yang, W., et al., *Inactivation of p21(WAF1/cip1) Enhances Intestinal Tumor Formation in Muc2(-/-) Mice*. The American Journal of Pathology, 2005. **166**(4): p. 1239-1246.
174. Jonckheere, N., et al., *Transcriptional activation of the murine Muc5ac mucin gene in epithelial cancer cells by TGF-beta/Smad4 signalling pathway is potentiated by Sp1*. Biochemical Journal, 2004. **377**(Pt 3): p. 797-808.
175. Taupin, D.R., K. Kinoshita, and D.K. Podolsky, *Intestinal trefoil factor confers colonic epithelial resistance to apoptosis*. Proceedings of the National Academy of Sciences of the United States of America, 2000. **97**(2): p. 799-804.
176. Dignass, A., et al., *Trefoil peptides promote epithelial migration through a transforming growth factor beta-independent pathway*. Journal of Clinical Investigation, 1994. **94**(1): p. 376-383.
177. Kandaswamy, K., et al., *Focal targeting by human β -defensin 2 disrupts localized virulence factor assembly sites in Enterococcus faecalis*. Proceedings

- of the National Academy of Sciences of the United States of America, 2013. **110**(50): p. 20230-20235.
178. Cadwell, K., et al., *A unique role for autophagy and Atg16L1 in Paneth cells in murine and human intestine*. Nature, 2008. **456**(7219): p. 259-263.
 179. Adolph, T.E., et al., *Paneth cells as a site of origin for intestinal inflammation*. Nature, 2013. **503**(7475): p. 10.1038/nature12599.
 180. Rioux, J.D., et al., *Genome-wide association study identifies five novel susceptibility loci for Crohn's disease and implicates a role for autophagy in disease pathogenesis*. Nature genetics, 2007. **39**(5): p. 596-604.
 181. Kaser, A., et al., *XBP1 links ER stress to intestinal inflammation and confers genetic risk for human inflammatory bowel disease*. Cell, 2008. **134**(5): p. 743-756.
 182. Khor, B., A. Gardet, and R.J. Xavier, *Genetics and pathogenesis of inflammatory bowel disease*. Nature, 2011. **474**(7351): p. 307-317.
 183. Fukata, M. and M.T. Abreu, *Pathogen recognition receptors, cancer and inflammation in the gut*. Current opinion in pharmacology, 2009. **9**(6): p. 680-687.
 184. Chen, G.Y., et al., *A Functional Role for Nlrp6 in Intestinal Inflammation and Tumorigenesis*. Journal of immunology (Baltimore, Md. : 1950), 2011. **186**(12): p. 7187-7194.
 185. Hu, B., et al., *Microbiota-induced activation of epithelial IL-6 signaling links inflammasome-driven inflammation with transmissible cancer*. Proceedings of the National Academy of Sciences of the United States of America, 2013. **110**(24): p. 9862-9867.
 186. Li, X.-D., et al., *Mitochondrial antiviral signaling protein (MAVS) monitors commensal bacteria and induces an immune response that prevents experimental colitis*. Proceedings of the National Academy of Sciences of the United States of America, 2011. **108**(42): p. 17390-17395.
 187. Brandl, K., et al., *MyD88 signaling in nonhematopoietic cells protects mice against induced colitis by regulating specific EGF receptor ligands*. Proceedings of the National Academy of Sciences of the United States of America, 2010. **107**(46): p. 19967-19972.
 188. Beck, P.L., et al., *Transforming Growth Factor- β Mediates Intestinal Healing and Susceptibility to Injury in Vitro and in Vivo Through Epithelial Cells*. The American Journal of Pathology, 2003. **162**(2): p. 597-608.
 189. Greten, F.R., et al., *NF- κ B is a negative regulator of IL-1 β secretion as revealed by genetic and pharmacological inhibition of IKK β* . Cell, 2007. **130**(5): p. 918-931.
 190. Nenci, A., et al., *Epithelial NEMO links innate immunity to chronic intestinal inflammation*. Nature, 2007. **446**(7135): p. 557-61.
 191. Lee, J., et al., *Maintenance of colonic homeostasis by distinctive apical TLR9 signalling in intestinal epithelial cells*. Nat Cell Biol, 2006. **8**(12): p. 1327-36.
 192. Halbleib, J.M. and W.J. Nelson, *Cadherins in development: cell adhesion, sorting, and tissue morphogenesis*. Genes Dev, 2006. **20**(23): p. 3199-214.
 193. Gooding, J.M., K.L. Yap, and M. Ikura, *The cadherin-catenin complex as a focal point of cell adhesion and signalling: new insights from three-dimensional structures*. Bioessays, 2004. **26**(5): p. 497-511.
 194. McGuckin, M.A., et al., *Intestinal barrier dysfunction in inflammatory bowel diseases*. Inflamm Bowel Dis, 2009. **15**(1): p. 100-13.

195. Su, L., et al., *Targeted epithelial tight junction dysfunction causes immune activation and contributes to development of experimental colitis*. Gastroenterology, 2009. **136**(2): p. 551-63.
196. Heller, F., et al., *Interleukin-13 is the key effector Th2 cytokine in ulcerative colitis that affects epithelial tight junctions, apoptosis, and cell restitution*. Gastroenterology, 2005. **129**(2): p. 550-64.
197. Weber, C.R., et al., *Claudin-1 and claudin-2 expression is elevated in inflammatory bowel disease and may contribute to early neoplastic transformation*. Lab Invest, 2008. **88**(10): p. 1110-20.
198. Kucharzik, T., et al., *Neutrophil transmigration in inflammatory bowel disease is associated with differential expression of epithelial intercellular junction proteins*. Am J Pathol, 2001. **159**(6): p. 2001-9.
199. Muise, A.M., et al., *Polymorphisms in E-cadherin (CDH1) result in a mis-localised cytoplasmic protein that is associated with Crohn's disease*. Gut, 2009. **58**(8): p. 1121-7.
200. Prasad, S., et al., *Inflammatory processes have differential effects on claudins 2, 3 and 4 in colonic epithelial cells*. Lab Invest, 2005. **85**(9): p. 1139-62.
201. Zeissig, S., et al., *Downregulation of epithelial apoptosis and barrier repair in active Crohn's disease by tumour necrosis factor alpha antibody treatment*. Gut, 2004. **53**(9): p. 1295-302.
202. Yi, J.Y., et al., *TNF-alpha downregulates E-cadherin and sensitizes response to gamma-irradiation in Caco-2 cells*. Cancer Res Treat, 2009. **41**(3): p. 164-70.
203. Wang, F., et al., *Interferon-gamma and tumor necrosis factor-alpha synergize to induce intestinal epithelial barrier dysfunction by up-regulating myosin light chain kinase expression*. Am J Pathol, 2005. **166**(2): p. 409-19.
204. Graham, W.V., et al., *Tumor necrosis factor-induced long myosin light chain kinase transcription is regulated by differentiation-dependent signaling events. Characterization of the human long myosin light chain kinase promoter*. J Biol Chem, 2006. **281**(36): p. 26205-15.
205. Iliev, I.D., et al., *Human intestinal epithelial cells promote the differentiation of tolerogenic dendritic cells*. Gut, 2009. **58**(11): p. 1481-9.
206. Cooney, R., et al., *NOD2 stimulation induces autophagy in dendritic cells influencing bacterial handling and antigen presentation*. Nat Med, 2010. **16**(1): p. 90-7.
207. Levine, B., N. Mizushima, and H.W. Virgin, *Autophagy in immunity and inflammation*. Nature, 2011. **469**(7330): p. 323-35.
208. Noguchi, E., et al., *A Crohn's disease-associated NOD2 mutation suppresses transcription of human IL10 by inhibiting activity of the nuclear ribonucleoprotein hnRNP-A1*. Nat Immunol, 2009. **10**(5): p. 471-9.
209. van Heel, D.A., et al., *Muramyl dipeptide and toll-like receptor sensitivity in NOD2-associated Crohn's disease*. Lancet, 2005. **365**(9473): p. 1794-6.
210. Zhou, L., et al., *TGF-beta-induced Foxp3 inhibits T(H)17 cell differentiation by antagonizing RORgamma function*. Nature, 2008. **453**(7192): p. 236-40.
211. Berg, D.J., et al., *Enterocolitis and colon cancer in interleukin-10-deficient mice are associated with aberrant cytokine production and CD4(+) TH1-like responses*. J Clin Invest, 1996. **98**(4): p. 1010-20.
212. Elson, C.O., et al., *Monoclonal anti-interleukin 23 reverses active colitis in a T cell-mediated model in mice*. Gastroenterology, 2007. **132**(7): p. 2359-70.
213. Fuss, I.J., et al., *Disparate CD4+ lamina propria (LP) lymphokine secretion profiles in inflammatory bowel disease. Crohn's disease LP cells manifest*

- increased secretion of IFN-gamma, whereas ulcerative colitis LP cells manifest increased secretion of IL-5. J Immunol, 1996. 157(3): p. 1261-70.*
214. Powrie, F., et al., *Inhibition of Th1 responses prevents inflammatory bowel disease in scid mice reconstituted with CD45RBhi CD4+ T cells. Immunity, 1994. 1(7): p. 553-62.*
 215. Neurath, M.F., et al., *The transcription factor T-bet regulates mucosal T cell activation in experimental colitis and Crohn's disease. J Exp Med, 2002. 195(9): p. 1129-43.*
 216. Wirtz, S., et al., *Cutting edge: chronic intestinal inflammation in STAT-4 transgenic mice: characterization of disease and adoptive transfer by TNF- plus IFN-gamma-producing CD4+ T cells that respond to bacterial antigens. J Immunol, 1999. 162(4): p. 1884-8.*
 217. Anderson, C.A., et al., *Investigation of Crohn's disease risk loci in ulcerative colitis further defines their molecular relationship. Gastroenterology, 2009. 136(2): p. 523-9.e3.*
 218. Cho, J.H., *The genetics and immunopathogenesis of inflammatory bowel disease. Nat Rev Immunol, 2008. 8(6): p. 458-66.*
 219. Kamada, N., et al., *Unique CD14 intestinal macrophages contribute to the pathogenesis of Crohn disease via IL-23/IFN-gamma axis. J Clin Invest, 2008. 118(6): p. 2269-80.*
 220. Pastorelli, L., et al., *Central role of the gut epithelial barrier in the pathogenesis of chronic intestinal inflammation: lessons learned from animal models and human genetics. Front Immunol, 2013. 4: p. 280.*
 221. DeVoss, J. and L. Diehl, *Murine models of inflammatory bowel disease (IBD): challenges of modeling human disease. Toxicol Pathol, 2014. 42(1): p. 99-110.*
 222. Kontoyiannis, D., et al., *Impaired on/off regulation of TNF biosynthesis in mice lacking TNF AU-rich elements: implications for joint and gut-associated immunopathologies. Immunity, 1999. 10(3): p. 387-98.*
 223. Wagner, S.J., et al., *Semisynthetic diet ameliorates Crohn's disease-like ileitis in TNFDeltaARE/WT mice through antigen-independent mechanisms of gluten. Inflamm Bowel Dis, 2013. 19(6): p. 1285-94.*
 224. Schaubeck, M., et al., *Dysbiotic gut microbiota causes transmissible Crohn's disease-like ileitis independent of failure in antimicrobial defence. Gut, 2015.*
 225. Kontoyiannis, D., et al., *Genetic dissection of the cellular pathways and signaling mechanisms in modeled tumor necrosis factor-induced Crohn's-like inflammatory bowel disease. J Exp Med, 2002. 196(12): p. 1563-74.*
 226. Apostolaki, M., et al., *Role of beta7 integrin and the chemokine/chemokine receptor pair CCL25/CCR9 in modeled TNF-dependent Crohn's disease. Gastroenterology, 2008. 134(7): p. 2025-35.*
 227. Mahler, M., et al., *Differential susceptibility of inbred mouse strains to dextran sulfate sodium-induced colitis. Am J Physiol, 1998. 274(3 Pt 1): p. G544-51.*
 228. Okayasu, I., et al., *A novel method in the induction of reliable experimental acute and chronic ulcerative colitis in mice. Gastroenterology, 1990. 98(3): p. 694-702.*
 229. Wirtz, S., et al., *Chemically induced mouse models of intestinal inflammation. Nat Protoc, 2007. 2(3): p. 541-6.*
 230. Fukata, M., et al., *Toll-like receptor-4 is required for intestinal response to epithelial injury and limiting bacterial translocation in a murine model of acute colitis. Am J Physiol Gastrointest Liver Physiol, 2005. 288(5): p. G1055-65.*

231. Williams, K.L., et al., *Enhanced survival and mucosal repair after dextran sodium sulfate-induced colitis in transgenic mice that overexpress growth hormone*. *Gastroenterology*, 2001. **120**(4): p. 925-37.
232. Jess, T., et al., *Risk of intestinal cancer in inflammatory bowel disease: a population-based study from olmsted county, Minnesota*. *Gastroenterology*, 2006. **130**(4): p. 1039-46.
233. Velayos, F.S., et al., *Predictive and protective factors associated with colorectal cancer in ulcerative colitis: A case-control study*. *Gastroenterology*, 2006. **130**(7): p. 1941-9.
234. Tanaka, T., et al., *A novel inflammation-related mouse colon carcinogenesis model induced by azoxymethane and dextran sodium sulfate*. *Cancer Sci*, 2003. **94**(11): p. 965-73.
235. Cooper, H.S., et al., *Clinicopathologic study of dextran sulfate sodium experimental murine colitis*. *Lab Invest*, 1993. **69**(2): p. 238-49.
236. Katakura, K., et al., *Toll-like receptor 9-induced type I IFN protects mice from experimental colitis*. *J Clin Invest*, 2005. **115**(3): p. 695-702.
237. Hemmerling, J., et al., *Fetal gut laser microdissection in combination with RNA preamplification enables epithelial-specific transcriptional profiling*. *J Immunol Methods*, 2014.
238. Catoire, M., et al., *Pronounced effects of acute endurance exercise on gene expression in resting and exercising human skeletal muscle*. *PLoS One*, 2012. **7**(11): p. e51066.
239. Huang da, W., B.T. Sherman, and R.A. Lempicki, *Systematic and integrative analysis of large gene lists using DAVID bioinformatics resources*. *Nat Protoc*, 2009. **4**(1): p. 44-57.
240. Caporaso, J.G., et al., *Global patterns of 16S rRNA diversity at a depth of millions of sequences per sample*. *Proc Natl Acad Sci U S A*, 2011. **108** **Suppl 1**: p. 4516-22.
241. Edgar, R.C., *UPARSE: highly accurate OTU sequences from microbial amplicon reads*. *Nat Methods*, 2013. **10**(10): p. 996-8.
242. Caporaso, J.G., et al., *QIIME allows analysis of high-throughput community sequencing data*. *Nat Methods*, 2010. **7**(5): p. 335-6.
243. Cole, J.R., et al., *The Ribosomal Database Project (RDP-II): previewing a new autoaligner that allows regular updates and the new prokaryotic taxonomy*. *Nucleic Acids Res*, 2003. **31**(1): p. 442-3.
244. Edgar, R.C., et al., *UCHIME improves sensitivity and speed of chimera detection*. *Bioinformatics*, 2011. **27**(16): p. 2194-200.
245. Hemmerling, J., et al., *Fetal exposure to maternal inflammation does not affect postnatal development of genetically-driven ileitis and colitis*. *PLoS One*, 2014. **9**(5): p. e98237.
246. Roulis, M., et al., *Intestinal epithelial cells as producers but not targets of chronic TNF suffice to cause murine Crohn-like pathology*. *Proc Natl Acad Sci U S A*, 2011. **108**(13): p. 5396-401.
247. Cohen, C.D., et al., *Laser microdissection and gene expression analysis on formaldehyde-fixed archival tissue*. *Kidney Int*, 2002. **61**(1): p. 125-32.
248. Espina, V., et al., *Laser-capture microdissection*. *Nat Protoc*, 2006. **1**(2): p. 586-603.
249. Lotz, M., et al., *Postnatal acquisition of endotoxin tolerance in intestinal epithelial cells*. *J Exp Med*, 2006. **203**(4): p. 973-84.

250. McMullin, R.P., L.N. Mutton, and C.J. Bieberich, *Hoxb13 regulatory elements mediate transgene expression during prostate organogenesis and carcinogenesis*. Dev Dyn, 2009. **238**(3): p. 664-72.
251. Noble, C.L., et al., *Regional variation in gene expression in the healthy colon is dysregulated in ulcerative colitis*. Gut, 2008. **57**(10): p. 1398-405.
252. Gruber, L., et al., *Maternal High-fat Diet Accelerates Development of CD-like Ileitis in TNFΔARE/WT Offspring While Hardly Affecting Fetal Epithelial Gene Expression*. Inflammatory Bowel Diseases, 2015: p. 1.
253. Heerwagen, M.J., et al., *Maternal obesity and fetal metabolic programming: a fertile epigenetic soil*. Am J Physiol Regul Integr Comp Physiol. **299**(3): p. R711-22.
254. Yan, X., et al., *Maternal obesity induces sustained inflammation in both fetal and offspring large intestine of sheep**. Inflamm Bowel Dis.
255. Zhu, M.J., et al., *Maternal obesity up-regulates inflammatory signaling pathways and enhances cytokine expression in the mid-gestation sheep placenta*. Placenta. **31**(5): p. 387-91.
256. Chang, J.S., et al., *Endoplasmic reticulum stress response promotes cytotoxic phenotype of CD8αβ⁺ intraepithelial lymphocytes in a mouse model for Crohn's disease-like ileitis*. J Immunol, 2012. **189**(3): p. 1510-20.
257. Powrie, F., et al., *Phenotypically distinct subsets of CD4⁺ T cells induce or protect from chronic intestinal inflammation in C. B-17 scid mice*. Int Immunol, 1993. **5**(11): p. 1461-71.
258. Gevers, D., et al., *The treatment-naive microbiome in new-onset Crohn's disease*. Cell Host Microbe, 2014. **15**(3): p. 382-92.
259. Challis, J.R., et al., *Inflammation and pregnancy*. Reprod Sci, 2009. **16**(2): p. 206-15.
260. Jones, H.N., et al., *High-fat diet before and during pregnancy causes marked up-regulation of placental nutrient transport and fetal overgrowth in C57/BL6 mice*. Faseb j, 2009. **23**(1): p. 271-8.
261. Lin, Y., et al., *Effect of maternal dietary energy types on placenta nutrient transporter gene expressions and intrauterine fetal growth in rats*. Nutrition, 2012. **28**(10): p. 1037-43.
262. Gaccioli, F., et al., *Maternal overweight induced by a diet with high content of saturated fat activates placental mTOR and eIF2α signaling and increases fetal growth in rats*. Biol Reprod, 2013. **89**(4): p. 96.
263. Yang, Q.Y., et al., *Maternal obesity induces epigenetic modifications to facilitate Zfp423 expression and enhance adipogenic differentiation in fetal mice*. Diabetes, 2013. **62**(11): p. 3727-35.
264. Jansson, N., et al., *Activation of placental mTOR signaling and amino acid transporters in obese women giving birth to large babies*. J Clin Endocrinol Metab, 2013. **98**(1): p. 105-13.
265. Yu, Z., et al., *Pre-pregnancy body mass index in relation to infant birth weight and offspring overweight/obesity: a systematic review and meta-analysis*. PLoS One, 2013. **8**(4): p. e61627.
266. Freeman, D.J., *Effects of maternal obesity on fetal growth and body composition: implications for programming and future health*. Semin Fetal Neonatal Med, 2010. **15**(2): p. 113-8.
267. Sewell, M.F., et al., *Increased neonatal fat mass, not lean body mass, is associated with maternal obesity*. Am J Obstet Gynecol, 2006. **195**(4): p. 1100-3.

268. Lau, E.Y., J. Liu, and E. Archer, *Maternal weight gain in pregnancy and risk of obesity among offspring: a systematic review*. 2014. **2014**: p. 524939.
269. Sarr, O., K. Yang, and T.R. Regnault, *In utero programming of later adiposity: the role of fetal growth restriction*. *J Pregnancy*, 2012. **2012**: p. 134758.
270. Kwon, G.S., et al., *Tg(Afp-GFP) expression marks primitive and definitive endoderm lineages during mouse development*. *Dev Dyn*, 2006. **235**(9): p. 2549-58.
271. Morey, J.S., J.C. Ryan, and F.M. Van Dolah, *Microarray validation: factors influencing correlation between oligonucleotide microarrays and real-time PCR*. *Biol Proced Online*, 2006. **8**: p. 175-93.
272. Mouralidarane, A., et al., *Maternal obesity programs offspring nonalcoholic fatty liver disease by innate immune dysfunction in mice*. *Hepatology*, 2013. **58**(1): p. 128-38.
273. Xue, Y., et al., *Maternal obesity induces gut inflammation and impairs gut epithelial barrier function in nonobese diabetic mice*. *J Nutr Biochem*, 2014. **25**(7): p. 758-64.
274. Marleau, A.M. and N.E. Sarvetnick, *IL-18 is required for self-reactive T cell expansion in NOD mice*. *J Autoimmun*, 2011. **36**(3-4): p. 263-77.
275. Lee, P.Y., et al., *Ly6 family proteins in neutrophil biology*. *J Leukoc Biol*, 2013. **94**(4): p. 585-94.
276. Delporte, C., et al., *Low-density lipoprotein modified by myeloperoxidase in inflammatory pathways and clinical studies*. *Mediators Inflamm*, 2013. **2013**: p. 971579.
277. Stenman, L.K., et al., *Genetically obese mice do not show increased gut permeability or faecal bile acid hydrophobicity*. *Br J Nutr*, 2013. **110**(6): p. 1157-64.
278. Levy, O., *Innate immunity of the newborn: basic mechanisms and clinical correlates*. *Nat Rev Immunol*, 2007. **7**(5): p. 379-90.
279. Teixeira, L.G., et al., *The combination of high-fat diet-induced obesity and chronic ulcerative colitis reciprocally exacerbates adipose tissue and colon inflammation*. *Lipids Health Dis*, 2011. **10**: p. 204.
280. Collado, M.C., et al., *Effect of mother's weight on infant's microbiota acquisition, composition, and activity during early infancy: a prospective follow-up study initiated in early pregnancy*. *Am J Clin Nutr*, 2010. **92**(5): p. 1023-30.
281. Simmons, R., *Developmental origins of adult metabolic disease: concepts and controversies*. *Trends Endocrinol Metab*, 2005. **16**(8): p. 390-4.
282. Vignini, A., et al., *Environmental and genetical aspects of the link between pregnancy, birth size, and type 2 diabetes*. *Curr Diabetes Rev*, 2012. **8**(3): p. 155-61.
283. Caron, E., et al., *Distribution of leptin-sensitive cells in the postnatal and adult mouse brain*. *J Comp Neurol*, 2010. **518**(4): p. 459-76.
284. Jequier, E., *Leptin signaling, adiposity, and energy balance*. *Ann N Y Acad Sci*, 2002. **967**: p. 379-88.
285. Bouret, S.G., S.J. Draper, and R.B. Simerly, *Formation of projection pathways from the arcuate nucleus of the hypothalamus to hypothalamic regions implicated in the neural control of feeding behavior in mice*. *J Neurosci*, 2004. **24**(11): p. 2797-805.
286. Proulx, K., D. Richard, and C.D. Walker, *Leptin regulates appetite-related neuropeptides in the hypothalamus of developing rats without affecting food intake*. *Endocrinology*, 2002. **143**(12): p. 4683-92.

6. Appendix

Table 9 Dietary compositions

	normal diet	HFD experiments	
company	ssniff	ssniff	
comment	"Chow" diet	"experimental control diet"	"high-fat diet (HFD)"
order number	V1534-000 R/M-H	S5745-E702	S5745-E712
metabl energy MJ/kg	12.80	15.50	19.70
micronutrients			
%kcal fat	9.00	12.00	48.00
%kcal protein	33.00	23.00	18.00
%kcal carb	58.00	65.00	34.00
crude fat %weight	3.30	5.10	25.10
crude protein %weight	19.00	20.80	20.80
crude ash %weight	6.40	5.60	5.60
crude fiber %weight	4.90	5.00	5.00
corn starch %weight	36.50	47.80	27.80
maltodextrin %weight		5.60	5.60
sucrose %weight	4.70	5.00	5.00
sucrose %kcal			
casein		24.00	24.00
vitamin pre-mix		1.20	1.20
mineral-pre-mix		6.00	6.00
cellulose %weight		5.00	5.00
soybean oil %weight		5.00	5.00
palm oil %weight			20.00
C14:0 %	0.01	0.03	0.22
C16:0 %	0.47	0.55	8.87
C16:1 %	0.01	0.03	0.13
C18:0 %	0.08	0.24	1.19
C18:1 %	0.62	1.34	8.75
C18:2 %	1.80	2.65	4.67
C18:3 %	0.23	0.33	0.43
C20:0 %	0.01	0.03	0.13
C20:1 %	0.02		
C20:2 %			
C20:4 %			
C20:5 %			
C22:0 %			
C22:5 %			
C22:6 %			
n3 %			
n6 %			
ration n6/n3			

micronutrients			
l-cystin %		0.20	0.20
cholin-chlorid %	0.29	0.20	0.20
lysin %	1.00	1.71	1.71
methionin %	0.30	0.75	0.75
met+cys %	0.65	1.04	1.04
threonin %	0.68	0.93	0.93
calcium (mg/kg)	1.00	0.92	0.92
phosphor (mg/kg)	0.70	0.63	0.63
sodium (mg/kg)	0.24	0.19	0.19
magnesium (mg/kg)	0.22	0.21	0.21
iron (mg/kg)	179.00	168.00	168.00
aluminium (mg/kg)			
selenium (mg/kg)	0.3		
iodine (mg/kg)	2.2		
copper (mg/kg)	16		
manganese (mg/kg)	69		
molybdenum (mg/kg)			
zinc (mg/kg)	94		
fluorine (mg/kg)			
cobalt (mg/kg)	2.1		

7. List of Figures

Figure 1 Immunoregulatory effects in the feto-maternal cross talk under physiological and inflammatory conditions.....	10
Figure 2 Early development of the intestinal epithelium adopted from [136].....	16
Figure 3 Neonatal development of the intestinal immune system.	19
Figure 4 Offspring groups in maternal inflammation studies.....	26
Figure 5 Offspring groups in maternal obesity studies	27
Figure 6 Regimen of maternal and offspring's dietary exposure.	28
Figure 7 Severity of CD-like ileitis in response to diet and hygiene stage.....	38
Figure 8 TNF-driven maternal inflammatory environment at weaning	39
Figure 9 Severity of CD-like ileitis is not influenced by maternal inflammation.	40
Figure 10 Loss of lysozyme and infiltration of neutrophils in distal ileum of $Tnf^{\Delta ARE/+}$ mice is not affected by maternal inflammation.	41
Figure 11 Immunophenotyping of offspring's mesenteric and splenic lymphocytes in response to maternal inflammation.	42
Figure 12 Offspring's body weight and fat depot masses in response to maternal inflammation.	43
Figure 13 Microbial ecology in WT and ARE offspring after disease onset.	44
Figure 14 Inflammation-driven changes of bacterial taxa in 8 week-old offspring.....	45
Figure 15 Metabolic differences between pregnant lean and HFD mothers equalize by postnatal HFD during breastfeeding.	47
Figure 16 Transcriptional analysis of placental cytokines.....	48
Figure 17 Laser microdissection of fetal intestinal epithelial cells from ileum and colon.	50
Figure 18 Proof of concept by comparative analysis of <i>Muc2</i> gene expression in fetal ileum and colon.....	51
Figure 19 Fetal transcriptional programming is hardly affected by maternal HFD.	52
Figure 20 Overlapping and top regulated genes in fetal intestinal epithelial cells in response to mDIO or fetal genotype.	54
Figure 21 Postnatal development of CD-like ileitis in $Tnf^{\Delta ARE/+}$ offspring is accelerated by fetal exposure to maternal diet-induced obesity (mDIO).....	55
Figure 22 Neutrophil infiltration into distal ileum of $Tnf^{\Delta ARE/+}$ offspring is accelerated by maternal diet-induced obesity, without affecting loss of Lysozyme+ cells in crypts.	56
Figure 23 Myeloperoxidase (MPO)-positive cell-infiltration is not affected by maternal diet-induced obesity (mDIO).....	57
Figure 24 The development of ileitis in $Tnf^{\Delta ARE/+}$ offspring is associated with increased TNF plasma levels and elevated portal vein endotoxin.....	58

Figure 25 Body weight development in response to mDIO and postnatal HFD. 59

Figure 26 MDIO protects WT offspring from excessive energy storage and shows no metabolic influence on $Tnf^{\Delta ARE/+}$ offspring. 60

Figure 27 Cumulative DSS exposure is equal among studies in (A) WT and iWT offspring (maternal inflammation) or (B) WT and oWT offspring (maternal diet-induced obesity). 61

Figure 28 Maternal inflammation, but not mDIO protects offspring against DSS colitis. 62

Figure 29 Fetal transcriptional programming of the colonic epithelium is hardly affected by maternal inflammation. 63

8. List of Tables

Table 1 <i>Previously conducted rodent studies about maternal obesity with different setting of maternal dietary exposure.</i>	13
Table 2 <i>Commonly used mouse models of IBD.</i>	23
Table 3 <i>Primary antibodies</i>	31
Table 4 <i>Secondary antibodies</i>	31
Table 5 <i>H&E staining protocol for laser microdissection</i>	32
Table 6 <i>Primer sequences</i>	34
Table 7 <i>Fluorochrome-conjugated antibodies</i>	35
Table 8 <i>Top 10 up- and downregulated genes</i>	63
Table 9 <i>Dietary compositions</i>	91

9. List of Supplementary Tables

Table X Maternal obesity studies: list of significantly regulated genes in the ileal epithelium of oWT fetuses compared to WT fetuses. Data were filtered according to a p-value <0.05 and a $FC \pm 1.3$. [Supplementary information\TableX.xlsx](#)

Table XI Maternal obesity studies: list of significantly regulated genes in the ileal epithelium of ARE fetuses compared to WT fetuses. Data were filtered according to a p-value <0.05 and a $FC \pm 1.3$. [Supplementary information\TableXI.xlsx](#)

Table XII Maternal obesity studies: list of significantly regulated genes in the ileal epithelium of oARE fetuses compared to ARE fetuses. Data were filtered according to a p-value <0.05 and a $FC \pm 1.3$. [Supplementary information\TableXII.xlsx](#)

Table XIII Maternal obesity studies: list of significantly regulated genes in the ileal epithelium of oARE fetuses compared to oWT fetuses. Data were filtered according to a p-value <0.05 and a $FC \pm 1.3$. [Supplementary information\TableXIII.xlsx](#)

Table XIV Maternal obesity studies: list of significantly regulated genes in the ileal epithelium of WT fetuses compared to oARE fetuses. Data were filtered according to a p-value <0.05 and a $FC \pm 1.3$. [Supplementary information\TableXIV.xlsx](#)

Table XV Maternal inflammation studies: list of significantly regulated genes in the colonic epithelium of iWT fetuses compared to WT fetuses. Data were filtered according to a p-value <0.05 and a $FC \pm 1.3$. [Supplementary information\TableXV.xlsx](#)

Table XVI Sampling data of 8 week-old offspring in maternal inflammation studies [Supplementary information\TableXVI.xlsx](#)

Table XVII Histological scores of 12 week-old $Tnf^{ARE/+}$ mice on Chow or experimental diet in different housing conditions [Supplementary information\Table XVII.xlsx](#)

Table XVIII Sampling data of 8 and 12 week-old offspring in maternal obesity studies [Supplementary information\TableXVIII.xlsx](#)

10. List of Abbreviations

Abbreviation	Explanation
AA	Antibiotics/Antimycotics
ABC	Avidin Biotin Complex
AIEC	Adherent-E Invasive <i>Escherichia Coli</i>
AJ	Adherens Junctions
AMP	Antimicrobial Peptide
ANOVA	Analysis Of Variance
AOM	Aazoxymethan
ARC	Arcuate Nucleus Of The Hypothalamus
ARE	AU-Rich Element
ATG16	Autophagy-Related Protein 16
AgRP	Agouti-Related Peptide
BMI	Body Mass Index
BW	Body Weight
CARD	Caspase Activation And Recruitment Domain
CCR5	C-C Chemokine Receptor Type 5
CD	Crohn's Disease
CD-like	Crohn's Disease-Like
CD	Cluster Of Differentiation
CDH1	E-Cadherin
CDNA	Complementary DNA
CED	Chronisch Entzündliche Darmerkrankungen
CI	Confidence Intervall
CRAMP	Cathelicidin-Related Antimicrobial Peptide
CT	Cycle Threshold
CTRLD	Control Diet
DAI	Disease Activity Index
DC	Dendritic Cell
DEPC	Diethylpyrocarbonate
DIO	Diet-Induced Obesity
DNA	Desoxyribonucleic Acid
DNase	DNA Degrading Enzyme
DSS	Dextrane Sulfate Sodium
EDTA	Ethylenediaminetetraacetic Acid

Abbreviation	Explanation
EFW	Endotoxin-Free Water
EGFP	Eukaryotic Green Fluorescent Protein
ELISA	Enzyme-Linked Immunosorbent Assay
EU	Endotoxin Unit
EtOH	Ethanol
F-Test	Fisher-Test
FACS	Fluorescent
FC	Fold Change
FCS	Fetal Calf Serum
Fc(R)	Fragment Crystallisable Receptor
FITC	Fluorescein isothiocyanate
FOXP3	Forkhead Box Protein 3
GALT	Gut-Associated-Lymphoid Tissue
GDM	Gene Distance Measurement
GF	Germ-Free
GO	Gene Ontology
GWAS	Genome-Wide Association Studies
HFD	High Fat Diet
HRP	Horseradish Peroxidase
IBD	Inflammatory Bowel Diseases
IBMT	Intensity-Based Moderated T-Statistic
IEC	Intestinal Epithelial Cells
IEL	Intraepithelial Lymphocytes
IFN	Interferon
IKK	Inhibitor Of NF-Kb (Ikb) Kinase
IL	Interleukin
ILC	Innate Lymphoid Cells
IQR	Inter Quartile Range
IRGM	Immunity-Related Gtpase Family M Protein
Ig	Immunoglobulin
JAK	Janus Kinase
KIT	Tyrosine-Protein Kinase Kit
KO	Knock-Out
LAL	Limulous Amoebocyte Lysate
LMD	Laser Microdissection
LPL	Lamina Propria Lymphocytes

Abbreviation	Explanation
LPS	Lipopolysaccharide
LRR	Leucine-Rich Repeat,
LTi	Lymphoid Tissue Inducer
Ly6G	Lymphocyte Antigen 6 Complex Locus G
MAPK	Mitogen-Activated Protein Kinase
MDIO	Maternal Diet-Induced Obesity
MHC	Major Histocompatibility Complex
MIAME	Minimum Information About A Microarray Experiment
MJ	Mega Joule
MLCK	Myosin Light Chain Kinase
MLN	Mesenteric Lymph Nodes
MPO	Myeloperoxidase
MUC	Mucin
MW	Molecular Weight
MyD88	Myeloid Differentiation Primary Response Gene 88
NAFLD	Non-Alcoholic Fatty Liver Disease
NCBI	National Center For Biotechnology Information
NEMO	NF-Kb Essential Modulator
NF-κB	Nuclear Factor Kb
NK	Natural Killer
NKT cell	Natural Killer T Cell
NLR	Nucleotide-Binding Oligomerization Domain -Like Receptor
NLRP	NOD-, LRR And Pyrin-domain-Containing 3
NOD	Nucleotide-Binding Oligomerization Domain
NPY	Neuropeptide Y
NSAID+	Non-Steroidal- Anti-Inflammatory Drug
NaCl	Sodium Chloride
O.C.T.	Optimal Cutting Temperature
OTUs	Operational Taxonomic Units
PBMCs	Peripheral Blood Mononuclear Cells
PBS	Phosphate Buffer Saline
PBST	Phosphate Buffered Saline Tween-20
PCR	Polymerase Chain Reaction
PCoA	Principal Coordinates Analysis
PND	Postnatal Day
POMC	Pro-Opiomelanocortin

Abbreviation	Explanation
PRR	Pattern Recognition Receptors
PSA	Polysaccharide A
QPCR	Quantitative PCR
RAG	Recombination-Activating Gene
RANTES	Regulated On Activation, Normal T Cell Expressed And Secreted
REG3	Regenerating Islet Derived 3
RELM β	Resistin-Like Molecule-B
RIG	Retinoic Acid-Inducible Gene 1
RIN	RNA Integrity Number
RIP2	Receptor-Interacting Protein 2
RLR	RIG-I-Like Receptor
RMA	Robust Multi-Array Average
RNA	Ribonucleic Acid
RNase	Ribonuclease
ROI	Region Of Interest .
ROR	Retinoic Acid Receptor-Related Orphan Receptor
RPMI	Roswell Park Memorial Institute
RT	Room Temperature
RT-qPCR	Reverse-Transcriptase-Quantitative PCR
SAMP1	"Senescence-Prone" Mice
SCFA	Short Chain Fatty Acid
SD	Standard Discrepancy
SDS	Sodium Dodecyl Sulfate
SFB	Segmented Filamentous Bacteria
SIgA	Secretory Immunoglobulin A
SNPs	Single Nucleotide Polymorphism
SPF	Specific Pathogen-Free
SPIA	Single Primer Isothermal Amplification
STAT	Signal Transducer And Activator Of Transcription
T1D	Type 1 Diabetes
TFF3	Trefoil Factor 3
TGF	Transforming Growth Factor
TJ	Tight Junctions
TLR	Toll-Like Receptor
TNBS	Trinitrobenzenesulfonic Acid

Abbreviation	Explanation
TNF	Tumor Necrosis Factor
TNFR	Tumor Necrosis Factor Receptor
TNFRSF	Tumor Necrosis Factor Receptor Super Family
TRADD	Tumor Necrosis Factor Receptor Type 1-Associated DEATH Domain
TRUC	T-Bet ^{-/-} RAG2 ^{-/-} Ulcerative Colitis
TS	Theiler Stage
UC	Ulcerative Colitis
UPL	Universal Probe Library
UPR	Unfolded Protein Response
UV	Ultra Violet
WHO	World Health Organization
WT	Wildtype
WTA	Whole Transcriptome Amplification
mRNA	Messenger RNA
mT1D	Maternal Type 1 Diabetes
rRNA	Ribosomal RNA

11. Acknowledgments

Es ist vollbracht! Nach vielen Jahren intensiver Arbeit liegt sie nun vor Euch: meine Dissertation.

Damit ist es an der Zeit, mich bei all denjenigen zu bedanken, die mich in dieser herausfordernden, aber auch ungemein lohnenden Phase meiner akademischen Laufbahn begleitet haben.

Zu besonderem Dank bin ich Prof. Dr. Dirk Haller verpflichtet. Als erster Gutachter hat er mich stets mit seinen wissenschaftlichen Anregungen unterstützt und herausgefordert. Ebenfalls bedanke ich mich sehr bei Prof. Dr. Martin Klingenspor für sein zweites Gutachten und für die wissenschaftliche Unterstützung im Rahmen des Epigenetik-Kollegs.

Meinen weiteren Dank richte ich an meine ehemaligen Kommilitonen und Mitarbeiter des Lehrstuhls für Ernährung und Immunologie, die mich in den vergangenen Jahren mit bereichernden Tipps, Diskussionsbeiträgen und vor allem mit viel Spaß und Freude wiederholt in neue kraftvolle und fruchtbare Bahnen gelenkt haben: Elena Lobner, Irina Sava-Piroddi, Amira Metwaly, Thomas Clavel, Nico Gebhardt, Silvia Pitariu, Caroline Ziegler, Sandra Hennig, Monika Bazzanella, Annemarie Schmidt, Sigrid Kisling, Valentina Schüppel, Gabriele Hörmannspurger, Katharina Heller, Sarah Just, Ingrid Schmöller, Simone Daxauer und Brita Sturm.

Mein ganz besonderer Dank geht an die Kollegen, die über die Doktorarbeit hinaus zu meinen Freunden zählen. Ich danke euch für die großartige Zeit im Labor, wenn wir „die Zukunft nach nebenan geschickt haben“ und freue mich auf zukünftige tolle Momente mit euch: Emanuel Berger, Natalie Steck, Lisa Richter, Marie-Anne von Schillde, Sören Ocvirk, Jelena Calasan, und meine „Epigenetik-Mädels“ Veronika Flöter und Kirsten Uebel.

Eine herausragende Stellung in jeglicher Hinsicht nimmt meine Familie und ganz besonders mein „Lieblingsmensch“ Ulf ein. Ohne seine liebevolle und geduldige Unterstützung und zahlreiche motivierende Gespräche wäre diese Arbeit nicht zu dem Werk geworden, welches sie heute ist. Vielen lieben Dank dafür.

DANKE

12. Curriculum Vitae

Personal Data

Name	Jana Hemmerling
Date of birth	May 1 st 1980
Current Address	Hangenham 31C, 85417 Marzling, Germany

Occupational Experience

08/2014-today	Medical Writer at <i>Advanced Medical Services GmbH</i> , Munich
04/2010-07/2014	PhD Student at <i>Technical University of Munich</i> , ZIEL, Chair of Nutrition and Immunology, " <i>Murine susceptibility to intestinal inflammation by in utero exposure to maternal inflammation and maternal obesity</i> "
05/2008-01/2010	Diploma student at the <i>German Institute of Human Nutrition (DIfE)</i> , Biochemistry of Micronutrients, Prof. Dr. R. Brigelius-Flohe, Potsdam-Rehbrücke, " <i>Vitamin E im vesikulären Transport von RBL-2H3-Zellen</i> "
05/2008-9/2008	Student research assistant at the <i>German Institute of Human Nutrition (DIfE)</i> , Potsdam-Rehbrücke
04/2002-12/2009	Purser at <i>Condor Berlin GmbH</i> , Berlin
06/2000-03/2002	Flight attendant at <i>Condor Berlin GmbH</i> , Berlin
08/1999-04/2000	Voluntary social year at <i>KITA "Fuchsbau"</i> , Rehfelde

Education

- 04/2010-06/2014 PhD thesis at *Technical University of Munich*, Chair for Nutrition and Immunology, Prof Dr. D. Haller, ZIEL-research center for nutritional and food sciences: “*Murine susceptibility to intestinal inflammation by in utero exposure to maternal inflammation and maternal obesity*”.
- 10/2003-01/2010 Studies of Nutritional Sciences at the *University Potsdam*, Diploma thesis at the *German Institute of Human Nutrition (DIfE)*, Biochemistry of Micronutrients, Prof. Dr. R. Brigelius-Flohe, Potsdam-Rehbrücke, „*Vitamin E im vesikulären Transport von RBL-2H3-Zellen*“

Scientific Qualifications

- 11/2010 Felasa B course for laboratory animals, Munich
- 01/2008-02/2008 Internship at the *Griffith University*, School of Biomolecular and Physical Sciences, Prof. Dr. D. Crane, Brisbane, Australia,
- 02/2007 Seminar “*Ambulante enterale Ernährungstherapie*“ of the *Deutsche Gesellschaft für Ernährungsmedizin (DGEM)*, Berlin

Publications

- 2015 Schiffner-Rohe, J., Witt A. Hemmerling J., von Eiff C. Leverkus F., *Efficacy of PPV23 in preventing pneumococcal pneumonia in elderly - a systematic review and meta-analysis*, PLoS One, 2015, *in revision*
- 2015 Gruber, L.#, Hemmerling, J.## *et al.*, *Maternal high-fat diet accelerates development of CD-like ileitis in $Tnf^{flARE/WT}$ offspring while hardly affecting fetal epithelial gene expression*. *Inflammatory Bowel Diseases* 2015:1.

shared first authorship

- 2014 Hemmerling, J.*, et al., *Fetal gut laser microdissection in combination with RNA preamplification enables epithelial-specific transcriptional profiling*. J Immunol Methods, 2014.
- 2014 Hemmerling, J.*, et al., *Fetal exposure to maternal inflammation does not affect postnatal development of genetically-driven ileitis and colitis*. PLoS One, 2014. **9**(5): p. e98237.
- 2010 Hemmerling, J., et al., *Alpha-Tocopherol enhances degranulation in RBL-2H3 mast cells*. Mol Nutr Food Res, 2010. **54**(5): p. 652-60.

* publications in the context of PhD thesis

Grants

- 2013 Young investigator travel award, Society of mucosal immunology, USA
- 2011 Danone research grant: Nutrition and Epigenetics
"Impact of maternal obesity on fetal gut programming and susceptibility to intestinal inflammation", Danone Institute, Haar
- 2010 Poster award, Seeon conference, *"Impact of maternal gut inflammation on the gene expression profile of the offspring's intestinal epithelial cells"*, Seeon

Oral presentations

- 07/2013 ICMI (International Conference for Mucosal Immunology), *"Fetal exposure to inflammation affects the transcriptional program in the intestinal epithelium and accelerates TNF-driven pathology"*, Vancouver, Canada
- 09/2012 NuGO week (Nutrigenomics week), *"Fetal gut programming by maternal inflammation and maternal diet-induced obesity in context of offspring's susceptibility to chronic intestinal disease"*, Helsinki, Finland

10/2009 FSV-Meeting 2009 (14th European Meeting on Fat Soluble Vitamins), " *α -Tocopherol enhances degranulation in RBL-2H3 mast cells.*", Potsdam

Poster presentations

03/2013 DGE (Deutsche Gesellschaft für Ernährung) congress "Disease-conditioning by fetal programming in the context of maternal inflammation and obesity", Bonn

05/2012 DDW (Digestive Disease Week), "Impact of maternal inflammation on fetal gut programming and susceptibility to chronic disease", San Diego, CA, USA

03/2012 DGE congress (Deutsche Gesellschaft für Ernährung), "Impact of maternal inflammation on fetal gut programming and susceptibility to chronic disease", Freising

09/2011 NuGO week (Nutrigenomics week), "Impact of maternal inflammation on fetal gut programming and disease susceptibility", Wageningen, The Netherlands

07/2011 ICMI (International Conference for Mucosal Immunology), "Impact of maternal inflammation on fetal gut programming and disease susceptibility", Paris, France

04/2011 Seeon conference, "Impact of maternal inflammation on the gut epithelial transcriptome", Seeon

06/2010 Seeon conference, "Impact of maternal gut inflammation on the gene expression profile of the offspring's intestinal epithelial cells", Seeon